

Overview: Recent advances on the understanding of the Northern Eurasian environments and of the urban air quality in China - Pan Eurasian Experiment (PEEX) program perspective

Hanna K. Lappalainen^{1,2}, Tuukka Petäjä^{1,2}, Timo Vihma³, Jouni Räisänen¹, Alexander Baklanov⁴, Sergey Chalov⁵, Igor Esau⁶, Ekaterina Ezhova¹, Matti Leppäranta¹, Dmitry Pozdnyakov^{7,46}, Jukka Pumpanen⁸, Meinrat O. Andreae^{9,42,43}, Mikhail Arshinov¹⁰, Eija Asmi³, Jianhui Bai^{11,44}, Igor Bashmachnikov⁷, Boris Belan¹⁰, Federico Bianchi¹, Boris Biskaborn¹², Michael Boy¹, Jaana Bäck¹³, Bin Cheng³, Natalia Ye Chubarova⁵, Jonathan Duplissy^{1,45}, Egor Dyukarev¹⁴, Konstantinos Eleftheriadis¹⁵, Martin Forsius¹⁶, Martin Heimann¹⁷, Sirkku Juhola²⁰, Vladimir Konovalov¹⁸, Igor Konovalov¹⁹, Pavel Konstantinov^{5,33}, Kajar Koster¹³, Elena Lapsina²¹, Anna Lintunen^{1,13}, Alexander Mahura¹, Risto Makkonen³, Svetlana Malkhazova⁵, Ivan Mammarella¹, Stefano Mammola^{22,23}, Stephany Mazon¹, Outi Meinander³, Eugene Mikhailov^{24, 25}, Victoria Miles⁶, Stanislav Myslenko⁵, Dmitry Orlov⁵, Jean-Daniel Paris²⁶, Roberta Pirazzini³, Olga Popovicheva²⁷, Jouni Pulliainen³, Kimmo Rautiainen³, Torsten Sachs²⁸, Vladimir Shevchenko²⁹, Andrey Skorokhod³⁰, Andreas Stohl³¹, Elli Suhonen¹, Erik S. Thomson³², Marina Tsidilina³⁹, Veli-Pekka Tynkkynen³⁴, Petteri Uotila¹, Aki Virkkula³, Nadezhda Voropay³⁵, Tobias Wolf⁶, Sayaka Yasunaka³⁶, Jiahua Zhang³⁷, Yubao Qiu³⁷, Aijun Ding³⁸, Huadong Guo³⁷, Valery Bondur³⁹, Nikolay Kasimov⁵, Sergej Zilitinkevich (†)^{1,2,3}, Veli-Matti Kerminen¹ and Markku Kulmala^{1,2,39,40,41}

¹ Institute for Atmospheric and Earth System Research / Physics, Faculty of Science, University of Helsinki, Finland

² Tyumen State University, Department of Cryosphere, 625003 Tyumen, Russia

³ Finnish Meteorological Institute, 00101 Helsinki, Finland

⁴ World Meteorological Organization, WMO, Geneva, Switzerland

⁵ Faculty of Geography, Lomonosov Moscow State University, Lenin Hills, 119991, Moscow, Russia

⁶ Nansen Environmental and Remote Sensing Center/Bjerknes Centre for Climate Research, Bergen, Norway

⁷ Nansen International Environmental and Remote Sensing Centre³⁹, Nansen Centre, NIERSC, St. Petersburg, Russia

⁸ Department of Environmental and Biological Sciences, PO Box 1627 (Address: Yliopistonranta 1 E), FI-70211 Kuopio, Finland

⁹ Max Planck Institute for Chemistry, Mainz, Germany

¹⁰ V.E. Zuev Institute of Atmospheric Optics (IAO) SB RAS, Tomsk, 634055, Russia

¹¹ LAGEO, Institute of Atmospheric Physics, Chinese Academy of Sciences (IAP-CAS), Beijing, 100029, PR, China

¹² Alfred Wegener Institute, Helmholtz Centre for Polar and Marine Research, Potsdam, Germany

¹³ Institute for Atmospheric and Earth System Research /Forest Sciences, University of Helsinki, Helsinki, Finland

- 38 ¹⁴ Institute of Monitoring of Climatic and Ecological Systems SB RAS, Tomsk, 634055, Russia; Yugra
39 State University, Khanty-Mansiysk, 628012, Russia
- 40 ¹⁵ ERL, Institute of Nuclear and Radiological Science & Technology, Energy & Safety, NCSR
41 Demokritos, Attiki, Greece
- 42 ¹⁶ Finnish Environment Institute SYKE, Latokartanonkaari 11, 00790 Helsinki, Finland
- 43 ¹⁷ Max-Planck-Institute for Biogeochemistry, Jena, Germany
- 44 ¹⁸ Institute of Geography RAS, Moscow, Russia
- 45 ¹⁹ Institute of Applied Physics, Nizhny Novgorod, Russia
- 46 ²⁰ Faculty of Biological and Environmental Sciences, University of Helsinki, Helsinki, Finland
- 47 ²¹ Yugra State University, Khanty-Mansiysk, 634012, Russia
- 48 ²² Finnish Museum of Natural History (LUOMUS), University of Helsinki, Helsinki, 00100, Finland
- 49 ²³ Molecular Ecology Group (MEG), Water Research Institute (IRSA), National Research Council of Italy
50 (CNR), Verbania Pallanza, 28922, Italy
- 51 ²⁴ St. Petersburg State University, 7/9 Universitetskaya nab, St. Petersburg, 199034, Russia
- 52 ²⁵ Multiphase Chemistry and Biogeochemistry Departments, Max Planck Institute for Chemistry, 55020
53 Mainz, Germany
- 54 ²⁶ Laboratoire des Sciences du Climat et de l'Environnement, IPSL CEA-CNRS-UVSQ, 91190 Gif-sur-
55 Yvette, France
- 56 ²⁷ Institute of Nuclear Physics, Lomonosov Moscow State University, Moscow, Russia
- 57 ²⁸ GFZ German Research Centre for Geosciences, Telegrafenberg, Potsdam, Germany
- 58 ²⁹ Shirshov Institute of Oceanology, Russian Academy of Sciences, Moscow, Russia
- 59 ³⁰ A.M. Obukhov Institute of Atmospheric Physics, Moscow, Russia
- 60 ³¹ Department of Meteorology and Geophysics, University of Vienna, Vienna, Austria
- 61 ³² Department of Chemistry & Molecular Biology, University of Gothenburg, Göteborg, 41296, Sweden
- 62 ³³ Peoples' Friendship University of Russia (RUDN), Laboratory of sSart technologies for sustainable
63 development of urban environment under global changes, Moscow, Russian Federation
- 64 ³⁴ Aleksanteri Institute, University of Helsinki, Helsinki, Finland
- 65 ³⁵ V B Sochava Institute of Geography SB RAS, Irkutsk, 664033, Russia; Institute of Monitoring of
66 Climatic and Ecological Systems SB RAS, Tomsk, 634055, Russia
- 67 ³⁶ Japan Agency for Marine-Earth Science and Technology (JAMSTEC), Yokosuka, Japan
- 68 ³⁷ Aerospace Information Research Institute, Chinese Academy of Sciences, Beijing, 100094, China
- 69 ³⁸ Joint International Laboratory of Atmospheric and Earth System sciences (JirLATEST), Nanjing
70 University, Nanjing, China
- 71 ³⁹ Institute for Scientific Research of Aerospace Monitoring "AEROCOSMOS", Moscow, 105064, Russia
- 72 ⁴⁰ Aerosol and Haze Laboratory, Beijing Advanced Innovation Center for Soft Matter Sciences and
73 Engineering, Beijing University of Chemical Technology (BUCT), Beijing, China
- 74 ⁴¹ Guangzhou Institute of Geography, Guangzhou Academy of Sciences, Guangzhou, China
- 75 ⁴² Department of Geology and Geophysics, King Saud University, Riyadh, Saudi Arabia

76 ⁴³ Scripps Institution of Oceanography, UCSD, La Jolla, CA, USA

77 ⁴⁴ Interdisciplinary Scientific and Educational School of M.V.Lomonosov Moscow State

78 University «Future Planet and Global Environmental Change, Russia

79 ⁴⁵ Helsinki Institute of Physics, University of Helsinki, 00014 Helsinki, Finland

80 ⁴⁶ St. State Petersburg University (St. Petersburg State University, 7/9 Universitetskaya nab. St. Petersburg,
81 199034. Russia

82
83 **Corresponding author(s):** Hanna Lappalainen, hanna.k.lappalainen@helsinki.fi, Veli-Matti Kerminen, [veli-](mailto:veli-matti.kerminen@helsinki.fi)
84 matti.kerminen@helsinki.fi

85

86 **Keywords**

87 Grand Challenges, climate change, land-atmosphere interactions and feedbacks, biogeochemical cycles,
88 Arctic Ocean, Northern Eurasia, China, Arctic marine ecosystem, atmospheric composition, air quality,
89 Arctic greening, land use change, permafrost, Pan-Eurasian Experiment (PEEX), Global Earth Observatory,
90 Digital Earth, Silk Road Economic Belt, Arctic societies, energy policy, boreal region, science diplomacy
91

92 **ABSTRACT**

93 The Pan-Eurasian Experiment (PEEX) Science Plan, released in 2015, addressed a need for a holistic system
94 understanding and outlined the most urgent research needs for the rapidly changing Arctic-boreal region. Air
95 quality in China, together with the long-range transport of atmospheric pollutants, was also indicated as one
96 of the most crucial topics of the research agenda. These two geographical regions, the Northern Eurasian
97 Arctic-boreal region and China, especially the megacities in China, were indentified as a “PEEX region”. It
98 is also important to recognize that the PEEX geographical region is an area where science-based policy
99 actions would have significant impacts on [the](#) global climate. This paper summarizes results obtained
100 during the last five years in the Northern Eurasian region, together with recent observations on the air quality
101 in the urban environments in China, in the context of the PEEX program. The main regions of interest are the
102 Russian Arctic, Northern Eurasian boreal forests (Siberia) and peatlands, and the megacities in China. We
103 frame our analysis against research themes introduced in the PEEX Science Plan in 2015. We summarize
104 recent progress towards an enhanced holistic understanding of the land – atmosphere – ocean systems
105 feedbacks. We conclude that although the scientific knowledge in these regions has increased, the new
106 results are in many cases insufficient and there are still gaps in our understanding of large-scale climate-
107 Earth surface interactions and feedbacks. This arises from limitations in research infrastructures, especially
108 the lack of coordinated, continuous and comprehensive in situ observations of the study region as well as
109 integrative data analyses, hindering a comprehensive system analysis. The fast-changing environment and
110 ecosystem changes driven by climate change, socio-economic activities like the China Silk Road Initiative,
111 and the global trends like urbanization further complicate such analyses. We recognize new topics with an
112 increasing importance in the near future, especially “the enhancing biological sequestration capacity of
113 greenhouse gases into forests and soils to mitigate the climate change” and the “socio-economic
114 development to tackle air quality issues”.

Field Code Changed

115	
116	Contents
117	Table of contents
118	ABSTRACT
119	1. INTRODUCTION
120	2. RESULTS
121	2.1. LAND ECOSYSTEMS
122	2.1.1 Changing land ecosystem processes (Q1)
123	<i>High-latitude photosynthetic productivity</i>
124	<i>Vegetation changes</i>
125	<i>New methodologies determining Earth surface characteristics</i>
126	2.1.2 Thawing permafrost (Q2)
127	<i>Observations of ground temperature evolution</i>
128	<i>Changing GHG fluxes and VOCs due to permafrost thaw</i>
129	2.1.3 Ecosystem structural change (Q3)
130	<i>Changes in microbial activity</i>
131	<i>Effects of forest fires on soils</i>
132	2.2. ATMOSPHERIC SYSTEM
133	2.2.1 Atmospheric composition and chemistry (Q4)
134	<i>Boreal forests carbon balance</i>
135	<i>Arctic methane (CH₄) balance</i>
136	<i>Northern Eurasian carbon monoxide (CO)</i>
137	<i>Northern Eurasian Ozone (O₃)</i>
138	<i>Sources and properties of atmospheric aerosols in boreal and Arctic environments</i>
139	<i>Black carbon and dust in the atmosphere and snow</i>
140	<i>Methodological and model developments related to atmospheric chemistry and physics</i>
141	2.2.2 Urban air quality and megacities (Q5)
142	<i>Air quality in China – recent observations</i>
143	2.2.3 Weather and atmospheric circulation (Q6)
144	<i>Cold and warm episodes</i>
145	<i>Cyclone density dynamics and atmosphere-ocean interaction</i>
146	<i>Circulation effect on temperature</i>
147	<i>Cloudiness in Arctic</i>
148	<i>Boundary layer dynamics and urban heat islands</i>
149	2.3 ARCTIC-BOREAL AQUATIC SYSTEM
150	2.3.1 Changing water systems, snow, sea ice and ocean sediments (Q7)
151	<i>Sea ice and thermodynamics with atmospheric and ocean dynamics</i>
152	<i>Snow depth/mass and sea ice thickness</i>

153	<i>Ocean floor and Sediments: composition and fluxes</i>
154	2.3.2 Marine ecology (Q8)
155	<i>Living marine organisms weaken or even subdue CO₂ accumulation</i>
156	<i>Organic carbon in lakes</i>
157	<i>Lake ice cover</i>
158	<i>Lake Baikal and Selenga River delta</i>
159	<i>Asian water lakes</i>
160	2.4 SOCIETY
161	2.4.1. Anthropogenic impact (Q10)
162	<i>Mitigation</i>
163	2.4.2 Environmental impact (Q11)
164	<i>Reindeer (Rangifer tarandus L.) grazing and ground vegetation structure and biomass</i>
165	2.4.3 Natural hazards (Q12)
166	<i>Naturally-determined diseases</i>
167	<i>UV variations</i>
168	3. SYNTHESIS AND FUTURE PROSPECTS
169	3.1 Future research needs from the system perspectives
170	3.2 Feedback mechanisms under changing climate, cryosphere conditions and urbanization
171	3.3 Climate scenarios for the Arctic-boreal region
172	ACKNOWLEDGEMENTS
173	REFERENCES
174	
175	

176

177 1. INTRODUCTION

178 Earth system is facing major challenges, including climate change, biodiversity loss, ocean acidification,
 179 epidemics and energy demand on a global scale (Ripple et al., 2017). These “Grand Challenges” are highly
 180 connected and interlinked. This creates a need for an approach of a multidisciplinary scientific program,
 181 which could deliver science-based messages to fast-tracked policy making (Kulmala et al., 2015). The recent
 182 estimates based on observed atmospheric concentrations of CO₂
 183 (ftp://aftp.cmdl.noaa.gov/products/trends/co2/co2_mm_mlo.txt) and business-as-usual scenario show that
 184 humankind should find solutions to answer the Grand Challenges (IPCC, 2021). Deep understanding of the
 185 feedbacks and interactions between the land, atmosphere and ocean domains, and accounting for social
 186 aspects in the regions of substantial changes, are needed for effective technical solutions, mitigation and
 187 adaption policy actions. The northern regions (> 45°N), together with the arctic coastal zone and Siberian
 188 region in Russia, are among the most critical areas for the global climate (Smith 2011; Kulmala et al., 2015;
 189 Kasimov et al., 2015).

190

191 The idea of the Pan-Eurasian Experiment (PEEX) (www.atm.helsinki.fi/peex), originating from a group of
 192 Finnish and Russian scientists and research organizations in 2012, is a bottom-up research and capacity
 193 building program concentrating on the sustainable development of the Arctic-boreal regions of the Northern
 194 Eurasia under changing climate and socio-economic megatrends (Kulmala et al., 2015, Lappalainen et al.,
 195 2016). The program was laid on four interconnected parts, namely research agenda, research infrastructures,
 196 capacity building and societal impacts (Lappalainen et al., 2014; Kulmala et al., 2016a, Lappalainen et al.,
 197 2017, Kulmala 2018). In addition to a strong involvement of the Russian partners, the PEEX China
 198 collaboration was established in 2013. China has a strong economic interest ~~on~~in Arctic regions (Tillman et
 199 al. 2018). Furthermore, China is already facing extensive environmental and air pollution challenges and has
 200 a major ~~interest to find~~interests toward finding technical solutions for environmental monitoring of the Silk
 201 Road Economic Belt Program (SREB) initiated by the President XI Jinping in 2013 (Kulmala 2018,
 202 Lappalainen et al., 2018, Dave and Kobayashi, 2018). ~~In Russia the~~The PEEX program is an umbrella for
 203 several bilateral scientific projects and activities ~~in Russia~~ (e.g. Chalov et al., 2015, 2018; Esau et al., 2016;
 204 Alekseychik et al., 2017; Bobylev et al., 2018; Malkhazova et al., 2018; Kukkonen et al., 2020; Ezhova et
 205 al., 2018b; Ziltinkevich et al., 2019; Petäjä et al., 2020 submitted; ; Bondur et al, 2019 a,b,c,d,e,f; Yuanhui
 206 He et al, 2020), ~~while~~whereas in China the primary focus is on the development of atmospheric in-situ
 207 stations and advanced air quality monitoring in megacity environments (e.g. Ding et al., 2016 b; Yao et al.,
 208 2018; Ying et al., 2020; Wang et al., 2020). Furthermore, PEEX is closely collaborating with the Digital Belt
 209 and Road (DBAR) Program coordinated by the Institute for Digital Earth and Remote Sensing (RADI). The
 210 PEEX collaboration with DBAR is driven by a need for a novel in-situ station network and ground-based
 211 data as a complementary information for the remote sensing in the Silk Road economic region. Long-term

development ~~of~~ a “Station Measuring the Earth Surface and Atmosphere Relations” (SMEAR) concept could provide baselines for this (Hari et al. 2016; Kulmala 2015, Kulmala 2018; Lappalainen et al., 2018).

The PEEEX program is motivated by the need for obtaining scientific information that combines research in the Arctic and boreal environments, and for understanding large-scale feedbacks and interactions operating in land-atmosphere-ocean systems (Kulmala et al., 2004; Kulmala et al., 2016a; Vihma et al., 2019) and large-scale weather impacts related to the Arctic amplification (e.g. Coumou et al., 2014; Vihma et al., 2020). One of the scientific backbones of PEEEX is the previously coordinated research frameworks and their synthesis. For example, the latest comprehensive overview on the interactions between the atmosphere, cryosphere and ecosystems at northern high latitudes was performed by the Nordic Center of Excellence in “Cryosphere-atmosphere interactions in a changing Arctic climate“, CRAICC) community (Boy et al., 2019). The PEEEX program can upscale the CRAICC results into a wider geographical context.

Climate change, as a main driver ~~for~~ environmental changes in the Northern Eurasian Arctic-boreal region and China, sets environmental boundaries for the future socio-economic activities of these regions in general. The harsh climate of this region puts a pressure on the ecosystems and living conditions of the local people (e.g. IPCC, 2019). PEEEX introduced fifteen large-scale research questions, which would ~~also~~ help us to fill the key gaps in our holistic understanding of land-atmosphere interactions and their connections to societies living in the northern Eurasian region (Kulmala et al., 2015; Lappalainen et al., 2018). This approach also sets the framework of the current paper. Here we introduce the recent research progress in the large-scale scientific themes relevant to the PEEEX region. The PEEEX study region consists of the Northern Eurasian Arctic and boreal (taiga) environments, thus the major geographical part of the environments is located in the Russian territory. China was added to the study area in 2013 as it was seen as locally and globally consequential region for climate change, air quality and long-term transport of atmospheric pollutants (Kulmala et al., 2015 a,b; Lappalainen et al., 2016, 2018).

Here we introduce the scientific results from PEEEX scientific output, review the main results from PEEEX scientific papers and present an analysis of the key gaps in the current scientific understanding. We use the PEEEX research agenda structure (Kulmala et al. 2016, Lappalainen et al. 2018) as a reference and mirror new ~~a~~ rising themes and results against this plan. For the literature material, we used the following sources for demonstrating the results: (i) individual ~~input~~ ~~inputs~~ sent by the PEEEX research community, (ii) ~~content~~ ~~contents~~ of the scientific papers published in Atmospheric Chemistry and Physics (ACP) PEEEX special issue in 2016-2019 (www.atmos-chem-phys.net/special_issue395.html) and (iii) scientific ~~output~~ ~~outputs~~ from PEEEX-labeled projects (www.atm.helsinki.fi/peex/index.php/projects) and other relevant results reported by the PEEEX partners. For the individual input, we asked the PEEEX research community to identify the main published papers in peer reviewed journals for each question out of their own work and ~~to~~ connect the work ~~to~~ ~~with~~ one of the 15 science questions introduced in the PEEEX science plan. Based on the abstracts we listed “addressed research themes” over last 5 years per PEEEX key topical areas (Table 1),

249 which we review in more detail in section 2. The results are first discussed with a holistic approach and then
 250 we categorize the advances through a set of identified feedbacks and interactions within the Arctic boreal
 251 environment. We follow up with a discussion on the need for a future research infrastructure to be able to
 252 provide relevant data and underline the future socio-economics development of the region setting the
 253 boundaries for proposed new science-based concepts and technical solutions.

254 2. RESULTS

255 In the PEEEX Science Plan, we indicated four main thematic research domains: the land system, the
 256 atmospheric system, the water system and the society with 15 thematic research areas and related large-scale
 257 research questions (Q) presented in Table 1 (Lappalainen et al., 2015), also indicated in the structure of the
 258 “Table of Contents”. This is the framework we re-visited and utilized in the synthesis of new results of the
 259 PEEEX community brought together in this paper. Furthermore, we synthesized the results and discuss their
 260 contribution to the large - scale feedbacks and interactions in the Arctic context in the sections below.

261

262 2.1. LAND ECOSYSTEMS

263

264 2.1.1 Changing land ecosystem processes (Q1)

265

266 *High-latitude photosynthetic productivity*

267

268 High-latitude terrestrial ecosystems are crucial to the global climate system and its regulation by vegetation.
 269 These ecosystems are typically temperature limited, and thus also considered especially sensitive to climate
 270 warming. Better understanding of an inter-annual and seasonal dynamics and resilience of the photosynthetic
 271 activity of forest vegetation as a whole is needed for the quantification of photosynthesis, or gross primary
 272 production (GPP), and for analyzing the carbon balance of the boreal forestforests. The carbon sink and
 273 source dynamics of the boreal forests have been intensively studied during the last five years at the SMEAR
 274 (Stations Measuring Atmosphere Ecosystem Relations) II station in Finland (Hari and Kulmala 2005; Hari et
 275 al., 2009). Recent results show that the Norway spruce and Scots pine ecosystems are rather resilient to a
 276 short-term weather variability (Matkala et al., 2020). Overall, the analyses by Kulmala et al. (2019) and
 277 Matkala et al. (2020) on subarctic Scots pine and Norway spruce stands at the northern timberline in Finland
 278 serve as examples of the canopy scale dynamics, showing that these ecosystems are generally weak carbon
 279 sinks but have a clear annual variation. Kulmala et al. (2019) observed that there is a difference between tree
 280 canopy photosynthesis compared to forest floor photosynthesis which starts to increase after the snowmelt.
 281 Thus, the models for photosynthesis should also address the snow cover period in order to better capture the
 282 seasonal dynamics of photosynthesis of the Northern forests (Kulmala et al., 2019).

283

284 The abundance of tree species, stand biomass, increasing tree growth and coverage of broadleaf species may
 285 also affect biogenic volatile organic compound (BVOC) emissions from the forest floor and impact the total

286 BVOC emissions from northern soils. At least the stand type has been shown to affect BVOCs fluxes from
287 the forest floor in a hemi boreal-boreal region (Mäki et al., 2019). As a whole, BVOCs emitted by boreal
288 evergreen trees are connected to the photosynthetic activity with a strong seasonality and have a crucial role
289 in atmospheric aerosol formation processes over the boreal forest zone. BVOC emissions have low rates
290 during photosynthetically inactive winter and increasing rates towards summer (Aalto et al., 2015). High
291 emission peaks caused by enhanced monoterpene synthesis were found in spring periods simultaneously with
292 the photosynthetic spring recovery (Aalto et al., 2015). This suggests that monoterpene emissions may have
293 a protective functional role for the foliage during the spring recovery state, and that these emission peaks
294 may contribute to atmospheric chemistry in the boreal forest in springtime. Vanhatalo et al. (2018) studied
295 the interplay between needle monoterpene synthase activities, its endogenous storage pools and needle
296 emissions in two consecutive years at a boreal forest in Finland. They found no direct correlation between
297 monoterpene emissions and enzyme activity or the storage pool size. Monoterpene- synthase activity of
298 needles was different depending on seasonality and needle ontogenesis. However, the pool of stored
299 monoterpenes did not change with the needle age (Vanhatalo et al., 2018). Also, clear annual patterns of
300 primary biological aerosol particles have been measured from a boreal forest, with late spring and autumn
301 being the seasons of a dominant occurrence. Increased levels of free amino acids and bacteria were observed
302 during the pollen season in the SMEAR II station in Finland, whereas the highest levels for fungi were
303 observed in autumn (Helin et al., 2017).

304
305 Extensive measurements of Scots pine photosynthesis and modelling resulted in optimized predictions of the
306 daily behavior and annual patterns of photosynthesis in a subarctic forest (Hari et al., 2017). The study
307 connected theoretically the fundamental concepts affecting photosynthesis with the main environmental
308 drivers (air temperature and light), and the theory gained strong support through empirical testing.
309 Understanding stomatal regulation is fundamental in predicting the impact of changing environmental
310 conditions on photosynthetic productivity. Lintunen et al. (2020) showed that the canopy conductance and
311 soil-to-leaf hydraulic conductance are strongly coupled, and that both soil temperature and soil water content
312 influence the canopy conductance through changes in the belowground hydraulic conductance. In particular,
313 the finding that the soil temperature strongly influences the belowground hydraulic conductance in mature,
314 boreal trees may help to better understand tree behavior and photosynthetic productivity in cold
315 environments. The plant photosynthetic rate is concurrently limited by stomatal and non-stomatal limitations,
316 and recent modelling (Hölttä et al., 2017) and empirical (Salmon et al., 2020) studies suggest that stomatal
317 and non-stomatal controls are coordinated to maximize leaf photosynthesis, i.e. non-stomatal limitations to
318 photosynthesis increase with a decreasing leaf water potential and/or increasing leaf sugar concentration.
319 This new approach allows including the effects of non-stomatal limitations in models of tree gas-exchange
320 (Fig. 1).

321
322 Due to climate warming, it seems that trees in high-latitudes have been progressively decreasing their
323 regional growth coherence in the last decades (Shestakova et al., 2019). Shestakova et al. (2019) showed

324 results that unequivocally linked a substantial decrease in the temporal coherence of forest productivity in
325 boreal ecosystems to a less temperature-limited growth that is concurrent with regional warming trends. This
326 emerging pattern points, for example, to an increasing dependence of the carbon balance on local drivers
327 and the role of forests as carbon sinks in the northern Ural region.

328

329 Vegetation gross primary production (GPP) is the largest CO₂ flux of the carbon cycle in terrestrial
330 ecosystems and impacts all of the carbon cycle variables (Beer et al., 2010). Ecosystem models usually
331 overestimate GPP under drought and during spring, late fall and winter (Ma et al., 2015). Several new
332 methodological improvements for a better quantification and scaling of GPP have been reported (Zhang et
333 al., 2018; Pulliainen et al., 2017; Kooijmans et al., 2019). The GPP, measuring photosynthesis, is crucially
334 important for the global carbon cycle and its accurate estimation is essential for ecosystem monitoring and
335 simulation. Pulliainen et al. (2017) introduced a new proxy indicator for spring recovery from *in situ* flux
336 data on CO₂ exchange. This made it possible to quantify the relation between spring recovery and carbon
337 uptake, and to assess changes in the springtime carbon exchange, demonstrating a major increase in the CO₂
338 sink. Zhang et al. (2018) introduced a new water-stress factor that effectively mitigates the overestimation of
339 GPP under drought conditions, while Bai et al. (2018 a,b) developed a method for quantifying the
340 evapotranspiration of crops by using a remote sensing-based two-leaf canopy conductance model. These
341 methods can provide novel insights into the quantification of GPP under different conditions and, in general,
342 into the impacts of biosphere-atmosphere relations on a larger scale.

343

344 Methods for satellite-based remote sensing of photosynthesis have been developed recently based on solar-
345 induced chlorophyll fluorescence signal, such as the OCO-2 product that has an improved spatial resolution,
346 data acquisition and retrieval precision, as compared with earlier satellite missions with solar-induced
347 chlorophyll fluorescence (SIF) capability, which allows for validation of the data directly against ground and
348 airborne measurements (Sun et al., 2017). Interpretation of the solar-induced chlorophyll fluorescence signal
349 has also been improved by many *in situ* studies. For example, Liu et al. (2019a, 2019b) simulated SIF in
350 realistic 3D birch stand reconstructed from terrestrial laser scanning data and found a large contribution of
351 the understory layer to the remote sensing signal.

352

353 *Vegetation changes*

354

355 The normalized difference vegetation index (NDVI) is used for detecting large-scale changes in vegetation
356 productivity. In the past decades, these changes include an increasing NDVI, called “greening”, taking place
357 in the tundra regions and a decreasing NDVI, called “browning”, in the Northern forest regions (Miles and
358 Esau, 2016). A deeper analysis behind these changes are needed. For example, in Northern West Siberia only
359 18% of the total area had statistically significant changes in productivity either towards greening or
360 browning, and having these opposite trends for different species within the same bioclimatic zone. The
361 observed complexity of the patterns and trends in the vegetation productivity underlines the need for new

362 studies on how forest types and different species are responding to climate and environmental changes in the
363 Northern environments (Miles and Esau, 2016). Also understanding the variations in small-scale plant
364 communities, seasonality and biogeochemical properties are needed for modeling the functioning of the
365 arctic tundra in global carbon cycling. Also the rapid development of the leaf area index (LAI, leaf area per
366 ground area, $m^2 m^{-2}$) during the short growing season and the yearly climatic variation address the
367 importance of optimal timing of the satellite data images when it is compared with the field verification data
368 in the Arctic region (Juutinen et al., 2017).

369
370 Bondur and Vorobyev (2015) analyzed the vegetation indices and complex spectral transformations derived
371 from processed long-term satellite data (1973-2013) for areas around the cities of Arkhangelsk and
372 Zapolyarny (Murmansk oblast). They demonstrated that these areas are subject to a peak anthropogenic
373 impact associated with specific industrial facilities, leading to changes in landscapes and depletion of natural
374 ecosystems, consequently leading to the decline in the quality of life and health conditions (Bondur and
375 Vorobyev, 2015). Region-wide changes in the vegetation cover and changes in and around several urbanized
376 areas in Siberia reveal robust indications of an accelerated greening near the older urban areas. Many
377 Siberian cities have turned greener while their surroundings have been dominated by wider browning. The
378 observed urban greening could be associated not only with a special tending of within-city green areas but
379 also with urban heat islands and succession of more productive shrub and tree species growing on warmer
380 sandy soils (Koronatova and Milyaeva 2011, Sizov and Lobotrosova 2016). Tundra and forest-tundra biomes
381 are sensitive to mean summer temperatures, which increases production and greening. Taiga biomes are
382 sensitive to precipitation and soil moisture with increased production in wet summer (Miles et al., 2019).

383
384 *New methodologies determining Earth surface characteristics*

385
386 Earth surface characteristics are fundamental knowledge to the understanding and quantification land-
387 atmosphere processes. The methods for determining Earth surface characteristics from satellites are
388 improving. As an example, a method for recognition of the Earth surface types according to space images
389 using an object-oriented classification was developed. The classification relies on Markov stochastic
390 segmentation for object extraction and supervised classification of the objects (Gurchenkov et al., 2017).
391 Furthermore, a prototype algorithm for hemispheric scale detection of autumn soil freezing using space-
392 borne L-band passive microwave observations was developed (Rautiainen et al., 2016) and is currently an
393 operative soil freeze and thaw product that delivers freely available data (<ftp://litdb.fmi.fi/outgoing/SMOS-FTService/>). The CryoGrid 3 land surface model provides improved descriptions of possible pathways of ice-
394 wedge polygon evolution and describes better the complex processes affecting ice-rich permafrost
395 landscapes (Nitzbon et al., 2019). In addition, there are new observations for validating satellite observations
396 and permafrost models. Boike et al. (2016) introduced a new, 16-year permafrost and meteorology data set
397 from the Samoylov Island Arctic research site, north-eastern Siberia. Terentieva et al. (2016) introduced

399 maps used as a baseline for validation of coarse-resolution land cover products and wetland data sets at high
 400 latitudes. Other examples of available data for the model validation are “BC emissions from agricultural
 401 burns and grass fires in Siberia” by Konovalov et al. (2018) and permafrost records at the Lena River delta”
 402 by Boike et al. (2016).

403
 404 Tundra ecosystems are under pressure and intensifying permafrost thawing, plant growth and ecosystem
 405 carbon exchange under the changing climate. The heterogeneity of Arctic landscapes is an extra challenge
 406 for environmental monitoring. For example, remote sensing methods are not able to capture variations in
 407 moss biomass, which is dominating the plant biomass and controlling soil properties in the Arctic. The
 408 general accuracy of landscape level predictions in the land cover type (LCT) is good, but the spatial
 409 extrapolation of the vegetation and soil properties relevant for the regional ecosystem and global climate
 410 models still needs to be improved (Mikola et al., 2018). Furthermore, for the future, we need to have a land
 411 characterization, in order to perform quantification and assessment of the ecosystem services at different
 412 scales using integrative techniques and integrated field observations together with remote sensing and
 413 modelling at the landscape scale (Burkhard et al., 2009, Fu and Forsius, 2015). At smaller scales, the isotopic
 414 composition of carbon and oxygen in peat can be used for the climate reconstruction (Granath et al., 2018).

415
 416 2.1.2 Thawing permafrost (Q2)

417
 418 *Observations of ground temperature evolution*

419
 420 Permafrost regions of the Northern Eurasia are warming along with the climate (IPCC, 2019). During the
 421 Global Terrestrial Network for Permafrost reference decade, 2007 - 2016, the temperature at the depth of
 422 zero annual amplitude increased by 0.39 ± 0.15 °C in the continuous permafrost zone and by 0.20 ± 0.10 °C
 423 in the discontinuous permafrost zone. At the same time, the mountain permafrost warmed by 0.19 ± 0.05 °C.
 424 The global average of the permafrost temperature increased by 0.29 ± 0.12 °C (Biskaborn et al., 2019). The
 425 observed trend in the continuous permafrost zone follows the air temperature trend in the Northern
 426 Hemisphere.

427
 428 The changes in the permafrost region affect climate, hydrology and ecology from local to global scales
 429 (Arnet et al., 2010; Hinzman et al., 2005). Several local studies focused on differences introduced by
 430 vegetation, soil and hydrological characteristics at the same site (Göckede et al., 2017, 2019). Göckede et al.
 431 (2017, 2019) presented findings on shifts in energy fluxes from paired ecosystem observations in northeast
 432 Siberia comprising a drained and a corresponding control site. Drainage disturbance triggered a suite of
 433 secondary shifts in ecosystem properties, including alterations in vegetation community structure, which in
 434 turn influenced changes in snow cover dynamics and surface energy budget. First, the drainage reduced heat
 435 transfer into deeper soil layers, which may have led to shallower thaw depths. Second, the vegetation change
 436 due to the drainage led to an albedo increase, which decreased the total energy income, or net radiation, into

437 the system. Third, the drainage reduced water content available for evapotranspiration, which resulted in a
 438 reduced latent heat flux and increased sensible heat flux, transferring more energy back to the atmosphere.
 439 The reported affects led to surface and permafrost cooling (Göckede et al., 2019).

440
 441 Kukkonen et al. (2020) compared temperature data from several shallow boreholes in the Nadym region,
 442 Siberia, and predicted permafrost evolution for different climate scenarios. The Nadym area represents a
 443 typical site located in the discontinuous permafrost zone. Kukkonen et al. (2020) found that the permafrost
 444 thawed most rapidly in low-porosity soils, whereas high-porosity soils in the top layer (e.g., peatland)
 445 retarded thawing considerably. Similarly, the depth of a seasonally frozen layer and the temperature regime
 446 of peat soils in the oligotrophic bog in the southern taiga zone of Western Siberia showed significant
 447 differences between the sites with high and low levels of bog waters (Kiselev et al., 2019). Both Kukkonen et
 448 al. (2020) and Kiselev et al. (2019) results are in line with previous conclusions on the importance of
 449 volumetric water content and unfrozen water content for soil thermal properties governing heat transfer and
 450 phase change processes (Romanovsky and Osterkamp, 2000). Locally, the sites with a thin snow cover (e.g.,
 451 hill tops) demonstrated a higher resistance to the thawing (Williams and Smith, 1989; Kukkonen et al.,
 452 2020). To follow-up on the development of permafrost thaw in different soil types require continuous and
 453 comprehensive observations during the coming decades.

454
 455 *Changing GHG fluxes and VOCs due to permafrost thaw*

456
 457 Biogenic GHG emissions are strongly connected with permafrost conditions and changes in other related
 458 environmental conditions, such as soil temperature and moisture conditions. Here we discuss recent results
 459 on the observed emissions from these permafrost perspectives and, later in section 2.2.1, address the
 460 connections between GHG fluxes and the other environmental factors, like deforestation and forest fires.

461
 462 During the permafrost thaw, even small changes in the soil carbon cycle can turn a terrestrial ecosystem from
 463 a sink into a source (Schuur et al., 2008). Based on regional *in situ* observations of CO₂ fluxes, Natali et al.
 464 (2019) estimated a winter-time carbon loss of 1 662 TgC per year, which is more than predicted by the
 465 process models estimates. Furthermore, Natali et al. (2019) found that even if the soil CO₂ loss were
 466 enhanced due to winter warming, the growing season might start earlier and onset the carbon uptake under
 467 warming climate conditions. For a better understanding of these connections and both spatial and temporal
 468 dynamics of the Arctic carbon cycle, we need more observations from permafrost ecosystems. Additional
 469 flux measurements are urgently needed to understand the variation between the current measurements and,
 470 especially extended measurements on the CH₄ emissions to better quantify their role in the carbon balance.
 471 For example, a new data assimilation system estimates an Arctic carbon sink of -67 g C m⁻² yr⁻¹, but this
 472 value is associated with very high uncertainties. Furthermore, these estimates do not include methane, which
 473 is even more difficult to evaluate (López-Blanco et al., 2019). Based on the field flux measurements, the
 474 Carbon Cycle Report 2018 (Schuur et al., 2018) estimated that the Eurasian boreal wetland is a source of 14

475 Tg CH₄ per year. On the other hand, Kirschke et al. (2013) estimations, based on atmospheric
476 measurements, ended up to the value of 9 Tg CH₄ per year. Locally, methane fluxes measured in 2005-2013
477 showed significant year-to-year variations. Interestingly, the observed variability in North America,
478 specifically in the Hudson Bay lowlands, appears to have been driven partly by the soil temperature, while in
479 the Western Siberian lowlands the variability was dependent on the soil moisture (Thompson et al., 2017).
480 The comparison of high-resolution modelling of atmospheric CH₄ to CH₄ observations already in 2012 from
481 the East Siberian Arctic Shelf (ESAS), a potentially large CH₄ source, confirms that methane releases are
482 highly variable and inhomogeneous (Berchet et al., 2016).

483
484 Long-term flux measurements provide insight into the carbon sink - source dynamics. The flux
485 measurements from the moist tussock tundra in the north-eastern Siberia indicated that drainage influences
486 the carbon cycle and that the tundra is changing to a weaker CO₂ sink and CH₄ source. Another relevant
487 observation was that the time outside the growing season influences the carbon balance of ecosystem
488 processes, especially during the zero-curtain period (Kittler et al. 2017). This is in line with similar studies in
489 Alaska (Commane et al., 2017; Euskirchen et al., 2017). Therefore, the autumn temperature was identified as
490 a major driving factor describing the differences between the annual GHG fluxes. Notably, however, the
491 seasonal amplitudes of CO₂ concentrations in Siberia were found to be significantly higher than those in the
492 North American continent, likely due to the more intense biological activity here (Timokhina et al., 2015a).
493 A recent study showed that the Siberian carbon cycle is a major contributor to the Northern Hemisphere
494 amplitude of CO₂ variation (Lin et al., 2020).

495
496 Observations from non-permafrost sites may give us a clue on the future dynamics of fluxes, as the
497 permafrost is thawing. The chamber measurements of CH₄ and CO₂ fluxes from a non-permafrost site in the
498 Siberian peatland in August, 2015, showed that the highest values of methane fluxes were obtained in burnt
499 wet birch forest and the lowest ones in seasonally waterlogged forests (Glagolev et al., 2018). The fluxes can
500 vary even between different sites of a bog, as measured by Dyukarev et al. (2019). The net ecosystem
501 exchange (NEE), ecosystem respiration (ER) and gross primary production (GPP), based on the measured
502 CO₂ fluxes at a ridge-hollow complex bog and a model for ridge and hollow sites at oligotrophic bog in
503 Middle Taiga Zone of West Siberia, showed that a two-year-average NEE at the hollow site was 1.7 times
504 higher than at the ridge site (Dyukarev et al., 2019). The ecosystem processes are influenced by drying in
505 tundra ecosystems. Kwon et al. (2019) reported from Alaska that drying in the tundra ecosystems increased
506 contributions of modern soil carbon to the ecosystem respiration but, at the same time, decreased
507 contributions of old soil carbon. These changes were attributed mainly to modified soil temperatures at
508 different soil layers due to the altered thermal properties of organic soils following drainage. Furthermore,
509 the drainage lowered CH₄ fluxes by a factor of 20 during the growing season, with post drainage changes in
510 microbial communities, soil temperatures, and plant communities also affecting the flux reduction in an
511 Arctic wetland ecosystem (Kwon et al., 2017).

512

513 Voigt et al. (2016) reported that, under warming conditions, the vegetated tundra in north-eastern European
 514 Russia shifted from a GHG sink to a source. The positive warming response was dominated by CO₂;
 515 however, N₂O emissions were also significant. N₂O was emitted not only from bare peat, already identified
 516 as a strong source, but also from vast vegetated peat areas not emitting N₂O under current climate conditions.
 517 These results can be explained by the dynamics between the temperature, nitrogen assimilation by plants and
 518 soil microbial activity, having a strong impact on the future GHG balance in Arctic (Voigt et al., 2016; Gil et
 519 al., 2017). Studying N₂O emissions from a typical permafrost peatland in Finnish Lapland, it was concluded
 520 that about 25% of the Arctic territory are areas that potentially emit nitrous oxide (Voigt et al., 2017). It
 521 seems that there is positive feedback mechanism between the permafrost thawing and moisture regime.
 522 Predicting the response of soils to climate change or land use is central to understanding and managing N₂O
 523 emissions. According to recent results, the N₂O flux can be predicted by models that incorporate soil nitrate
 524 concentration (NO₃⁻), water content and temperature (Pärn et al., 2018).

525
 526 In addition to CO₂ and CH₄, thawing or collapsing of arctic permafrost can release volatile organic
 527 compounds (VOCs). Li et al. (2020a) examined the release of VOCs from thawing permafrost peatland soils
 528 sampled from Finnish Lapland in laboratory. The average VOC fluxes were four times as high as those from
 529 the active layer, and mainly attributed to direct release of old, trapped gases from the permafrost. These
 530 results demonstrate a potential for substantive VOC releases from thawing permafrost and suggests that
 531 future global warming could stimulate VOC emissions from the Arctic permafrost.

533 2.1.3 Ecosystem structural change (Q3)

535 *Changes in microbial activity*

536
 537 Climate change is likely to cause an increased appearance of trees on open peatlands, but we do not know
 538 how this vegetation change will influence the below-ground microbiology and composition. Changes along
 539 bog ecotones at three Russian peatland complexes suggest that tree encroachment may reduce the trophic
 540 level of *Testate Amoeba* communities and reduce the contribution of mixotrophic *Testate Amoebae* to
 541 primary production. Thus, it seems that increased tree recruitment on open peatlands will have important
 542 consequences for both microbial biodiversity and microbial-mediated ecosystem processes (Payne et al.,
 543 2016). We also need to understand better the dynamics affecting the bacteria, fungi and other related species
 544 in the ground air layer. Recent studies by Korneykova and Evdokimova (2018) and Korneikova et al. (2018
 545 a, 2018b) showed the influences of anthropogenic sources (Copper-Nickel Plant) and acidic soils in Russian
 546 northern taiga and tundra on the portion of the airborne fungi, and on the structure of algological and
 547 mycological complexes (Korneikova et al., 2018 a, 2018b). New methods were reported on how to improve
 548 soil conditions, developed on all kinds of materials made or exposed by human activity that otherwise would
 549 not occur at the Earth's surface, referred as "Techno sol engineering" (Slukovskaya et al., 2019), and how to

550 monitor climate change impacts on the functional state of bogs by using *Sphagnum* mosses (Preis et al.,
551 2018).

552

553 *Effects of forest fires on soils*

554

555 Forest fires, a significant environmental factor in the Northern Eurasian region, change soil chemical and
556 physical properties and may influence greenhouse gas fluxes and emissions of BVOCs. Recent results
557 indicate that a slower post-fire litter decomposition has a clear impact on the recovery of soil organic matter
558 following forest fires in northern boreal coniferous forests due to accumulated soil organic matter. The soil
559 recovery is related to slow litter composition and reduced enzymatic and microbial activity (Köster et al.,
560 2016).

561

562 Post-fire studies on the long-term evolution of the structure and functioning of bacterial communities are
563 sparse. Sun et al. (2016) showed that the major drivers influencing bacterial community are the soil
564 temperature, pH and moisture. Furthermore, Köster et al. (2015) analyzed long-term effects of fire on soil
565 CO₂, CH₄ and N₂O fluxes in pine forest stands in the Finnish Lapland, and discussed the role of microbial
566 bio mass in this context. They did not detect significant effects of fires on CO₂ emissions or N₂O fluxes, but
567 there were long-lasting strengthening of the CH₄ sink by the soil. Interestingly, Köster et al. (2018) did not
568 find a similar kind of long-term effect on the CH₄ sink dynamics in studies carried out in Siberia.

569

570 Forest wildfires also regulate the BVOC emissions from boreal forest floors by changing the ground
571 vegetation. Total BVOC emissions from a forest floor were found to decrease after a forest fire and then to
572 increase again along with the succession of forests (Zhang-Turpeinen et al., 2020). For a comparison, Bai et
573 al. (2017) showed that biomass burning resulted in increased BVOC emission fluxes and ozone
574 concentration above canopy in a subtropical forest in China.

575

576 2.2. ATMOSPHERIC SYSTEM

577

578 Concerning critical atmospheric processes and large-scale climate implications, we concentrate here on
579 greenhouse gases and aerosol particles over Northern Eurasia and Arctic, urban air quality, and issues related
580 to the weather and atmospheric circulation. We summarize the recent measurements on the atmospheric
581 composition relevant to sink and source dynamics in Siberia, on the sources and properties of atmospheric
582 aerosols in Arctic-boreal environments, including black carbon and dust in the atmosphere and snow, and on
583 the methodological and model developments related to atmospheric chemistry and physics (Q4, section
584 2.2.1). Furthermore, we introduce new results and observations on atmospheric pollution in rural, suburban
585 and mega city environments in China and Russia (Q5, section 2.2.2). We briefly show some recent results
586 related to synoptic-scale weather in Arctic-boreal regions, focusing on cold and warm episodes, cyclone

587 density and atmosphere–ocean interaction, effects of circulation on temperature and moisture, cloudiness in
 588 the Arctic, and boundary layer dynamics (Q6, section 2.2.3).

589

590 2.2.1 Atmospheric composition and chemistry (Q4)

591

592 *Boreal forests carbon balance*

593

594 As already discussed in section 2.1.1, boreal forests as a carbon sink and the related role of forestation have
 595 been under international debate. It seems that early snowmelt increases springtime carbon uptake of the
 596 boreal forests of Eurasia and North America and shows a major advance in the CO₂ sink (Pulliainen et al.,
 597 2017). A scenario of a complete global deforestation by Scott et al. (2018), combining radiative forcing to
 598 CO₂, surface albedo and short-lived climate forcers (SLCFs), suggests that global deforestation could cause a
 599 0.8 K warming after 100 years, with SLCFs contributing 8% of the effect. However, deforestation as
 600 projected by the RCP8.5 scenario leads to zero net radiative forcing from SLCF, primarily due to
 601 nonlinearities in the aerosol indirect effect. Tuovinen et al. (2019) showed that methane fluxes vary strongly
 602 with a wind direction in a tundra ecosystem ~~with~~having heterogeneous vegetation. By combining very high-
 603 spatial-resolution satellite imagery and footprint modelling, they were able to estimate the relation between
 604 the main land cover types and ecosystem-level measurements. CH₄ emissions originated mainly from wet fen
 605 and graminoid tundra patches, whereas the areas of bare soil and lichen acted as strong CH₄ sinks (Tuovinen
 606 et al. 2019. Tsuruta et al. (2017) reported posterior mean global total emissions of 516±51 Tg CH₄ yr⁻¹ during
 607 2000–2012, which indicates that these emissions had increased by 18 Tg CH₄ yr⁻¹ from the period 2001–2006
 608 to the period 2007–2012. This increase can be ~~explain~~explained by increased emissions from the temperate
 609 region in South America and from the temperate region and tropics in Asia.

610

611 Analysis of the trends and the diurnal, weekly and seasonal cycles of CO₂ and CH₄ mixing ratios derived
 612 from the long-term data of the “Japan–Russia Siberian Tall Tower Inland Observation Network” showed that
 613 the frequency of identified events of elevated concentration differs for CO₂ and CH₄ and may reach up to
 614 20% of days in some months (Belikov et al., 2019). These observations made it possible to reduce
 615 uncertainties in the biosphere surface CO₂ uptake (Kim et al., 2017). Although the CO₂ uptake in boreal
 616 Eurasia estimated by Kim et al. (2017) was about 30% lower than that obtained without the assimilation of
 617 Siberian observation data, Siberia still remains a key contributor to the terrestrial CO₂ sink in the Northern
 618 Hemisphere.

619

620 There are tendencies of a significant growth or suppression of soil CO₂ fluxes across different types of
 621 human impacts, such as forest fires, trampling, settlements, reindeer grazing and clearcuts on cryogenic
 622 ecosystems in Russia (Karelin et al., 2017). For example, Ivanhov et al. (2019) analyzed CO₂ measurements
 623 during 2010–2017 and reported CO₂ concentration increases of 20 ppm in Tiksi at a coast of Laptev Sea and
 624 of 15 ppm at the Cape Baranov station. They also detected that wildfires in Siberia can lead to a parallel

625 increase of the CO₂ concentration at the Russian Arctic. Furthermore, the measurements showed that the
 626 atmospheric CO₂ concentration increased on average by 2.0 ppm yr⁻¹ during 2006-2013 in central Siberia,
 627 with a large inter-annual variations. The highest increase were found in 2010 and 2012 (3.6 and 4.3 ppm yr⁻¹
 628 ¹, respectively), when large wildfires released huge amounts of CO₂ in Siberia (Timokhina et al., 2015b).
 629 Repeated wildfires in boreal forests can combust a portion of the thick organic soil layer characteristic for
 630 this ecosystem, and change the forests from a carbon sink into a carbon source (Walker et al., 2019). A study
 631 on a fire chronosequence of the central Siberian permafrost soil showed that soils affected by fires over
 632 decades act as CO₂ sources, and that the CO₂ emissions from these soils increased with an increasing time
 633 since the last fire (Köster et al., 2018). However, there were no similar effects on CH₄ emissions, with soils
 634 acting as a CH₄ sink without any connection to forest fires. In addition to CO₂, wildfires also release large
 635 amounts of other trace gases and aerosols. Emission factors of several trace gases and aerosols from Siberian
 636 fires measured from the Trans-Siberian railway were reported by Vasileva et al. (2017). The impact of
 637 Siberian fires as elevated aerosol concentrations was at times observed to extend up on the Arctic coast
 638 (Asmi et al., 2016).

639

640 *Arctic methane (CH₄) balance*

641 Deep understanding on the dynamics of methane emissions in the Arctic is needed for identifying and
 642 quantifying GHG-related feedbacks and global methane cycle (Dean et al., 2018). ~~The main source of~~ During
 643 ~~the winter,~~ methane ~~in Arctic during winter is originates mostly from~~ anthropogenic ~~sources,~~ while on a
 644 smaller ~~scale,~~ scales also emissions from ~~the~~ oceans, including the Eastern Siberian Arctic Shelf (ESAS), can
 645 play an important role. During the warm season, the balance is dominated by emissions from wetlands and
 646 freshwater bodies. Thonat et al. (2017) employed the CHIMERE model for an assessment of the methane
 647 cycle in Arctic. They reported that all methane sources, except biomass burning, contributed to
 648 measurements at six study sites. That study emphasizes the importance of a joint model-measurements
 649 approach for studies of complex phenomena at large spatial scales. Accounting for OH oxidation and soil
 650 uptake, two important sinks of methane, improved the agreement between observed and modelled methane
 651 concentrations (Thonat et al., 2017). Peltola et al. (2019) up-scaled CH₄ fluxes measured at 25 northern
 652 wetland sites and showed three different maps of wetland distribution with the annual methane emissions
 653 varying from 31 to 38 Tg(CH₄) yr⁻¹. (For the monthly up scaled CH₄ flux data products see
 654 doi.org/10.5281/zenodo.2560163). Multiple sources, together with different spatiotemporal dynamics and
 655 magnitudes, are influencing the total Arctic CH₄ budget and addresses the need for the further improved
 656 assessments (Peltola et al., 2019; Thonat et al., 2017).

657

658 *Northern Eurasian carbon monoxide (CO)*

659 Analysis of long-term trends in the atmospheric composition in remote Northern Eurasia (1998–2016)
 660 showed that the total column carbon monoxide (CO) amount has been stabilized or increased in summer and
 661 autumn months (Rakitin et al., 2018). The changes in the global photochemical system, especially changes in
 662 the ratio between the sources and sinks of minor atmospheric chemical species, could explain these trends

663 (Skorokhod et al., 2017). A comparative study (1998–2014) on the atmospheric total column CO amount in
 664 background and polluted regions of Eurasia indicated that this amount has decreased remarkably in the
 665 Moscow urban environments ($3.73\% \pm 0.39\%$ per year) compared to the background regions (0.9–1.7% per
 666 year) (Wang et al., 2018a).

667

668 *Northern Eurasian Ozone (O_3)*

669 Atmospheric measurements of ozone, its precursors and other pollutants over Siberia are important for the
 670 atmospheric chemistry modelling, satellite product validation and comparisons between Siberia and other
 671 regions of the Northern Hemisphere. Isoprene and monoterpenes together with nitrogen oxides impact
 672 tropospheric O_3 formation and lead to an increase in the daytime ozone-forming potential (OFP) in urban
 673 environments. Bai et al. (2021) showed that O_3 may respond either positively or negatively to isoprene and
 674 monoterpene emissions depending on the level of solar radiation and atmospheric loadings of trace gases and
 675 aerosol particles. It was demonstrated that monoterpenes have a major contribution to tropospheric O_3
 676 formation, especially in cities in Siberia having high atmospheric NO_x concentration (10–20 ppb) and
 677 daytime temperatures ($>25\text{ }^\circ\text{C}$) (Berezina et al., 2019). In contrast, isoprene is dominating the O_3 formation
 678 and the increasing OFP in the cities in Far East. The isoprene-derived OFP can originate from deciduous
 679 vegetation growing in city environments or nearby regions, or from an anthropogenic isoprene source. The
 680 monoterpene-derived OFP was found to be the lowest in medium-size cities and the highest in small cities
 681 (Berezina et al., 2019). The total contribution of benzene and toluene to photochemical O_3 production was
 682 found to be up to 60–70% in urbanized environments, indicating anthropogenic pollutant sources
 683 (Skorokhod et al., 2017). In addition to atmospheric chemistry, the connection between [stratospheric](#) O_3 , UV
 684 radiation and health effects needs to be addressed in the populated urban environments of Siberia. Chubarova
 685 et al. (2019b) estimated that [winterthe wintertime](#) O_3 depletion in northern regions of Siberia is not critical,
 686 but [the much larger \$O_3\$ reductionreductions observed](#) in the early spring can lead to dangerous levels of
 687 erythema UV radiation (see also section 2.4.3 Natural Hazards and UV variation) .

688

689 *Sources and properties of atmospheric aerosols in boreal and Arctic environments*

690

691 Atmospheric new particle formation (NPF) is the largest contributor to the number concentration of aerosol
 692 particles in the global troposphere. During the past couple of decades, NPF has been measured in more than
 693 10 boreal forest sites (Kerminen et al., 2018). The annual frequency of NPF event days varies between about
 694 10 and 30% in the boreal forest zone, being the highest in the western part of this region and lowest in the
 695 northern edge and Siberian part of it. Similar high nucleation frequencies were found at two very remote
 696 sites in boreal North America (Andreae et al., 2019). In contrast, annual NPF event frequencies below 2%
 697 were reported from central Siberia (Wiedensohler et al., 2019). Similarly, in the northern Siberia on the
 698 Arctic coast, NPF events were mainly connected with marine and coastal air masses and rarely observed in
 699 continental air masses (Asmi et al., 2016). Seasonally, NPF tend to be most frequent during spring, even
 700 though high NPF event frequencies can also be observed during summer or autumn. Winter-time NPF is rare

701 throughout the boreal forest region. In the Arctic, NPF appears to be a major aerosol particle source from
702 spring to summer, after which this source collapses during autumn and is practically absent over the whole
703 winter (Freud et al., 2017). 20 years of NPF observations in a boreal forest at the SMEAR II station in
704 Finland show higher frequency of NPF events under clear-sky conditions in comparison to cloudy conditions
705 (Dada et al. 2017). Also oxidized organic vapors showed a higher concentration during the clear-sky NPF
706 event days, whereas the condensation sinks and some trace gases had higher concentrations during the
707 nonevent days.

708
709 The overall importance of atmospheric NPF in boreal and Arctic areas depends on the growth of freshly-
710 formed particles to cloud condensation nuclei. In the boreal forest environment, both observations and model
711 simulations indicate that the particle growth is tied strongly with the oxidation products of biogenic volatile
712 organic compounds originating from forest ecosystems (Paasonen et al., 2018; Östrom et al., 2017). The
713 important compound group in this respect are monoterpenes, even though also sesquiterpenes were found to
714 have high secondary organic aerosol yields in boreal forest environments (Hellén et al., 2018). The observed
715 particle growth rates were found to increase with an increasing particle size and to be highest in summer
716 (Paasonen et al., 2018). The chemistry of new particle growth in the Arctic atmosphere is not well
717 characterized, even though available observations suggest that this growth is associated mainly with biogenic
718 emissions from high-latitude marine areas (Giamarelou et al., 2016; Heintzenberg et al., 2017; Kecorius et
719 al., 2019).

720
721 Wildfires are an important source of particulate pollutants on a global scale and are affecting both air quality
722 and climate (Andreae, 2019; Bondur et al., 2020). Satellite observations indicate that the annual burned area
723 by wildfires in Russia decreased by a factor of 2.6 during 2005–2016 owing to early detection and
724 suppression of fire sources, whereas in Ukraine the relative size of burned-out areas increased by a factor of
725 6–9 from 2010–2013 to 2014–2016 (Bondur et al., 2017; 2019d). For Siberia, Ponomarev et al. (2016)
726 reported a strong ~~increase~~increases in both ~~in~~-number and burned areas based on satellite data, ~~1996–2015~~.
727 ~~Based on their data, the~~with burned areas ~~in Siberia doubled~~doubling from 2005 to 2016. While biomass
728 burning emissions have been measured widely over Russia (Bondur, 2016; Bondur and Ginzburg, 2016;
729 Bondur et al., 2019d), there is still a need for further information on the atmospheric composition of wildfire
730 emissions and related emission ratios from the Siberian region. Fire experiments provide important
731 information on the emission and aging characteristics of smoke aerosols (e.g. Kalogridis et al., 2018).

732
733 Luoma et al. (2019) presented a detailed trend analysis for aerosol optical properties at the SMEAR II station
734 in Finland. They found a statistically significantly decreasing trend for the scattering coefficient, and even a
735 stronger decreasing trend for the absorption coefficient during 2006 – 2017. These trends are very likely
736 indicative of decreasing influence of anthropogenic emissions, with the contribution from emissions
737 containing black carbon decreasing even faster.

738

739 Measurements of carbonaceous aerosols over central Siberia during 2010-2012 showed that in fall and
740 winter, high concentrations of such aerosols were caused by long-range transport from the cities located in
741 southern and southwestern regions of Siberia (Mikhailov et al., 2015a). In spring and summer, pollution
742 levels were high due to regional forest fires and agricultural burning in the Russian-Kazakh region. The
743 variability of the background concentration of organic aerosols correlated with the air temperature in
744 summer, implying that biogenic sources dominated the formation of organic particles at that time of the year
745 (Mikhailov et al., 2015b). Based on a five-year study by Mikhailov et al. (2017), it seems that the
746 atmospheric pollution originating from the biomass burning and anthropogenic emissions is
747 significantly affecting the Siberian region. However, in summer precipitation is removing the
748 pollutants from the air and leading to relatively clean atmospheric conditions in this region.

749
750 At circumpolar sites over the Arctic, aerosol optical properties were found to vary both seasonally and
751 spatially (Schmeisser et al., 2018). Arctic haze aerosols in late winter and spring are characterized by
752 increased concentrations of sulfate, whereas in summer rich organic chemistry seems to be associated with
753 vegetation, local urban and shipping sources as well as secondary aerosol formation influenced by emissions
754 from low latitude Siberia (Popovicheva et al., 2019a). In a longer perspective, Arctic observations show large
755 decreases in both sulfate and black carbon concentrations since the early 1980s (Breider et al., 2017).

756
757 Observations on the elemental composition of surface aerosols on the coastal Kandalaksha Bay of the White
758 Sea were indicative of the dominance of biogenic aerosol particles during summer time, with heavy metal
759 concentrations in aerosols being at Arctic background levels (Starodymova et al., 2016). Increases in Ni and
760 Cu concentrations were observed in air masses arriving from the western part of the Kola Peninsula
761 indicative of emissions from the smelters in that region.

762
763 *Black carbon and dust in the atmosphere and snow*

764
765 Black carbon (BC) is a potentially large contributor to climate forcing in the Arctic region, however, the
766 assessment of its pollution is hampered by the lack of aerosol studies in Northern Siberia (Popovicheva et al.,
767 2019). ~~Spatial~~The spatial variability of Arctic BC was studied using a harmonized dataset from ~~six~~
768 circumpolar Arctic observatories (Backman et al., 2017). These data suggested a significant spatial and
769 seasonal variability (Schmeisser et al., 2018), addressing a need for more year-round data. BC observations
770 (Sep 2014 – Sep 2016) at the Hydrometeorological Observatory Tiksi at a coast of the Laptev Sea showed a
771 seasonal variation, with the highest concentrations (up to 450 ng/m³) from January to March and the lowest
772 ones (about 20 ng/m³) in June and September. During winter, stagnant weather and stable atmospheric
773 stratification resulted in the accumulation of pollution, depending also on the wind direction and air mass
774 transport (Popovicheva et al., 2019a).

775

776 For Arctic, important sources of BC include industrial regions of Northern Europe, gas flares of the oil fields
777 in the North Sea and Siberia, and Siberian biomass burning (Shevchenko et al., 2015; Konovalov et al.,
778 2018). ~~For~~~~In 2012, for~~ ~~example~~ ~~in 2012~~, approximately a quarter of the biogenic BC emissions from Siberia
779 after fire season were transported into the Arctic (Konovalov et al., 2018). Popovicheva et al. (2017a)
780 analyzed the BC origins over the Russian Arctic seas together with simulated BC concentrations.
781 Concentrations were observed to be high (100-400 ng m⁻³) ~~in~~~~over~~ the Kara Strait, Kara Sea and Kola
782 Peninsula, and extremely high (about 1000 ng m⁻³) ~~in~~~~over~~ the White Sea. It seems that the gas-flaring
783 emissions from the Yamal-Khanty-Mansiysk and Nenets-Komi regions affected the measurements made
784 ~~in~~~~over~~ the Kara Strait (northerly 70 °N) region, while the Near Arkhangelsk (White Sea) region was
785 connected to the biomass burning in mid-latitudes. Combustion in Central and Eastern Europe were also
786 identified as important BC sources.

787
788 Atmospheric aging promotes an internal mixing of BC with other aerosol constituents, leading to enhanced
789 light absorption and radiative forcing. *In situ* observations at Arctic stations demonstrated an absorption
790 enhancement due to the internal mixing of BC, which is a systematic effect and should be considered for
791 quantifying the aerosol radiative forcing in this region (Zanatta et al., 2018).

792
793 Regional modelling of the Arctic aerosol pollution showed that long-range transported anthropogenic
794 emissions and biomass burning are the main contributors to direct aerosol radiative effects in the region
795 (Marelle et al., 2018). However, a scenario for 2050 indicates that shipping emissions in the Arctic Ocean
796 could become the main source of surface aerosol and local flaring as a major source of BC, as the flaring
797 already is a major source of BC in northwestern Russia. Kühn et al. (2020) assessed the effects of different
798 BC mitigation measures on Arctic climate and showed that reducing BC emissions by the Arctic Council
799 member states can reduce BC deposition by about 30 % compared to the current situation. A full execution
800 of recommendation by the Arctic Council member and observer countries could reduce the annual global
801 premature deaths due to PM by ~9 % by 2030 (Kühn et al. 2020). Evangelidou et al. (2018) estimated the
802 origin of elemental carbon (EC) in snow and showed that for western Siberia where gas flaring emissions is a
803 major contributor, the model underestimation was significant. Furthermore, the model was evaluated by
804 independent BC measurements in snow over the Arctic showed and, again, the model underestimated BC
805 concentrations, especially in spring.

806
807 Climatically significant cryosphere effects of light-absorbing, high-latitude dust can be similar to the albedo
808 and melt effects of BC (Peltoniemi et al., 2015; Svensson et al., 2016, 2018; Meinander et al. 2020a, 2020b).
809 Iceland is the most significant source for European Arctic dust and plays a role in the cryosphere-
810 atmosphere-biosphere interactions and feedbacks (Boy et al., 2019; Dragosics et al., 2016, Dagsson-
811 Waldhauserova and Meinander, 2019). Dust storms from technogenic mining industry tailing dumps on the
812 Kola Peninsula are also an important source of local atmospheric pollution for neighbor cities, e.g., Apatity

813 and Kirovsk (Amosov et al., 2020). Besides regional-scale dust storms from deserts in Kazakhstan, also
814 Mongolia and China are significant sources of aerosol pollution for these regions and for the Northern Asia.

815
816 *Methodological and model developments related to atmospheric chemistry and physics*

817
818 Several methods to characterize the atmospheric chemistry were introduced or improved. Motivated by the
819 ability of atmospheric ion measurements to identify new particle formation (NPF) events in the atmosphere
820 (Leino et al., 2016), a new classification method for atmospheric NPF was developed (Dada et al., 2018).
821 The new method uses both ion and aerosol particle number concentration measurements in the size ranges of
822 2-4 nm and 7-25 nm, respectively, is complementary to the traditional event analysis, and can also be used as
823 an automatic way of determining new particle formation events from large data sets. Zaidan et al. (2018b)
824 used a mutual information approach for a variety of simultaneously monitored ambient variables, including
825 trace gas and aerosol particle concentrations and several meteorological variables, in order to identify key
826 factors contributing to atmospheric NPF. This method can be used in the atmospheric studies also to discover
827 other interesting phenomena and relevant variables. The NPF is directly observed by monitoring the time
828 evolution of ambient aerosol particle size distributions. A new machine learning-based approach, a Bayesian
829 neural network (BNN) classifier, points out the potential of these methods and suggest further exploration in
830 this direction (Zaidan et al., 2018a).

831
832 The condensation sink, being proportional to the surface area of an aerosol population, is one of the major
833 parameters controlling NPF. A simple model for the time evolution of the condensation sink in the
834 atmosphere for intermediate Knudsen numbers was developed to describe the coupled dynamics of the
835 condensing vapor and the condensation sink (Ezhova et al., 2018a). The model gives reasonable predictions
836 of condensation sink dynamics during periods of particle growth by condensation in the atmosphere. A new
837 empirical relation between the atmospheric cloud condensation nuclei (CCN) concentration and aerosol
838 optical properties was derived (Shen et al., 2019), making it possible to estimate CCN concentrations at sites
839 with continuous observations of aerosol optical properties.

840
841 Empirical models of solar radiation were developed and used for calibrations of solar radiometers (Bai,
842 2019). This method can be used to calibrate all kinds of solar radiometers. A solar radiation model combined
843 with ceilometer and pyranometer measurements was used to classify clouds at SMEAR II (Ylivinkka et al.,
844 2020) It opens new possibilities for studies of aerosol-cloud interactions.

845
846 Che et al. (2016) made an inter-comparison of three satellite (AATSR Level 2) aerosol optical depth (AOD)
847 products (SU, ADV and ORAC) over China. The SU algorithm performs very well over sites with different
848 surface conditions in mainland China from March to October, but slightly underestimates AOD over barren
849 or sparsely vegetated surfaces in western China. The ADV product has the same precision and error
850 distribution as the SU product. The main limits of the ADV algorithm are underestimation and applicability.

851 The ORAC algorithm has the ability to retrieve AOD at different ranges, including high values of AOD, but
852 its stability decreases significantly with an increasing AOD, especially when $AOD > 1.0$ (see also section
853 [2.2.2 Urban air quality and megacities](#)).

854
855 One of the major problems for both interpretation of satellite data and applications of empirical models of
856 solar radiation is related to elevated aerosol layers in the atmosphere. It was demonstrated that their origin
857 can be attributed at a higher confidence when back trajectories are combined with lidar and radiosonde
858 profiles (Nikandrova et al., 2018).

859
860 Black carbon measurement methods have progressed. A representative value for the multiple scattering
861 enhancement factor, a fundamental quantity correcting atmospheric black carbon measurement using an
862 aethalometer, was derived for the first time in the Arctic environment (Backman et al., 2017). By analyzing
863 BC measurements made with an Aethalometer in Nanjing, Virkkula et al. (2015) showed that the
864 compensation parameter of a widely-used data processing method depends both on single-scattering albedo
865 and backscatter fraction of the aerosol (see also section 2.2.2 Urban air quality and megacities). The
866 multiple-scattering correction factor of quartz filters and the effect of filtering particles mixed in snow was
867 estimated by Svensson et al. (2019) who applied the method for analyzing light absorption and BC in snow
868 samples taken from the Finnish Lapland and the Indian Himalayas.

869
870 Measurement of atmospheric sub-10 nm particle number concentrations has been of substantial interest
871 recently. A new high flow differential mobility particle sizer (HF-DMPS) was built, calibrated and operated
872 in field conditions for one month (Kangasluoma et al. 2018). The counting uncertainties of the HFDMP
873 were reduced by about 50% as compared to the traditional DMPS. The HFDMP detected about two times
874 more particles than the DMPS in the size range of 3–10 nm. Below 3 nm, the HF-DMPS is currently limited
875 by the inability of diethylene glycol to condense on biogenic particles. For collecting BVOC samples, a
876 novel collection method offering portability and improved selectivity and capacity was developed. A solid-
877 phase microextraction (SPME) Arrow sampling (Barreira et al. 2018) can be used for static and dynamic
878 collection of BVOCs in the field conditions. A significant improvement on sampling capacity was observed
879 with the new SPME Arrow system over SPME fibers. A fully automated online dynamic in-tube extraction
880 (ITEX)–gas chromatography/mass spectrometry (GC/MS) method was introduced for continuous and
881 quantitative monitoring of volatile organic compounds in air (Lan et al. 2019). The stability and suitability of
882 the developed system was validated with a measurement campaign, and the ITEX method provided 2–3
883 magnitudes lower quantitation limits than established methods. Parshintsev et al. (2015) introduced a new,
884 fast analysis method for the desorption atmospheric pressure photoionization high-resolution (Orbitrap) mass
885 spectrometry (DAPPI-HRMS). The DAPPI results agreed with the aerosol particle number measured with an
886 established method and was found to detect different compounds and giving complementary information
887 about the aerosol samples.

888

Formatted: Font: Times New Roman, 11 pt

889 Fragmentation of molecular clusters inside mass spectrometers is a significant uncertainty-source in many
890 chemical applications. A novel model, capable of quantitatively predicting the extent of fragmentation of
891 sulfuric acid clusters was developed (Passananti et al. 2019). The fragmentation cannot be described in terms
892 of rate constants under equilibrium conditions, because clusters accelerate under electric fields (Zapadinsky
893 et al. 2019). A model describing an energy transfer to the cluster internal modes caused by collisions with
894 residual carrier gas molecules was developed. The model can be used to interpret experimental
895 measurements done with atmospheric pressure interface mass spectrometers.

896
897 Recently, a new atmospheric observation site equipped with state-of-the-art atmospheric aerosol
898 instrumentation was deployed in Beijing, China (Liu et al. 2020). At the Beijing University of
899 Chemical and Technology (BUCT), the Aerosol and Haze Laboratory (AHL) was established in
900 2018 - 2019, providing novel insights into air pollution in a comprehensive manner. The station
901 hosts comprehensive instrumentation to concentrations of atmospheric trace gases, aerosol particle
902 size distributions and mass concentrations, particle chemical composition on the levels from
903 molecules, clusters and nanometer to micrometer sized aerosol particles. For example, the first
904 results showed increased cluster mode particle number concentrations during NPF events, whereas
905 during haze days accumulation mode particle number concentrations were high (Zhou et al., 2020).
906 The observations have enabled to quantify number emission factors and underlined the importance of
907 traffic (Kontkanen et al. 2020). Daytime sulfuric acid concentrations in Beijing were typically
908 around $4.9 \times 10^6 \text{ cm}^{-3}$ (Lu et al. 2019). During these measurements, an evidence was found on
909 significant nighttime sulphuric acid production, yielding gaseous sulphuric acid concentrations of
910 1.0 to $3.0 \times 10^6 \text{ cm}^{-3}$ (Guo et al., 2021). For further results, see also section 2.2.2 Urban air quality
911 and megacities.

912
913 Besides Beijing, measurements have been performed in several other locations inside the PEEEX area. We
914 used novel instrumentation to measure new particle formation and its precursors at the background Fonovaya
915 station in the Tomsk region (Russia, Siberia), at the Värriö subarctic research station (Finland), in Ny-
916 Ålesund (Svalbard, Norway) and on the German icebreaker, the Polarstern, during the MOSAIC project. As
917 an example, the first results from Fonovaya station are shown in Fig. 2. -Thanks to these deployments, in the
918 next years we will be able to understand the identity of NPF precursors in those remote places. This will help
919 us to elucidate the human impact on aerosol formation and thereby on aerosol-cloud interactions at high
920 latitudes. In Siberia, we will finally understand why new particle formation occurs infrequently, and
921 hopefully also identify the human role in this phenomenon. In the Arctic, we will understand the marine
922 influence on NPF and will find out the detailed mechanism that leads to the formation of small clusters that
923 which initiate NPF.

924

925 Model developments were made at several scales. Aerosol-radiation and aerosol-cloud interactions are
926 among the main sources of uncertainties in climate models, and detailed information on anthropogenic
927 aerosol number emissions is needed to improve this situation. Anthropogenic aerosol number emissions in
928 current large-scale models are usually converted from corresponding mass emissions in pre-compiled
929 emission inventories using very simplistic methods. In the global aerosol-climate model ECHAM-HAM, the
930 anthropogenic particle number emissions, converted originally from the AeroCom mass emissions, were
931 replaced with recently-formulated number emissions from the Greenhouse Gas and Air Pollution Interactions
932 and Synergies (GAINS) model (Xausa et al., 2018). However, revisions are still needed in the new particle
933 formation and growth schemes currently applied in global modeling frameworks.

934

935 For regional and urban scales, a fully integrated /online coupled meteorology-chemistry-aerosol model
936 Enviro-HIRLAM was developed (Baklanov et al., 2017) and tested for several applications in Europe,
937 Russian Arctic and China (Shanghai) (Mahura et al., 2018, 2019). Key issues for seamless integrated
938 chemistry–meteorology modeling for Earth System prediction were analyzed and formulated (Baklanov et
939 al., 2018), highlighting the scientific issues and emerging challenges that require proper consideration to
940 improve the reliability and usability of these models for three main application areas: air quality,
941 meteorology, and climate modeling. Baklanov et al. (2018) also presents a synthesis of scientific progress in
942 the form of answers to nine key questions, and provides recommendations for future research directions and
943 priorities in the development, application, and evaluation of online coupled models.

944

945 2.2.2 Urban air quality and megacities (Q5)

946

947 The rapid urbanization and growing number of megacities and urban agglomerations requires new types of
948 research and services that make the best use of science and available technology. There are urgent needs for
949 examining what the rising number of megacities means for air pollution and local climate, and what effects
950 these changes have on global climate (Baklanov et al., 2016). Such integrated studies and services should
951 assist cities in facing hazards, such as storm surge, flooding, heat waves and air pollution episodes,
952 especially in changing climates (WMO, 2019). We discuss here the recent observation on the atmospheric
953 pollution in China and Russia.

954

955 *Air quality in China – recent observations*

956

957 China is one of the regions with highest concentrations of fine PM_{2.5} in the world (Wang et al., 2017a). This
958 has serious consequences on air pollution and the associated visibility reduction (haze) and adverse health
959 effects (Zhao et al., 2017). The number of haze days in China has been growing during the recent decades,
960 but detailed understanding of the factors governing the occurrence of haze is still not clear (Wang et al.,
961 2019). Both NO₂ and SO₂ concentrations showed increasing trends during the 2004-2012 period, and these
962 trends could be linked to increased power plant and traffic emissions (Wang et al., 2019). A key feature of

963 haze formation seems to be an increased inorganic fraction of the aerosol, suggesting that the reduction of
964 nitrate, sulfate and their precursor gases would improve air quality and visibility in China (Wang et al.,
965 2019). In northern China, PM_{2.5} concentrations declined over the period 2013–2017, and approximately half
966 of the inter-annual variability in this region was attributed to atmospheric circulation changes (Li et al.,
967 2020b). The maximum daily 8-h average O₃ concentrations increased over most of northern China during the
968 same time period, with again large influences due to atmospheric circulation on daily basis (Liu et al.,
969 2019b).

970
971 Compared with most other urban environments investigated so far, measurements in urban China
972 demonstrated a relatively frequent occurrence of atmospheric new particle formation (NPF), and the
973 observed NPF events were typically characterized by high particle formation rates and strongly size-
974 dependent growth of newly-formed particles (Kulmala et al., 2016b; Wang et al., 2017b; Chu et al., 2019).
975 Since the first reported sub-3 nm particle measurements in China a few years ago (Xiao et al., 2015), new
976 insight into the formation pathways of molecular clusters and their growth have been obtained, including the
977 relative roles of gaseous sulfuric acid, amines, ammonia and organic vapors in these processes (Yao et al.,
978 2018; Yan et al., 2021). While high pre-existing particle loadings appear to suppress NPF during severe haze
979 periods in Chinese megacities, it is unclear how NPF is possible at all under less but still quite polluted
980 conditions typical for these environments (Kulmala et al., 2017). Overall, the available observations suggest
981 NPF to be a major source of aerosol particles in urban China, with potentially large effects on haze formation
982 (Kulmala et al., 2021) and cloud properties (Chu et al., 2019).

983
984 Urban measurements of particle number size distributions give deep understanding into the sources and
985 atmospheric processing of fine particles. The longest urban continuous record is from the SORPES station in
986 the Yangtze River Delta (Qi et al., 2015), covering almost a decade of measurements, whereas the broadest
987 size range (1.5 nm – 1 μm) was measured in the winter Beijing atmosphere (Zhou et al., 2020). The latter
988 study found clear differences in particle sources in different size ranges: NPF was in general the largest
989 source of clusters and nucleation mode (<25 nm) particles, while traffic contributed to all the size ranges and
990 dominated both cluster and nucleation modes on haze days. Aitken mode (25–100 nm) particles originated
991 mainly from local emissions, with additional contributions from regional and transported pollution as well as
992 from the growth of nucleation mode particles. Regional and transported pollution were identified as the main
993 source of accumulation mode (>100 nm) particles.

994
995 Air pollution and chemical transformation, including annual and seasonal variations of the concentrations of
996 atmospheric constituents, were analyzed for North China for the period 2005–2015 (Bai et al., 2018a). A
997 photochemical link that related the production of fine PM and O₃ to VOCs was detected, and this mechanism
998 was found to be prominent in summer. An intensive measurement campaign (SORPES station, Yangtze
999 River Delta) was carried out to investigate sulfate formation and associated nitrogen chemistry (Xie et al.,
1000 2015). That study highlighted the effect of NO_x in enhancing the atmospheric oxidizing capacity, and

1001 indicated a potentially very important impact of increasing NO concentrations on particulate pollution
1002 formation and regional climate change in East Asia. In Changzhou, a highly-populated city in the Yangtze
1003 River Delta, primary organic aerosol concentrations outweighed secondary ones, indicating an important role
1004 of local anthropogenic emissions in aerosol pollution (Ye et al., 2017). The measurement also showed the
1005 abundance of organic nitrogen compounds in water-soluble organic aerosol, suggesting that these
1006 compounds are likely associated with traffic emissions.

1007
1008 Aerosol impacts on warm cloud properties were investigated over three major urban clusters in Eastern
1009 China and East China Sea using multi-sensor satellite observations (Liu et al., 2017, 2018). In addition to the
1010 amount of aerosol, evidence was provided that aerosol types and environmental conditions need to be
1011 considered to understand the relationship between cloud properties and aerosols. Aerosol-cloud interactions
1012 were found to be more complex and of greater uncertainty over land than over ocean.

1013
1014 The atmospheric boundary layer (ABL), and especially its dynamic behavior, is central to the evolution of
1015 near-surface air pollution. Using atmospheric observations combined with theoretical arguments, Petäjä et al.
1016 (2016) proposed a feedback mechanism connecting ABL properties with PM. According to such mechanism,
1017 high concentrations of PM enhance the stability of an urban boundary layer (BL) decreasing its height, thus
1018 causing further accumulation of pollution inside BL. Ding et al. (2016a) and Wang et al. (2018b)
1019 demonstrated an important role of BC aerosols in this feedback using model simulations combined with
1020 observations. A tight connection between the BL height and pollutant concentration, and indications of the
1021 presence of the above feedback mechanism, was also found based on comprehensive observations made on a
1022 325-m tower in Beijing (Wang et al., 2020). In order to understand these feedbacks, Kulmala (2018) and
1023 Hari et al. (2016) emphasized the crucial role of continuous, comprehensive measurements on a network of
1024 flagship stations in tackling the air pollution problem in urban China and megacities elsewhere in the world.
1025 They also introduced a so-called “Stations for Measuring Atmospheric and Earth surface Relations”
1026 (SMEAR) concept, which consists of integrated atmospheric and ecosystem observations allowing the
1027 analysis of Earth surface – atmosphere feedbacks and interactions. The first SMEAR-type station in China,
1028 the SORPES station located in the Yangtze River Delta, has been operating since 2011 (Ding et al., 2016b).

1029
1030 *Anthropogenic emissions and environmental pollution in Russia*

1031
1032 In the complex situation of the plurality of emissions, an important research task remains in the Moscow
1033 megacity environment for the assessment of the air quality and potential sources through aerosol
1034 composition analyses. Moscow aerosol pollution has been studied using a special AeroRadCity-2018
1035 experiment (Chubarova et al., 2019) and satellite data with the application of new MAIAC/MODIS aerosol
1036 algorithm with a 1-km resolution (Zhdanova et al., 2020). An advanced source apportionment for this
1037 environment was performed using combined Fourier-transform infrared spectroscopy data and statistical
1038 principal component analysis (Popovicheva et al., 2020b). The main principal component loadings revealed

1039 the source impacts of transport, biomass burning, biogenic, dust and secondary aerosol in spring.
1040 Identification of biomass burning-affected periods discriminated the daily aerosol composition change with
1041 respect to air mass transport and number of fires detected in the surrounding areas. Measurements of
1042 particulate BC were conducted at an urban background site (Meteorological Observatory of MSU) during the
1043 spring period of 2017-2018 (Popovicheva et al., 2020c). The mean BC concentrations displayed significant
1044 diurnal variations, with a poorly prominent morning peak and minimum at daytime. BC mass concentrations
1045 were higher at nighttime due the shallow boundary layer and intensive diesel traffic. The aerosol optical
1046 thickness (AOT) over Moscow showed a pronounced seasonal cycle, with a summer maximum and winter
1047 minimum (Chubarova et al., 2016a). It was found that during 2001–2014, the monthly-mean values of AOT
1048 declined by 1–5% per year, and this decline was attributed to decreased emissions of aerosols and their
1049 precursors.

1050
1051 In general, the atmospheric environment over remote areas of Siberia and Northern Asia is relatively clean
1052 compared with other surrounding regions of Asia and Eastern Europe (Baklanov et al., 2013). However, air
1053 pollution from Siberian industrial centers poses significant environmental threats. For Siberian cities (e.g.,
1054 Norilsk, Barnaul, Novokuznetsk), the air quality is among the worst in the Russian and European cities.
1055 Similar to Arctic cities, stable atmospheric stratification and temperature inversions dominate for more than
1056 half a year. This leads to pollution accumulation near the surface, which influences ecosystems and people.
1057 Moreover, not only severe climatic conditions, but also manmade impacts on the environment in industrial
1058 areas and large cities have intensified. The impacts manifest themselves as the pollution of environment, land
1059 use changes, hydrodynamic regimes and local climate. Ultimately, these impacts feed back to people,
1060 affecting their health and well-being.

1061
1062 The Russian part of the Barents Euro-Arctic region includes severe emission ‘hot spots’ for air pollutants.
1063 The Kola Peninsula, despite the presence of areas with undisturbed nature in the eastern part, is the most
1064 industrially developed and urbanized region in the Russian Arctic. The main polluters are the smelters of the
1065 Severonickel (Monchegorsk, central part of the peninsula) and the Pechenganickel (Nickel and Zapolyarnyi
1066 near the Russian-Norwegian border) enterprises. For comparison, emissions of SO₂ from the Nickel smelter
1067 alone are 5-6 times larger than the total Norwegian emissions (NILU, 2013). In 2015 the Norilsk Nickel in
1068 Siberia - the biggest mining and the metallurgical complex - emitted about 1.9 million tons of SO₂ (GGO,
1069 2016). With the nickel factory (located in the southern part of the city), copper factory (just to its north) and
1070 metallurgical plant (12 km to the east), the city of Norilsk is influenced by heavy industry no matter which
1071 way the wind blows. The Blacksmith Institute declared in 2007 that Norilsk is one of the top 10 worst-
1072 polluted places in the world. The impacts of emissions are manifested as deterioration of forest ecosystems
1073 and acidification of soils and surface waters (Derome and Lukina, 2011), even at considerable distances from
1074 the smelters. Heavy metals and alkaline pollutants contaminate areas around the sources of pollution within a
1075 few hundred kilometres, while acid sulphates can be transported over long distances (Mahura et al., 2018).

1076

1077 A recent analysis on the total deposition and loading on the population in North-Western Russia and
1078 Scandinavian countries caused by the continuous sulfur emissions from the Cu-Ni smelters in Murmansk
1079 indicates the dominance of wet deposition, especially in winter time (Mahura et al., 2018). North-Western
1080 Russia is influenced more by the Severonikel emissions compared with countries in the Scandinavian
1081 Peninsula. The cities of the Murmansk region (Kola Peninsula) are under highest impacts. On a yearly scale,
1082 the individual loadings on population are at the largest level (up to 120 kg/person) in the Murmansk region,
1083 much lower (15 kg/person) in northern Norway, and the smallest (< 5 kg/person) in eastern Finland, Karelia
1084 Republic and Arkhangelsk region. Distinct seasonal variability was identified, with the lowest contribution
1085 during summer and the highest contribution during winter-spring in Russia, during spring in Norway, and
1086 during autumn in Finland and Sweden.

1087
1088 The annual yearbook “The State of Atmospheric Pollution in Cities on the Territory of Russia” for 2018
1089 (Roshydromet and GGO, 2019) states the highest atmospheric emissions of PM were observed in Siberian
1090 and Ural cities. In Novokuznetsk and Omsk, the observed PM was the highest (> 30 000 tons per year) while
1091 emissions from other cities such as Angarsk and Chelyabinsk were lower (< 20 000 tons per year). Note that
1092 in the 2015-2019 yearbooks, emissions from only stationary sources were provided due to revisions
1093 (approved and implemented in November 2019 by the Russian Ministry of Natural Resources and Ecology,
1094 MNRE) of methods applied for estimation of emissions into the atmosphere from mobile sources. Depending
1095 on a source type, different methods to calculate emissions are applied (MNRE, 2019). For the gaseous
1096 compounds, such as SO₂, the maximum emissions included very high from Siberian cities (e.g. Norilsk,
1097 Novosibirsk, Novokuznetsk, Omsk, Ufa, Irkutsk, Angarsk) and from North-West Russia cities (Zapolyarny,
1098 Nickel, Monchegorsk). High NO₂ emissions were observed in Novosibirsk, Omsk, Angarsk and
1099 Chelyabinsk. The CO integral urban emissions depend on a city size. These varied from less than 10 Gg yr⁻¹
1100 ¹ (for small regional centers like Vladimir, Kursk, Samara) to 406 and 804 Gg yr⁻¹ for large metropolitan
1101 areas such as St. Petersburg and Moscow. As a whole, an analysis of spatio-temporal variation of trace gases
1102 in the boundary layer over Russian cities indicated significant emission variations between the urban
1103 environments and remote sites (Elansky et al., 2016).

1104 Cities, being not isolated systems, may distribute as much pollution to the surrounding areas as they receive
1105 it from outside them or from remote regions. The analysis of the transboundary atmospheric transport
1106 between Russian Siberia and bordering countries (e.g. China, Kazakhstan, and Mongolia) is part of a mutual
1107 risk assessment for urban areas/ cities and their surroundings. For example, the city of Ulaanbaatar
1108 (Mongolia) suffers from high levels of pollution due to excessive airborne particulate matter emanating from
1109 coal combustion mixed with traffic emissions and resuspended soil dust, resulting in variable chemical
1110 source profiles (Gunchin et al., 2019). Long-range transport from remote sources might be an additional
1111 contributor. Moreover, there are indications that such transport of biomass burning emissions from Siberia
1112 could lead to pollution episodes and impact on surface ozone as far as in western North America (Jaffe et al.,
1113 2004).

1114

1115 2.2.3 Weather and atmospheric circulation (Q6)

1116

1117 The observed evolution of weather and climate represents the combined effects of external forcing (changes
1118 in the concentrations of greenhouse gases and aerosols etc.) and internal variability, related to a large extent
1119 to the atmospheric circulation. It is also affected by local factors, particularly urban heat islands in cities.

1120 Here we discuss these interconnected processes, focusing on cold and warm episodes, cyclone density and
1121 atmosphere-ocean ~~interaction~~interactions, effects of circulation on temperature and moisture, cloudiness in
1122 the Arctic, and boundary layer dynamics relevant to the Arctic-boreal region.

1123 *Cold and warm episodes*

1124 The Arctic warming, ~~and as well as~~ the Arctic amplification, have been associated with changes in
1125 atmospheric large-scale circulation together affecting the European winter temperatures. In large parts of
1126 Europe, severe cold (warm) winter events are significantly correlated with warm (cold) Arctic episodes
1127 (Vihma et al., 2020). Air mass trajectory analysis revealed that air masses associated with extreme cold
1128 (warm) events typically originate from over continents (sea areas). Despite Arctic and European-wide
1129 warming, winter cooling has occurred in northeastern Europe in cases of air masses arriving from the
1130 southeast (Vihma et al., 2020).

1131

1132 *Cyclone density dynamics and atmosphere-ocean interaction*

1133 Transporting large amounts of heat and moisture from mid-latitudes to the central Arctic, synoptic-scale
1134 cyclones are vital for the Arctic climate system. Recent findings, based on atmospheric reanalysis, above all
1135 the global ERA-Interim reanalysis available from 1 January 1979 to 31 August 2019, are summarized below.
1136 During 1979–2016 in winter (Dec, Jan, Feb), the cyclone density increased in the areas around Svalbard and
1137 in northwestern Barents Sea, but decreased in southeastern Barents Sea (Wickström et al., 2020). This is
1138 related to a shift to more meridional winter storm tracks in the Norwegian, Barents and Greenland Seas. The
1139 shift is favored by a positive trend in the Scandinavian Pattern and, in the areas north of Svalbard, by a
1140 significant increase in the Eddy Growth Rate (Wickström et al., 2020).

1141

1142 Numerical model simulations of the storm activity in the White, Baltic and Barents Seas were analyzed for
1143 the period 1979–2015 (Myslenkov et al., 2018). A high interannual variability in the storm number was
1144 observed for all studied seas. No significant trends in the storm number during the period 1979–2015 were
1145 found in the studied sea areas. On average, the connection with global atmospheric circulation is stronger for
1146 the Baltic Sea than for the other two seas. Also, the future changes of wind wave climate were analyzed.
1147 According to the RCP8.5 scenario, in the second part of the 21st century the number of storm events will rise
1148 in the Baltic and Barents Seas.

1149

1150 In the Bjerknes compensation, changes in atmospheric heat transport co-occur with opposing changes in
1151 ocean heat transport. Observations and model simulations indicate a central role for ocean-atmosphere heat

1152 exchange in the Barents Sea area in maintaining this compensation in the Arctic (Bashmachnikov et al., 2018
1153 a, 2018b).

1154

1155 *Circulation effect on temperature*

1156 The effect of atmospheric circulation on temperature trends in years 1979-2018 was studied by Räisänen
1157 (2019, 2021) using a trajectory-based method. He found that [the](#) circulation trends had reduced the annual
1158 mean warming during this period in western and central Siberia locally by over 1°C, with a much larger
1159 cooling effect in autumn and winter (Fig. 3). His findings also confirmed a circulation-induced amplification
1160 of warming over the Barents and Kara seas particularly in winter. Yet, in most areas the circulation-related
1161 temperature trends have varied strongly from month to month, leaving only a relatively small effect on the
1162 annual mean temperature trends. The residual warming obtained after subtracting the circulation effect
1163 therefore tends to have a smoother seasonal cycle than the observed temperature trends, in better agreement
1164 with the multi-model mean trends in the CMIP5 simulations (Taylor et al., 2012).

1165

1166 *Circulation effect on moisture*

1167 The effects of large-scale circulation on moisture, cloud and longwave radiation occur mostly via the impact
1168 of horizontal moisture transport (Nygård et al., 2019). Evaporation is typically not efficient enough to shape
1169 those distributions, and much of the moisture evaporated in the Arctic is transported southward (Nygård et
1170 al., 2019). Strong moisture transport events avail a large part of the northwards moisture transport. The
1171 meridional net transport is only a small part of the water vapor exchange between the Arctic and mid-
1172 latitudes (Naakka et al., 2019). When a high-pressure pattern across the Arctic Ocean from Siberia to North
1173 America is lacking, the amounts of moisture, clouds and downward longwave radiation are anomalously
1174 high near the North Pole (Nygård et al., 2019). Using vertically-integrated water vapor as a metric, the Arctic
1175 (north of 70°N) has experienced a robust moistening trend since 1979, and in absolute numbers this trend is
1176 the smallest in March and the largest in August (Rinke et al., 2019). However, the relative trends are the
1177 largest in winter. Although different atmospheric reanalysis are consistent in spatiotemporal trend patterns,
1178 they scatter in the trend magnitudes.

1179

1180 Analysis of moisture and aridity estimated using the web-GIS "CLIMATE" and the ECMWF ERA-Interim
1181 reanalysis data for Southern Siberia (50-65 °N, 60-120 °E) from 1979 to 2010 with a $0.75^\circ \times 0.75^\circ$ grid
1182 resolution showed that the mountain regions of Eastern Siberia have been come more arid each month during
1183 the last 30 years (Ryazanova and Voropay, 2017). In Western Siberia, aridity increased in May and
1184 decreased in June, while in the other months positive and negative trends were found. The greatest
1185 differences in the trends of the aridity index, air temperature and precipitation were observed in July.

1186

1187 *Cloudiness in Arctic*

1188

1189 The climatology and inter-annual variability of Arctic cloudiness remains a wildcard in regional climate
 1190 change projections. Both climate models and satellite data products need *in situ* observations for calibration
 1191 and validation. Chernokulsky et al. (2017) and Chernokulsky and Esau (2019) collected and processed
 1192 manual cloud observations from meteorological stations in the PEEX area. The cloud records in the Arctic
 1193 are available since the end of the 19th century. Since 1936, cloud observations representatively cover the
 1194 Eurasian Arctic. This permits reconstructions of cloud type and cloud cover climatologies as well as studies
 1195 of inter-decadal variability of cloudiness. A problem of a special interest is related to the co-variability of the
 1196 total cloud cover and sea ice concentration or extent. Both clouds and sea ice affect the surface heat balance
 1197 through surface albedo, but their feedback mechanisms, dynamical impacts and climate sensitivities are
 1198 different. Chernokulsky et al. (2017) found that the annual-mean total cloud cover (TCO) decreases during
 1199 warmer climate periods with a lower sea ice concentration, but increases over sea ice in the Barents Sea as
 1200 more moisture is transported into the Arctic at higher temperatures. Furthermore, the increasing TCO
 1201 reduces the deficit of the surface heat, and the intra- and inter-annual variability of TCO over solid ice is
 1202 higher than that over open water (Chernokulsky et al. 2017). Long-term cloud climatological analysis based
 1203 on meteorological observations of the total and low cloud cover and cloud types from the Barents Sea to the
 1204 Chukchi Sea showed that significant transitions between cloud types has been taken place, especially the
 1205 low-level stratus and stratocumulus types have been transformed to convective cloud types (Chernokulsky
 1206 and Esau, 2019). Chernokulsky and Esau (2019) addressed that their results are relevant for understanding
 1207 Arctic cloud processes and feedbacks, and that new knowledge is needed to connect the changes in the
 1208 Arctic radiation balance with the Arctic cloud cover—cloud type climatology.

1209

1210 *Boundary layer dynamics and urban heat islands*

1211

1212 On the background of accelerated and amplified Arctic warming, anthropogenic heat release and metabolism
 1213 of cities add up to persistent warm temperature anomalies in urbanized areas (Fig. 4). Indeed, if the climate
 1214 change forcing approaches 2 W m^{-2} , the urban heat forcing could be $10\text{-}100 \text{ W m}^{-2}$ (Konstantinov et al.,
 1215 2018). The urban heating trapped in the shallow ~~the shallow~~ [PBLs](#) ~~planetary boundary layers~~ is potent to rise the local
 1216 temperatures by ~~1°C~~ [1 to 10°C](#) ~~and 10°C~~ or even more. This local climate phenomenon is known as the urban
 1217 heat island (UHI) (Esau et al., 2020). A series of *in situ* and satellite UHI studies in the northern cities
 1218 revealed strong and persistent warm temperature anomalies in almost all of 28 northern West Siberian cities
 1219 (Miles and Esau, 2017), in 5 cities covered by the UHIARC network (Konstantinov et al., 2019; Varentsov et
 1220 al., 2018a) and in 57 Scandinavian cities (Miles and Esau, 2020). The mean wintertime temperature
 1221 anomalies, the UHI intensity, varied from 0.8 K to 1.4 K and had extreme intensities of up to 7 K during cold
 1222 anticyclone weather conditions. The complete dataset of surface UHI intensity derived from MODIS LST
 1223 data products is freely available and published in Miles (2020). Such a UHI-induced strong mediation of
 1224 cold temperature spells might cause significant socio-economic and environmental impacts in the cities
 1225 (Konstantinov et al. 2018, Fig. 4). A survey of other UHI studies in 11 Arctic cities and towns confirmed that

1226 even relatively small cities at high latitudes may exhibit intensive UHIs. A recent analysis confirms the
1227 important role of the surrounding temperature in explaining spatial-temporal variation of [the](#) UHI intensity
1228 (Miles and Esau, 2017). The major contribution to the UHI was revealed for water, sparse vegetation,
1229 grassland and scrubland. The mechanisms and pathways of the UHI maintenance requires [an](#) involvement of
1230 numerical experiments with turbulence-resolving models to advance the understanding of the local climate
1231 features (Urban Heat Islands - UHIARC dataset see http://urbanreanalysis.ru/uhi_arc.html). We would need a
1232 denser meteorological network, especially high quality temperature data, to better understand the urban
1233 climatology and the thawing processes in urban soils and to better assess climatic trends relevant to Arctic
1234 societies and welfare (Konstantinov et al. 2018).

1235
1236 Urban climate anomalies may cause more extreme weather and climate phenomena in densely populated
1237 megacities. The Moscow agglomeration – the largest megacity in the boreal continental climate within the
1238 PEEEX domain – demonstrates profound effect of interactions between the UHI and urban winds, known as a
1239 cross-over effect (Varentsov et al. 2018b). The UHI creates an urban heat “dome” with near-surface air
1240 inflow into the urban central districts and air outflow at higher levels in the atmosphere. The air uplift in the
1241 urban dome is connected to the increase in summer rainfall at the lee side and over the central urban districts.
1242 Stable atmospheric stratification over rural area is strengthened by the downwind air motions coming from the
1243 urban region.

1244
1245 Atmospheric boundary layer over the Arctic Ocean has been studied on the basis of tethered sounding
1246 observations over sea ice (Palo et al., 2017) and research aircraft observations over the open ocean and sea
1247 ice (Suomi et al., 2016). Palo et al. (2017) found that in spring and summer, the occurrence and properties of
1248 temperature inversions were controlled by the surface melt and warm air advection rather than surface net
1249 radiation. During snow/ice melt, temperature inversions were frequently surface-based, and equally strong as
1250 winter inversions over the Arctic Ocean. To better understand atmospheric boundary layer processes in the
1251 Arctic, Suomi et al. (2016) developed a method to measure wind gusts from a research aircraft. It allows
1252 wind gust observations at altitudes not reached by traditional weather mast observations. The observed gust
1253 factors strongly depended on the surface roughness, which differed for sea ice and the open ocean.

1254

1255 2.3 ARCTIC-BOREAL AQUATIC SYSTEM

1256

1257 We discuss the recent results on Arctic sea ice dynamics and thermodynamics, snow depth and sea ice
1258 thickness, sea ice research supporting navigation, and rare elements in snow and the ocean sediments,
1259 especially from the perspective of improvements in the observation and modelling methods (Q7, section
1260 3.3.1). We introduce new results on the Arctic marine ecosystem and focus on the primary production and
1261 carbon cycle (Q8, section 3.3.2.). In section 3.3.3 for the Arctic – boreal lakes and rivers, we discuss the
1262 browning of lakes and lake sediment with a special attention on the Selenga River system of Lake Baikal
1263 (Q9).

1264
1265 2.3.1 Changing water systems, snow, sea ice and ocean sediments (Q7)
1266

1267 *Sea ice and thermodynamics with atmospheric and ocean dynamics*

1268
1269 Referring to the earlier discussion in section 2.2.3 on atmospheric circulation, we address here how the sea
1270 ice dynamics closely interacts with the atmospheric and ocean dynamics. A rapid decrease in the Arctic
1271 Ocean ice cover, particularly in the Barents and Kara Seas, has been taking place since the late 1970s
1272 simultaneously with the cooling of winters in central Eurasia (McCusker et al., 2016). This unexpected
1273 winter cooling is related to increasing northeasterly winds over the southeastern flank of an anomalous high
1274 that has developed over the northwestern coast of Russia (McCusker et al., 2016; Mori et al., 2019; Räisänen
1275 2021). However, the causality between the atmospheric circulation changes and the Arctic sea ice decrease is
1276 debated. Observations suggests a strong correlation between these two, but climate model simulations forced
1277 by reduced ice cover produce much weaker circulation changes than observed, resulting in only weak
1278 cooling in central Eurasia (Mori et al., 2014, 2019; McCusker et al., 2016). This suggests that either most
1279 models are underestimating the sensitivity of the atmospheric circulation to sea ice decrease, supported by
1280 Romanowsky et al. (2019), or that the circulation change has not been primarily caused by the decreasing sea
1281 ice. In the latter case, the correlation between the reduced ice cover and atmospheric circulation would
1282 mainly reflect the effect of circulation on sea ice. In support of this, Blackport et al. (2019) showed that a
1283 reduced sea ice coincides with an anomalous heat flux from the atmosphere to the ocean, and that on the sub-
1284 seasonal time scale, anomalies in atmospheric circulation tend to precede rather than follow those in sea ice.
1285 Thus, while the reduced sea ice might partly explain the observed changes in atmospheric circulation (Mori
1286 et al., 2019), the effect of circulation on sea ice appears to be stronger than the effect of sea ice on
1287 circulation.

1288
1289 Considering atmosphere-ice interactions, Jakobson et al. (2019) studied the linkages between sea ice
1290 concentration (SIC), atmospheric stratification, surface roughness and wind speed at the 10-m height (W10)
1291 and 850-hPa level (W850). In all the seasons except summer, a reduction in SIC favored reduced
1292 atmospheric stratification and aerodynamic surface roughness, which resulted in a stronger W10. The effect
1293 was the strongest in autumn, and positive trends in W10 and its ratio to W850 typically occurred in regions
1294 with the strongest negative trends in SIC. The relationships were stronger on inter-annual than on sub-
1295 seasonal time scales. Large-scale atmospheric circulation, characterized, e.g., by the Dipole Anomaly (DA),
1296 has also contributed to sea ice dynamics. A positive polarity in DA has contributed to the recent rapid loss of
1297 summer sea ice in the Pacific part of the Arctic Ocean by bringing warmer air masses from the south and
1298 transporting more ice towards the north enhancing the ice-albedo feedback (Lei et al., 2016). Another
1299 example of ice dynamics affecting the ice-albedo feedback was the weakened Transpolar Drift Stream in
1300 summer 2013. It reduced sea ice transport out of the Arctic Ocean, and restrained ice melt because of the low

1301 air temperatures, weakened albedo feedback, and a relative small oceanic heat flux in the central Arctic (Lei
1302 et al., 2018).

1303 Solar radiation, being the main forcing factor for a sea ice melt in summer, is difficult to parameterize in
1304 thermodynamic models. This is due to the large variability in the optical properties of sea ice in space and
1305 time. A two-stream model provides a time-efficient parameterization of the apparent optical properties
1306 (AOPs) for ponded sea ice, accounting for both absorption and scattering, and has a potential to be
1307 implemented into sea-ice thermodynamic models to explain the role of melt ponds in the summer decay of
1308 Arctic sea ice (Lu et al. 2016). This model was used to investigate the role of solar radiation in the Arctic sea
1309 ice during the melting season considering layers of melt ponds, underlying sea ice, and ocean beneath the
1310 ice. It was found that the energy absorption profiles depend strongly on the incident irradiance and ice
1311 scattering, but only weakly on the pond depth. It seems that the incident solar energy is largely absorbed by
1312 the melt pond rather than by the underlying sea ice (Lu et al., 2018a). The model was further applied to
1313 investigate the influence of a surface ice lid on the optical properties of a melt pond. The thickness of the ice
1314 lid determines the amount of solar energy absorbed. Visual inspections on the color of refreezing melt ponds
1315 also help to judge the significance of the influence of the ice lid. This will allow for an accurate estimation
1316 on the role of surface ice lid during field investigations on the optical properties of melt ponds (Lu et al.,
1317 2018a). The modelled pond color agrees with field observations from the Arctic sea ice in summer. The
1318 analysis of pond color is a new potential method to obtain ice thickness in summer, however, more validation
1319 data and improvements to the radiative transfer model would be needed (Lu et al., 2018b).

1320

1321 *Snow depth/mass and sea ice thickness*

1322 Snowpack on sea ice has a crucial role in insulating the sea ice from the colder atmosphere, accordingly
1323 reducing sea ice growth in winter, effectively reflecting the incoming solar radiation, reducing sea ice melt in
1324 spring and summer and contributing to its formation. The replacement of snow fall by rain strongly enhances
1325 the ice-albedo feedback in the Arctic Ocean (Dou et al., 2019). Shalina and Sandven (2018) refined the
1326 description of snow depth on sea ice in the central Arctic, providing new snow depth data for the Arctic
1327 marginal seas. High autumn and winter precipitation and thinning Arctic sea ice make snow-ice formation
1328 prevalent in the Atlantic sector of the Arctic (Merkouriadi et al., 2017).

1329

1330 Advance has been made in applying thermistor string based autonomous high-resolution Snow and Ice Mass
1331 Balance (IMB) Array (SIMBA) buoys to measure snow depth and ice thickness (Figs. 5 and 6.). SIMBA has
1332 a lower cost, allowing deployment in large numbers (Lei et al., 2015). The determination of snow depth and
1333 ice thickness from SIMBA temperature profiles has so far been largely a manual process. A SIMBA-
1334 algorithm was developed to process SIMBA data automatically (Liao et al., 2018), assuming a fixed snow-
1335 ice interface. Snow-ice formation results in snow-ice interface moving upward. The SIMBA-algorithm was
1336 further developed to tackle the moving interfaces (Cheng et al., 2020). The developed SIMBA-algorithm
1337 works well in cold condition for lakes and Polar Oceans. For Polar Oceans, the snow and ice are close to

1338 isothermal during summer, which prevents the identification of interfaces on the basis of the temperature
 1339 gradient. Under such conditions, thermodynamic modelling yields valuable information on snow depth and
 1340 ice thickness (Tian et al., 2017).

1341 A challenge in sea ice thermodynamic modelling is the uncertainty in the magnitude of the oceanic heat flux
 1342 at the ice base, especially for land-fast sea ice. Yang et al. (2015) applied a one-dimensional thermodynamic
 1343 model to investigate impact factors on land-fast sea ice in the East Siberian Sea. The modelled snow cover
 1344 was less than 10 cm, having a small influence on the ice thickness, but surface albedo and oceanic heat
 1345 fluxes were critical.

1346
 1347 Also in the terrestrial Arctic and boreal zone, there is a need for a better efficiency and coverage of an *in-situ*
 1348 snow observation network. Snow cover and snow mass are fundamental parameters for global energy and
 1349 water cycles, and the changes in the regional snowpack have societal impacts like on amount of drinking
 1350 water or capacity for the hydropower generation (Bormann et al., 2018). Snow depth data in the Arctic
 1351 region are available from the synoptic weather stations and snow mass data are systematically collected from
 1352 the snow courses, as demonstrated in Extended Data (fig. 2) by Pulliainen et al. (2020). The use of automatic
 1353 and cost-effective measurements together with harmonized snow measurement practices is the way forward.
 1354 A survey on a harmonized snow monitoring in Europe demonstrated that crucial parameters for operational
 1355 services, such as parameters characterizing precipitating and suspended snow, are measured by 74% of the
 1356 European snow network contributors (COST Action ES1404), but the parameters characterizing the snow
 1357 microstructural properties, electromagnetic properties and composition are currently measured by only 41%,
 1358 26% and 13%, respectively, of the network contributors (Pirazzini et al., 2018). The observations at the
 1359 continental scale, so far, demonstrate a widespread snow-cover retreat since the ~~1970s~~1970's across the
 1360 Northern Hemisphere, particularly in the Arctic (Derksen et al., 2012; Bormann et al., 2018). On the
 1361 contrary, the results from the mountains are mixed and there is no consistent picture of what is happening at
 1362 the regional scale (Bormann et al., 2018). Pulliainen et al. (2020) provided new insight into the seasonal
 1363 snow mass and its trend by using a bias-corrected GlobSnow 3.0 estimates. Pulliainen et al. (2020) is now
 1364 able to demonstrate different continental trends based on the 39-year satellite record: a decrease in North
 1365 America, a negligible trend in Eurasia, and a high regional variability in both areas.

1366 *Sea ice research supporting navigation*

1367
 1368 Recent research has addressed emerging opportunities for Arctic navigation and the importance of
 1369 operational sea ice analysis. Lei et al. (2015) showed trends along the Arctic Northeast Passage (NEP) and
 1370 demonstrated an increase in the spatially-averaged length of the open period (the ice concentration less than
 1371 50%) from 84 days in the ~~1980s~~1980's to 114 days in the 2000s. The summer sea ice along the High-
 1372 Latitude Sea Route (HSR) north of the eastern Arctic islands has decreased during the last decade, with the
 1373 ice-free period reaching 42 days in 2012. The HSR avoids shallow waters along the coast, which easier the
 1374 access to for deeper-draft vessels (Lei et al., 2015). Considering operational sea ice analyses for the Bohai

1375 Sea, work has been done to combine thermodynamic modelling and Earth Observation (EO) data from
 1376 synthetic aperture radar (SAR) and microwave radiometers (Karvonen et al., 2017). The SAR-based
 1377 discrimination between sea ice and open-water works well, and areas of thinner and thicker ice can be
 1378 distinguished. However, a larger comprehensive training dataset is needed to set up an operational algorithm
 1379 for the estimation of sea ice concentration and for the weighting scheme for sea ice thickness (Karvonen et
 1380 al., 2017).

1381
 1382 Multi-decadal Arctic sea-ice state estimates are important for the strategic planning of Arctic navigation.
 1383 These estimates are usually based on climate models with a thermodynamic-dynamic sea-ice models. An up-
 1384 to-date assessment of large-scale sea-ice models was with the aid of sea-ice models as a climate model
 1385 component, a comprehensive review was carried out by Leppäranta et al. (2020). Specifically, Uotila et al.
 1386 (2015) found that a model with the subgrid-scale sea-ice thickness distribution reproduces more realistic sea
 1387 ice and upper ocean, due to better captured spring evolution, than a model with just single sea-ice thickness
 1388 category. In terms of validity of initial conditions for multi-decadal predictions, Uotila et al. (2019) analyzed
 1389 a set of ocean reanalysis products, including Arctic sea ice, and found that the multi-model set mean is a
 1390 useful product as a state estimate. This finding increases confidence toward the use of the combination of
 1391 ocean reanalysis for both initialization of multi-decadal predictions and analysis of multi-decadal variability.

1392

1393 *Ocean floor and Sediments: composition and fluxes*

1394

1395 A significant content of illite and muscovite among layer silicates in most of the ice-rafted sediments
 1396 samples taken from selected Arctic regions suggests that sources of the sedimentary material are mainly
 1397 mineralogically similar to modern bottom sediments of the East Siberian and Chukchi seas, as well as
 1398 presumably sediments of the eastern Laptev Sea. A significant kaolinite fraction in the samples from the
 1399 North Pole area can be caused by the influx of ice-rafted fine-grained sedimentary material from the
 1400 Beaufort or Chukchi seas, where kaolinite is supplied from the Bering Sea. The samples contained variable
 1401 proportions of erosion products of both mafic and felsic magmatic rocks and/or sufficiently mature
 1402 sedimentary rocks (Maslov et al., 2018a).

1403

1404 Quantification of CH₄ sources is fundamental information for the climate change mitigation (Fletcher and
 1405 Schaefer 2019). Methane stored in ocean floor reservoirs can reach the atmosphere in the form of bubbles or
 1406 dissolved in water. Methane hydrates could destabilize with rising temperatures, further increasing
 1407 greenhouse gas emissions in a warming climate. Subsea permafrost and hydrates in the East Siberian Arctic
 1408 Shelf (ESAS) are acting as a substantial carbon pool, and source of methane to the atmosphere. Annual
 1409 methane emissions of the region varies from 0.0 to 4.5 TgCH₄/Tg CH₄ yr⁻¹ estimated by Berchet et al. (2016).
 1410 Yasunaka et al. (2018) estimated the monthly air-sea CO₂ fluxes in the Arctic Ocean and adjacent seas
 1411 located north of 60 degrees N for the period 1997 2014 and ended up to a net annual Arctic Ocean CO₂
 1412 uptake of 180 ± 130 TgC/Tg C per year.

1413

1414 The Zeppelin Observatory data for 2014 suggest that the CH₄ fluxes from the Svalbard continental platform
 1415 are smaller than 0.2 Tg yr⁻¹. All estimates are in the lower range of values reported earlier (Pisso et al.,
 1416 2016). Platt et al. (2018) reported a potential region with high ocean-atmosphere CH₄ flux located north of
 1417 Svalbard, but addressed that at the time of the measurements the meteorological conditions were unique,
 1418 including a short episode of the highly sensitive to emissions over an active seep site without a sensitivity to
 1419 land-based emissions.

1420

1421 *River runoff affecting the hydrological processes at coastal marine environments*

1422

1423 The Arctic Ocean, including the Hudson Bay, receives 55.6 % of its river inflow from Russia, mostly via 19
 1424 large rivers (Shiklomanov and Shiklomanov, 2003). This freshwater inflow of approximately 2920 km³ per
 1425 year (Shiklomanov, 2008) is associated with large sediment and heat transports, which together affect the
 1426 hydrography, marine climate and ecosystems across the Siberian shelf seas (Magritsky et al., 2018). A major
 1427 part of seasonal and interannual variations in the river runoff is anthropogenic, due to regulation in large
 1428 reservoirs (Georgiadi et al., 2016). In addition, Magritsky et al. (2018) detected an increased runoff trend of
 1429 5-10 %, compared to a reference period of 1936 to 1975, in most of the major Russian rivers discharging into
 1430 the Arctic Ocean. This trend is mostly due to a climate-induced increase since the second half of
 1431 ~~1980s~~1980's (Magritsky et al., 2018). However, due to gaps in the monitoring programs, these estimates
 1432 have a large uncertainty: focusing on river discharges from the six largest Eurasian rivers to the Arctic
 1433 Ocean, estimates of the increase range from 7% (Peterson et al., 2002) to 1.5 % (Shiklomanov and Lammers,
 1434 2009).

1435

1436 Permafrost thawing has resulted in releases of old carbon storages, but so far there is no clear evidence on
 1437 the impact of permafrost thawing on the net emissions of CO₂ and CH₄ to the atmosphere (IPCC, 2019). A
 1438 potential explanation of no or weak net increase is that a fraction of the released methane has been taken by
 1439 rivers instead of emitted to the atmosphere. Increased amounts of organic carbon in rivers impact the
 1440 regional and global biochemical and methane cycles (Shakhova et al., 2007; Wild et al., 2019). With the
 1441 accelerating permafrost thaw, also the atmospheric emissions are expected to increase, in particular for CO₂
 1442 but also for CH₄. Expected future changes in river ice regime are consistent with the expected changes in the
 1443 duration of the cold season and accumulated negative air temperatures. Significant changes are expected for
 1444 the rivers in the Kola Peninsula and the lower reaches of the rivers Northern Dvina and Pechora, whereas the
 1445 lowest changes are expected for the central parts of Eastern Siberia (Agafonova et al., 2017). Due to
 1446 anthropogenic activities (above all industry, municipal services, and filling of reservoirs), water withdrawal
 1447 from Russian Arctic rivers and related groundwater systems is approximately 20.6 km³ per year, and it is
 1448 expected to increase to 37 km³ per year by 2025 to 2030 (Magritsky et al., 2018). Features of these changes
 1449 at the marine margin of the Lena River delta are different compared to changes in the delta head area.

1450

1451 The hydrological representativeness of a glacier is a new characteristic, and of practical importance for
 1452 basin-wide tasks of hydrology and glaciology. For its evaluation, it is proposed to replace the seasonal air
 1453 temperatures with the glacier summer mass balance (BS) or to include BS in the multiple regression
 1454 equations for calculating the runoff of rivers fed by melting of snow and ice. This method can be
 1455 recommended for at least of some glaciers in the existing network of the World Glacier Monitoring Service
 1456 (WGMS) (Konovalov et al., 2019).

1457

1458 2.3.2 Marine ecology (Q8)

1459

1460 *Living marine organisms weaken or even subdue CO₂ accumulation*

1461 The important climatological role of the world's oceans is to reduce the CO₂ accumulation into the
 1462 atmosphere through its absorption. This mechanism is ordinarily viable as the partial pressure of dissolved
 1463 CO₂ in marine surface waters is less than the content of CO₂ in the overlying atmosphere. Due to the organic
 1464 pump, a net draw down of atmospheric CO₂ into the ocean is put into effect. It proceeds in the process of
 1465 sinking of particulate organic carbon of algal origin: organically bound CO₂ is released through
 1466 remineralization and further accumulated in the deep ocean. In contrast, owing to the processes of carbonate
 1467 counter pump, CaCO₃ is exported downward and, at depth, dissolves causing a net release of CO₂ to the
 1468 atmosphere (Balch et al., 2016). However, there are living marine organisms that are able to weaken or even
 1469 subdue CO₂ accumulation, at least within their habitat. Among this group of marine organisms, the leading
 1470 role belongs to coccolithophores. Among marine bio systems, coccolithophores (class Primmnesiophyceae) are
 1471 most productive calcifying algae (Taylor et al., 2017). They both produce particulate inorganic carbon (in the
 1472 form of calcite) and promote the increase of CO₂ partial pressure ($p\text{CO}_2$) in the ambient marine surface
 1473 waters. Thus, the biological activity of coccolithophores can exercise a direct influence on both the CO₂ flux
 1474 exchange at the atmosphere-ocean interface and the marine carbonate chemistry system (CCS). The rain
 1475 ratio, i.e. the ratio of particulate inorganic carbon to organic carbon, determines the intensity and direction of
 1476 CO₂ flux at the atmosphere-ocean interface. In the case of coccolithophores, the rain ratio is above unity
 1477 within their habitat area, which potentially can have climatic consequences but also drive alterations in
 1478 marine CCSs (Balch 2018).

1479

1480 *Emiliania huxleyi* is the most widespread coccolithophorid algal species in Earth's oceans, which, in light of
 1481 the above, naturally explains why this is one of the best-studied marine algae. Of all other coccolithophores,
 1482 *E. huxleyi* is probably the most successful in forming extensive blooms in world-wide marine waters ranging
 1483 from oligotrophic to eutrophic. Unlike diatoms and dinoflagellates, this alga is phenomenally immune to
 1484 both light-limitation and very high light intensities. As high levels of incident light/irradiance enhance
 1485 calcification (which is predominantly a light-dependent reaction), it is supposed that the calcification
 1486 machinery enables *E. huxleyi* cells to resist photodamage through dissipating excess energy. This specialty is
 1487 important in case of nutrient-depleted waters, especially in combination with the high affinity of *E. huxleyi*
 1488 for nutrients including nitrogen but especially phosphorous. The property of both mixotrophic nutrition, and

1489 resistance, at least partial, to zooplankton grazing and virus attacks (due to cell's coverage by calcite
 1490 scales/coccoliths) contribute to this alga ability to sustain a variety of unfavorable conditions and retain
 1491 steadfastly its ecological niche (Godrijan et al., 2020). Thus, the elaborate biology of *E. huxleyi* cells imparts
 1492 to them the intrinsic and rather rare property of pursuing growth-maximizing and loss-minimizing life
 1493 strategies. This property reveals itself through multiple manifestations, two of which are vastness and
 1494 sustainability of *E. huxleyi* bloom areas. A typical bloom surface is not less than thousands of square
 1495 kilometers, but in many marine environments it is far larger (Kondrik et al., 2018b). For example, in some
 1496 years, the value of S in the North and Norwegian Sea can be well above 100 000 km², in the Bering Sea
 1497 maximum bloom area (S) values were registered at 250 000 km², particularly large *E. huxleyi* bloom areas
 1498 (up to 380 000 km²) were observed in the Barents Sea (Kondrik et al., 2017). Within the subpolar and polar
 1499 zones of the Northern Hemisphere, in the waters around the Great Britain, in the North, Norwegian,
 1500 Labrador, Greenland, Barents, and Bering seas *E. huxleyi* blooms occur annually although with largely
 1501 varying intensity (Pozdnyakov et al., 2017). The duration of blooms in the Northern Atlantic and the Barents
 1502 Sea is on average about three-four weeks. The moment of onset of the *E. huxleyi* bloom area maximum shifts
 1503 from June-July to September-October for the seas located at the temperate, subpolar and polar latitudes of
 1504 the Northern Hemisphere, respectively. This sequence mimics the flow pattern of the Gulf Stream. In the
 1505 Bering Sea, the temporal pattern of S variations reveals two periods (1998-2001 and 2018-2020) of
 1506 extraordinary intense *E. huxleyi* outbursts. It is hypothesized that this phenomenon was driven by massive
 1507 advection of Fe-depleted North Pacific waters due to a significant weakening of the Alaskan Current. The
 1508 latter is supposed to be a teleconnected aftermath of exceptionally strong El Niño events in 1996-1997 and
 1509 2017, respectively (Pozdnyakov et al., 2020).

1510
 1511 Satellite-borne estimations made during 1998-2018 showed that *E. huxleyi* outbursts resulted in a release of
 1512 inorganic carbon (PIC) in the form of CaCO₃ in surface waters in amounts ranging from ~10 to several
 1513 hundreds of kilotons. In the Barents Sea, the released PIC content varied between ~100 kt and 250-300 kt,
 1514 whereas in the Bering Sea, during the two periods of exceptional activity, the PIC content was as high as 500
 1515 kt (Kondrik et al., 2017). There is ample evidence that the release of PIC was accompanied by a significant
 1516 increase in CO₂ partial pressure ($\Delta p\text{CO}_2$) within the bloom area: between 1998 and 2016, the mean and
 1517 maximum values of the ratio $\Delta p\text{CO}_2/(\Delta p\text{CO}_2)_{\text{background}}$, varied in the ~~ranges~~ ranges of ~ (20-40)%, and ~(30-
 1518 60)%, respectively. The highest numbers were registered in the Bering and Barents seas (Kondrik et al.,
 1519 2018a; 2019). Also, there is space borne evidence for the atmospheric columnar ΔCO_2 enhancement
 1520 (ΔCO_2)_{atm} over *E. huxleyi* blooms: numerous case studies in the aforementioned North Atlantic seas as well
 1521 as in the Barents and Black seas proved that (ΔCO_2)_{atm} could reach 2-3 ppm (Kondrik et al., 2019; Morozov
 1522 et al., 2019).

1523
 1524 Notwithstanding the remarkable ability of *E. huxleyi* to grow under conditions unfavorable for algae of other
 1525 functional groups (e.g. diatoms, flagellates, cyanobacteria), a highly irregular pattern of the registered two-
 1526 decadal (1998-present) time series of S , PIC, and $\Delta p\text{CO}_2$ are indicative of susceptibility of this alga outbursts

1527 to environmental conditions (Nissen et al., 2018; Kazakov et al., 2019; Silkin et al., 2019). Statistical
1528 prioritization of non-biogenic forcing factors (FFs) shows that the latter are sea- and time-period specific
1529 (Pozdnyakov et al., 2019). Thus, in the Barents Sea, sea water temperature (SWT) is the highest-ranked FF,
1530 followed by PAR (photosynthetic active radiation). In the Bering Sea, beyond the aforementioned periods
1531 (1998-2001 and 2018-present), sea surface salinity (SSS) is the FFs leader, with PAR as a runner up,
1532 whereas SWT is only third in the row. Although these assessments are done without explicitly considered
1533 nutrients concentrations (NCs), implicitly NCs were among the FFs. Indeed, arguably, variations in SWT,
1534 SSS, CHL, MLD, and surface current speed/advection (tested as FFs) indirectly account for the variations in
1535 NCs as well in such CCSs parameters as alkalinity and basicity (Durairaj et al., 2015; Pozdnyakov et al.,
1536 2019, and references therein).

1537
1538 In the long run, ~~under the conditions of~~ steady accumulation of CO₂ into the atmosphere, ~~this factor~~ should
1539 ~~be~~ closely ~~be~~ considered (Rivero-Calle et al., 2015). The action of a rising atmospheric CO₂ concentration is
1540 expected to proceed through a number of direct and indirect interactions (Fig. 7), both of which should
1541 ultimately cause alterations in the rain ratio. An increase in the atmospheric CO₂ concentration leads to the
1542 rising of the global temperature, and further to the strengthening of stratification, intensification of irradiance
1543 within the euphotic zone and cutting of nutrient fluxes from below. Although increases in CO₂ fluxes to the
1544 surface ocean cause a reduction of pH and CO₃²⁻ levels in water, the large pool of HCO₃⁻ remains to support
1545 the calcification machinery. Thus, it will lead to the establishment of environmental conditions unfavorable
1546 for non-calcifying phytoplankton (NCP), but beneficial (or at least endurable) for coccolithophores in
1547 general and *E. huxleyi* specifically. The reduction of NCP and uncontested growth of *E. huxleyi* drives a
1548 further reduction of dissolved CO₂ consumption by other groups of phytoplankton, increase in *p*CO₂ in the
1549 surface ocean and intensification of CO₂ fluxes into the atmosphere. Concurrently, through a system of
1550 feedback interactions, alterations in the rain ratio are bound to affect the carbon fluxes at the water-
1551 atmosphere interface. Therefore, the scenario of further increases atmospheric CO₂ concentration in the
1552 future, in all probability, implies a vaster proliferation of *E. huxleyi* in the world's oceans.

1553
1554 In combination with statistic-based-mathematical models of *E. huxleyi* blooms (Pozdnyakov et al., 2019), the
1555 available IPCC climate models permit mid-term projections of the forthcoming changes (Gnatiuk et al.,
1556 2020). However, our knowledge on the reciprocal influence of climate change and both the structure and
1557 functioning of marine ecosystems (even at the level of primary producers!) is still insufficient to confidently
1558 prognose the future dynamics of the *E. huxleyi* phenomenon. More studies are required even to fully
1559 understand the mechanism of intracellular light-dependent reaction of calcification, its dependency on both
1560 seawater carbonate chemistry and environmental FFs (Vihma et al., 2019). Creation of respective
1561 multidecadal databases (as in Kazakov et al., 2019) as well as further delivery of satellite and *in*
1562 *situ*/shipborne/laboratory data are necessary to improve our capacity to assess with certainty the
1563 climatological and ecological role of *E. huxleyi* blooms on regional and global scales (Fig. 7).

1564

1565 2.3.3 Lakes and rivers (Q9)

1566 *Organic carbon in lakes*

1567

1568 Spatial variability, an essential characteristic of lake ecosystems, has often been neglected in field research
 1569 and monitoring. The detected spatial "noise" strongly suggests that besides vertical variation also the
 1570 horizontal variation should be considered in the ecosystem monitoring and, most importantly when the role
 1571 of dissolved organic carbon (DOC) on the CO₂ flux is estimated (Manasypov et al., 2015; Leppäranta et al.,
 1572 2018). In natural waters with an increasing level of colored dissolved organic matter (CDOM) concentration,
 1573 the water color is shifted towards brown. The key "permanent" landscape variables, the coverage by lakes
 1574 and peatland in the catchment area can be strongly correlated with lake elevation above the sea level. A high
 1575 lake coverage indicates a low CDOM concentration, while a high peat coverage indicates the opposite
 1576 (Arvola et al., 2016). For example in Finland, recent results from inland water studies have not shown any
 1577 overall, consistent large-scale changes in CDOM concentrations over the last 101-year period (Arvola et al.,
 1578 2017). Rather, CDOM changes in individual lakes have been related to changes in land use in the drainage
 1579 basin. Manasypov et al. (2015) reported results from Siberian lakes, representing a discontinuous permafrost
 1580 zone, and addressed that although the concentration of most elements in the lakes are lowest in spring, the
 1581 maximal water coverage of land made it as an significant reservoir of DOC. The soluble metals in the water
 1582 column that can be easily mobilized to the hydrological network.

1583

1584 In very shallow freezing lakes, the volume liquid water is much reduced due to ice growth, and rejection of
 1585 nutrients and pollutants in the ice growth causes major enrichment of the water body. This has major
 1586 implications to the ecosystem of these lakes (Yang et al., 2016; Song et al., 2019). Freezing rejects some 80-
 1587 90 % of the impurities in freshwater lakes. On the other hand, ice cover accumulates atmospheric deposition
 1588 over several months but releases them into the water body within one month's melting phase. Rejection of
 1589 nutrients and pollutants in lake ice growth causes major enrichment of the water body in shallow lakes and
 1590 notable increases in nutrient concentrations in a shallow lake during seasonal ice growth (Fang et al., 2015).

1591

1592 *Lake carbon balance*

1593

1594 Arctic and boreal lakes are an important natural source of CH₄ ~~to~~ into the atmosphere (Bastviken et al, 2011).
 1595 Methane is ~~mainly~~ produced mainly in the bottom sediments and/or hypolimnion, where most of the
 1596 anaerobic decomposition of organic matter take place, and then is either oxidized to CO₂ in the water column
 1597 or emitted to the atmosphere. At Kuivajärvi, a typical meso humid lake located in Southern Finland, it was
 1598 found that 91% of available CH₄ was oxidized in the active CH₄ oxidation zone during hypolimnetic hypoxia
 1599 (Saarela et al., 2020). In warm springs, the early onset of thermal stratification with cold and well-
 1600 oxygenated hypolimnion delays the period of hypolimnetic hypoxia and thus limiting the production of
 1601 methane. At Kuivajärvi measured CO₂ fluxes (F-CO₂) showed that the lake acted as net source of carbon
 1602 during two open-water periods (Mammarella et al., 2015). During daytime, with typically high wind speeds,

1603 shear-induced water turbulence controls the water-air gas transfer efficiency, thus enhancing the vertical
 1604 diffusive fluxes across the water-air interface. However, during calm nighttime conditions, buoyancy-driven
 1605 turbulent mixing, associated with penetrative cooling of surface water, controls the gas exchange, and simple
 1606 wind speed-based transfer velocity models strongly underestimate F- CO₂ (Mammarella et al., 2015). Kiuru
 1607 et al. (2018) developed a model simulating CO₂ dynamics of a boreal lake in warming climate. The
 1608 simulations for 2070-2099 showed a 20–35% increase in the CO₂ flux from the lake compared to the
 1609 reference period of 1980–2009.

1610

1611 *Lake ice cover*

1612 Wei et al. (2016) studied the Lake Inari (67.14 N, 25.73 E), Finnish Lapland, in winters 1980/1981 -
 1613 2012/2013, and observed an increasing trend in the air temperature during the freezing season, associated
 1614 with an increasing trend in the water precipitation during winter. Low temperatures with less precipitation
 1615 lead to the formation of columnar ice, while strong winds together with heavy snowfall favored granular ice
 1616 formation. Karetnikov et al., (2017) analyzed long-term ice conditions in Lake Ladoga, Russia, for the period
 1617 of 1913–2015 and showed that the mean freezing and breakup dates were November 26 and May 15,
 1618 respectively, and that the annual frequency of complete freeze over of the lake was 0.83. The period from
 1619 1990 to present was much milder than the preceding years. The annual increase in the ice concentration
 1620 depended on the accumulated freezing-degree-days (AFDD) and the hypsographic curve, while the ice
 1621 thickness increased with the square root of AFDD.

1622

1623 An analysis of a Siberian thermokarst lake located in the Lena River Delta, characterized as a floating ice
 1624 lake, showed that the temporal dynamics and magnitude of heat fluxes and surface energy balance closures
 1625 are substantially different depending on lake surface conditions (Franz et al., 2018). Sensible heat and latent
 1626 heat fluxes, modelled using available heat bulk transfer models (Woolmay et al, 2015; Verburg and
 1627 Antenucci, 2010; Andreas et al, 2002), tend to underestimate the measured fluxes and show less variability
 1628 over freezing ice cover, melting ice in Spring, as well as over open water in Summer. However, the
 1629 performance of these models depends also on the accuracy of meteorological and hydrological input
 1630 parameters, which should be carefully measured especially during challenging winter conditions.

1631

1632 The seasonal lake ice cover is a sensitive indicator of climate variations in the Arctic (Kirillin et al., 2012;
 1633 Leppäranta, 2015). To work more on this question, Lake Kilpisjärvi (surface 37.1 km², max depth 57 m), a
 1634 tundra lake in northern Finland, has been under an intensive ice-related field programs in recent years. The
 1635 research covered the whole year but was focused on the melting period in May–June. The heat budget over
 1636 the ice season was dominated by the radiation balance. Turbulent fluxes were significant before the freeze-up
 1637 in fall, but in the ice season they were small. The evolution of ice thickness served as a very good
 1638 approximation to the total surface heat flux (Leppäranta et al., 2017) (Fig. 8). In the melting stage, solar
 1639 radiation, the strongest forcing of the water body beneath ice cover, breaks the stability and initiates
 1640 convective turbulent mixing. This brings heat from the deeper water to ice, enhancing melting at the ice

1641 bottom (Kirillin et al., 2018). Thus, the common assumption of the heat flux from the water to ice to be due
1642 to molecular conduction does not hold in the melting stage but it is much higher. The ice–water interaction
1643 under lake ice has not been well covered in earlier studies of ice growth and melting.

1644
1645 The ice melting process was studied in detail in Lake Kilpisjärvi. The melting progressed in the upper and
1646 lower surfaces and in the interior, with proportions depending on the solar flux and optical properties of the
1647 ice, and were therefore case-dependent. About one-third of the solar flux that penetrated the ice returned to
1648 ice bottom, providing heat for melting. This was consistent with the under-ice results by Kirillin et al. (2018).
1649 In 2013 a rapid ice breakage event completed the ice breakup in a short time interval, with final breakage at
1650 the ice porosity 40-50%. A lake ice melting model should include the thickness and porosity of ice, with
1651 porosity connected to an ice strength criterion (Leppäranta et al., 2019).

1652
1653 *Lake Baikal and Selenga River delta*

1654 The Selenga River, the main tributary of Lake Baikal, has a catchment area of 450 000 km² in the boundary
1655 region between Northern Mongolia and Southern Siberia. This area is well known by its climate, land use
1656 and dynamic socioeconomic changes which might have negative impacts on the ecosystems of Lake Baikal
1657 and thus was selected as PEEEX field laboratory within PEEEX subprogram Selenga-Baikal Network
1658 (www.atm.helsinki.fi/peex/index.php/baikal-selenga-network-basenet). In the recent past, hydroclimatic
1659 development together with land use changes led to a contaminant influx from mining areas and urban
1660 settlements increased. Additional hydrological modifications due to the construction of dams and
1661 abstractions/water diversions from the Selenga's Mongolian tributaries could lead to additional alterations
1662 (Karthe et al., 2017b). In addition to Selenga River, a key issue for an improved understanding of regional
1663 impacts of the environmental change is to disentangle the influence of climate change from that of other
1664 pressures within the catchment (Lychagin et al., 2017). The PEEEX subprogram Selenga-Baikal Network
1665 aims at integrated field-based and modeling knowledge to develop basin-wide conceptual framework of
1666 riverine fluxes (Kasimov et al., 2017a; Karthe et al., 2019).

1667
1668 As a PEEEX field laboratory, regional large-scale assessments made it possible to predict the comprehensive
1669 nature of hydrological and geochemical changes driven by climatic processes and human impacts. Heavy
1670 metals in water and sediments (Kasimov et al., 2020a, 2020b) and fish communities (Kaus et al., 2017) were
1671 measured since 2011 in over 50 locations around the catchment. The mining zones are potential hotspots for
1672 increasing metal loads to downstream river systems. Several metals (Al, Cd, Fe, Mn, Pb and V) are exported
1673 from mining sites to the downstream river system, as shown by net increasing mass flows. Based on a novel
1674 partitioning coefficient approach (Table Fig. 29), contrasting patterns with domination of both particulate and
1675 dissolved phases in different parts of the basin were found. Such heterogeneity in the metal partitioning is
1676 likely to be found in many large river systems.

1677

1678 Multi-scale modeling ranged from the basin wide (Malsy et al., 2017; Frolova et al., 2017) to specific sub-
 1679 regions, such as particular segments of the river system (Kaus et al., 2017; Thorslund et al., 2017; Garmaev
 1680 et al., 2019) or its delta (Chalov et al., 2017a, 2017b; Shinkareva et al., 2019), and identified reactions of
 1681 hydrogeochemical pathways on climate change. The mean flow reduction in the Selenga River was 3-5% ~~in~~
 1682 ~~the 2020s-2030s~~ during 2020's to 2030's and 4-25% ~~in the 2080s-2090s~~ during 2080's to 2090's, being a
 1683 crucial driver of ongoing and future hydrogeochemical changes. Increases in temperatures with permafrost
 1684 thaw and the expansion of agricultural, mining and urbanization processes may induce up to a 6% increase in
 1685 the particulate modes and 3% in the dissolved modes of some metals in the river system (Chalov et al.,
 1686 2018). Possible changes in the number or magnitude of high-flow events, caused by climatic or other
 1687 anthropogenic factors, could influence the total sediment deposition, which was primarily found to occur
 1688 during relatively short high-flow events. Such potential changes have important implications to the possible
 1689 spreading of polluted sediments (Pietron et al., 2015) and their storage in the Selenga River Delta, which is
 1690 an important wetland region forming the geochemical barrier which mitigate pollution of Lake Baikal by
 1691 riverine fluxes (Voropay and Kichigina, 2018, Chalov et al., 2015). The Selenga delta region sequester
 1692 various metals bound to Selenga River sediments (Chalov et al., 2015, Pietroń et al., 2018). The water
 1693 shortage decreases the processes of suspended sediment retention in the delta. The seasonal
 1694 hydrogeochemical patterns are explained by wetland inundation during floods and channel erosion or Baikal
 1695 wind surge during low flow periods (Chalov et al., 2017a, 2017b).

1696

1697 *Asian water lakes*

1698

1699 The largest internal drainage basins in the world are located in Central Asia, with a limited availability of
 1700 both surface and groundwater (Karthé et al., 2017a). Since the twentieth century, water resources of this
 1701 region have been over exploited and, for example, from small Mongolian headwater streams to the mighty
 1702 Aral Sea, surface waters have been partially desiccated. It seems that the implementation of the Integrated
 1703 Water Resources Management and water-food-energy nexus approaches would lead to a more
 1704 environmental-friendly future (Karthé et al., 2017). The lake-rich Qinghai-Tibet Plateau (QTP) has recently
 1705 been identified as the Third Pole of the Earth. Due to its high elevation and unique climate, QTP affects the
 1706 global and local climate and played an important role on the Central and Southern Asian water cycle (Zhang
 1707 et al., 2018). Lake-atmosphere interactions have been quantified over open-water periods, yet little is known
 1708 about the lake ice thermodynamics and heat and mass balance during the ice-covered season. A modelling
 1709 study for a thermokarst lake in the QTP was performed (Huang et al., 2019a). Strong diurnal cycles were
 1710 seen for all surface heat fluxes. The ice mass balance was dominated by the growth and melt at the base, but
 1711 the surface sublimation was also crucial for the ice loss, accounting for up to 40% of the maximum ice
 1712 thickness and 41% of the lake water loss during the ice-covered period. The strong penetration of solar
 1713 radiative flux is the dominant contributor to the high value of upward sensible heat flux at ice bottom,
 1714 resulting in a relatively thin ice cover compared with equivalent high-latitude climate.

1715

1716 2.4 SOCIETY

1717

1718 The anthropogenic impact has been addressed as one of the PEEX themes for the society system. The
 1719 discussion on the mitigation and adaptation, including urban infrastructure design and risk assessment, are
 1720 addressed in this context (Q10, section 2.4.1). The social transformations are discussed in terms how local
 1721 reindeer grazing interacts with the environment (Q11 section 2.4.2). The adaptive capacity of the Northern
 1722 societies depends on their environment, demographic structure and economic capacity, and the
 1723 environmental hazards and environmental health under changing climate are the key research areas in this
 1724 context (Q12 section 2.4.3.).

1725

1726 2.4.1. Anthropogenic impact (Q10)

1727

1728 *Mitigation*

1729 Arctic climate change generates a need for long-term planning and development of new socio-economic
 1730 infrastructures, such as dams, bridges, roads and transnational and regional energy networks. For this task,
 1731 new climate-based forecasting tools, cost and operational risk estimates as well as other methods and tools
 1732 for an infrastructure and urban design are needed. As an example, engineering calculations for maximal
 1733 discharges were provided for the Nadym River in Russia (Shevnina et al., 2017). Badina (2018) introduced a
 1734 method for the natural risk assessment by using indices based on socioeconomic potential data and spatial
 1735 distribution of natural hazards. This method has been tested and used to identify the most vulnerable
 1736 municipalities in South Siberia. Another example of new methods is a “Green Factor tool” to increase the
 1737 share and effectiveness of green areas in urban environments and cities. An ambitious target set in this tool
 1738 could encourage or force urban developers to aim higher with the planning of green areas and construction,
 1739 however the existing regulations challenge the use of this approach (Juhola, 2018).

1740

1741 The energy production is of fundamental importance for the society functions, and new clean energy
 1742 technologies are needed for hindering the climate change. The potential of hydropower production under
 1743 probabilistic projections of annual runoff rate and future changes in the potential hydropower production
 1744 need to be evaluated (Shevnina et al., 2019). All the Nordic countries are vulnerable to various degrees to
 1745 potential cross-border impacts, due to their energy sectors being highly globalized and interconnected.
 1746 However, cross-border impacts are not yet properly included in Nordic climate assessments or energy
 1747 strategies. The EU’s new Green Deal is pivotal in this respect, as for the first time emissions along the whole
 1748 supply chain (oil, gas, coal, renewables) become under scrutiny and as part of a normative governance.
 1749 Therefore, policy makers and energy planners should be assisted in making comprehensive vulnerability
 1750 assessments that address both domestic and international climate risks (Groundstroem and Juhola, 2019).

1751

1752 2.4.2 Environmental impact (Q11)

1753

1754 *Reindeer (Rangifer tarandus L.) grazing and ground vegetation structure and biomass*

1755

1756 Reindeer (*Rangifer tarandus L.*) grazing in the North affects the ground vegetation structure and biomass and
 1757 cover of lichens. It seems that reindeers affect GHG fluxes from the forest field layer. Grazing changes affect
 1758 the vegetation composition and thereby emissions (Köster et al., 2018). Köster et al. (2017) provided detailed
 1759 information on soil CO₂ effluxes, which were mostly affected by the year of measurement, time of
 1760 measurement, soil temperature and also by the management, resulting in higher CO₂ emissions on the grazed
 1761 areas. Soil moisture content did not affect the soil CO₂ efflux. For example, in the Finnish Lapland the
 1762 average soil CO₂ efflux values were significantly higher in 2014 compared with 2013, mainly due to
 1763 differences in the soil temperature at the beginning of the season (Köster et al., 2017). Furthermore, grazing
 1764 significantly decreased the biomass and cover of lichens and also the amount of tree regeneration. In a
 1765 subarctic mature pine forest, grazing did not affect the soil temperature or soil moisture. No statistically
 1766 significant effect of grazing on the soil CO₂ efflux, soil C stock or soil microbial C biomass was found. The
 1767 soil microbial N biomass was significantly lower in the grazed areas compared to the non-grazed areas. It
 1768 seems that in the boreal subarctic coniferous forests, grazing by reindeer can be considered as "C neutral"
 1769 (Köster et al., 2015). There is also indication that reindeer grazing affects the boreal forest soils e.g. their
 1770 fungal community structure and litter degradation (Santalahti et al., 2018).

1771

1772 2.4.3 Natural hazards (Q12)

1773

1774 Under this theme, the PEEX research has so far focused on environmental health issues. These include
 1775 diseases, impact of UV radiation, and air pollution in urban environments. The spread of diseases caused by
 1776 living pathogens is basically determined by environmental conditions. Medico-geographical assessments are
 1777 usually based on identification of the links between the spread of diseases and factors of the geographical
 1778 environment.

1779

1780 *Naturally-determined diseases*

1781 Climatic factors are deemed among the main determinants for the spread of naturally-determined diseases
 1782 (Malkhazova et al., 2018). Emerging zoonotic diseases are expected to be particularly vulnerable to climate
 1783 and biodiversity disturbances. Anthrax is an archetypal zoonosis that manifests its most significant burden on
 1784 vulnerable pastoralist communities. Ezhova et al. (2021) investigated the dynamics of environmental factors
 1785 that led to an anthrax outbreak in Yamal Peninsula, Siberia, during 2016. They found that the local
 1786 permafrost was thawing rapidly for the last 6 years before the outbreak, supporting the hypothesized role of
 1787 permafrost thaw in triggering this outbreak, and concluded further that the spread of anthrax was likely
 1788 intensified by the extremely dry summer of 2016 in the region. Overall, the recent findings highlight the

1789 significance of warming temperatures for anthrax ecology in northern latitudes, and suggest potential
1790 mitigating effects of interventions targeting megafauna biodiversity conservation in grassland ecosystems
1791 and animal health promotion among small to midsize livestock herds (Walsh, et al., 2018). Equally important
1792 is the monitoring of climatic factors, such warming and precipitation extremes, in Arctic regions previously
1793 contaminated by Anthrax (Ezhova et al., 2021).

1794

1795 *UV variations*

1796 Different geophysical parameters affecting the UV molecular number density show that especially at high
1797 altitudes, the increased surface albedo has a significant effect on the UV growth. The new parameterization
1798 of the on-line UV tool (*momsu.ru/uv/*) for Northern Eurasia allows us to determine the altitude dependence
1799 of UV and to estimate the possible effects of UV on human health considering different skin types and
1800 various open body fraction for January and April conditions in the Alpine region (Chubarova et al., 2016b).
1801 Using UV satellite retrievals, ERA-Interim data and the INM-RSHU chemistry-climate model, the changes
1802 in the UV irradiance and UV resources were estimated over Northern Eurasia for the 1979-2015 period,
1803 demonstrating significant UV increases over vast areas (Chubarova et al., 2020). Referring to long-term UV
1804 measurements and model simulations in Moscow, a statistically significant positive trend of more than 5%
1805 per decade since 1979 was evaluated (Chubarova et al., 2018). Related to the connection between UV
1806 variation and stratospheric O₃, see also the section 2.2.1 Atmospheric composition and chemistry.

1807

1808 *Examples of air pollution episodes*

1809

1810 Street-level urban air pollution is one of the key topics in urban environments. For example, in Norway,
1811 Bergen, the most extreme cases of repetitive wintertime air pollution episodes, followed by increased large-
1812 scale wind speeds above the valley, were transported by the local re-circulations to other less polluted areas
1813 with only slow dilution. This result underlines the need for better described assumptions on transport paths
1814 and weak dispersion in classical air pollution models, in order to improve the current air quality forecasts in
1815 urban areas (Wolf- Grosse et al., 2017b). A link between the persistence of the flow above the Bergen valley
1816 and the occurrence and severity of the local air pollution episodes was found. Analysis of the large-scale
1817 circulation over the North Atlantic-European region, with respect to air pollution in Bergen, revealed that the
1818 persistence in meteorological conditions connected with air pollution episodes is not necessarily caused by
1819 large-scale anomalies of the atmospheric circulation over the Norwegian west coast, but rather connected
1820 with anomalies as far away as Greenland (Wolf-Grosse et al., 2017a).

1821

1822 In Russia, especially intensive atmospheric pollution episodes have severe impacts on the environment and
1823 human health. Popovicheva et al (2019b) analyzed the Tver region, north of Moscow, which was
1824 considerably affected the secondary organic aerosol (SOA) formation originating from long-lasting peat bog
1825 fires. Spectral absorbance characteristics were similar to peat burning and traffic source emissions during fire
1826 and non-fire related days and confirmed the effect of transported peat smoke on air quality in a megacity

1827 environment (Popovicheva et al., 2019b). Popovicheva et al. (2019b) also showed that long-term transport
 1828 from the North-West Russia and Scandinavia influence the local population.

1829
 1830 Local Arctic air pollution alone can seriously affect public health and ecosystems locally, especially in
 1831 wintertime when the pollution can accumulate under inversion layers (Schmale et al., 2018a). We need more
 1832 research on the contributing emission sources and the relevant atmospheric pollution mechanisms, and more
 1833 detailed epidemiological or toxicological health impact studies in the Arctic. Socioeconomic changes
 1834 (shipping, tourism, natural resources extraction, increasing number of population) are already taking place in
 1835 the Arctic, and they will increase in the future. It is also expected that the emission types and magnitudes will
 1836 increase the number of exposed individuals (Arnold et al., 2016). There is still a large variation in the amount
 1837 of the location of emissions. Future predictions are even more difficult due to the yet unknown development
 1838 of the Arctic economic activities and their emissions (Arnold et al., 2016, Schmale et al., 2018a, 2018b).

1839

1840 3. SYNTHESIS AND FUTURE PROSPECTS

1841

1842 3.1 Future research needs from the system perspectives

1843

1844 For the Land ecosystem, the recent progress towards understanding of the Northern Eurasian Arctic - boreal
 1845 land ecosystems (section 3.1) are dealing with improved methodologies relevant to land processes (Q1),
 1846 observations on permafrost thawing (Q2), and observed changes in the Northern ecosystems, especially soil
 1847 conditions (Q3).

1848

1849 Improved satellite-based methods and (validation) data together with better quantification and, especially,
 1850 the scaling of the gross primary production (GPP) are enabling a better identification and quantification of
 1851 Earth surface characteristics and ecosystem carbon balance compared with the earlier capacity (Gurchenkov
 1852 et al., 2017, Rautiainen et al., 2016, Nitzbon et al., 2019, Boike et al., 2019, Terentieva et al., 2016), Zhang et
 1853 al, 2018, Pulliainen et al., 2017, Matkala et al., 2020; Bondur and Chimitdorzhiev, 2008 a,b). Intensive
 1854 research has been carried out on the quantification of the GPP, a key variable for biological activity, in
 1855 different conditions and at different scales (Pulliainen 2017, Kulmala et al., 2019, Matkala et al., 2020).
 1856 Further investigations are called for a more detailed understanding of the seasonal dynamics of the biological
 1857 activity.

1858

1859 The Northern Eurasian ecosystems' tipping points are related to multiple simultaneous stress factors. The
 1860 key stress factors here are the permafrost thawing and factors important for ecosystems, such as the
 1861 prolongation of the growing season, increase in the mean temperature of the growing season and forest fires
 1862 (Kukkonen et al. 2020, Biskaborn et al. 2019, Payne et al., 2016. Köster et al. 2016, Miles and Esau 2016,
 1863 Miles et al., 2019). New evidence on the progress of permafrost thawing in Siberia has been introduced by
 1864 Kukkonen et al. (2020) and Biskaborn et al. (2019). The permafrost thawing is also triggering yet not

1865 clearly-known processes related to changing fluxes, ecosystem processes and dynamics of greenhouse gas
1866 sinks and sources (Schuur et al., 2008, Thomson et al., 2017, Commane et al., 2017, Euskirchen et al., 2017,
1867 Dean et al., 2018, Thonat et al., 2017). The progress affecting permafrost thawing has not yet been analyzed
1868 in detail. For example, we need more information on the dynamics of how the thawing processes vary
1869 between soil types due to differences in water movement and, in the winter time, how the snow cover affects
1870 ground surface temperatures (Bartsch et al. 2010). In addition to permafrost processes, the recent advances in
1871 observed changes in the Northern ecosystem reveal a significant role of soil processes in biogeochemical
1872 cycles, especially the nitrogen cycle (Voigt et al., 2016, Pärn et al., 2018). Knowledge of the soil
1873 microbiological composition and the effect of forest fires have been improved (Köster et al., 2015, 2016,
1874 Zhang-Turpeinen et al., 2020), but further research is called for vegetation changes influencing the below-
1875 ground microbiology, its composition and enzymatic activity (Payne et al., 2016. Köster et al. 2016). The
1876 NDVI methods have made it possible to detect vegetation changes (Miles and Esau 2016). A range of
1877 vegetation cover changes in Siberia have been reported, such as the Arctic greening and browning processes,
1878 but e.g. the greening of Siberian cities remains an issue of intensive research also in the future (Miles and
1879 Esau 2016, Miles et al., 2019).

1880 For the Atmospheric system, the recent progress in understanding the Northern Eurasian Arctic - boreal land
1881 atmospheric system and the aspects of the megacity air quality (section 3.2) are dealing with atmospheric
1882 composition changes (Q4), key feedbacks between climate and air quality (Q5), and synoptic scale weather
1883 (Q6). Recent results demonstrate improved quantification of the carbon balance and CO₂ fluxes and
1884 concentrations due to land use change, forest fires in Siberia, and new understanding of aerosol sources and
1885 properties in the Arctic environment and across the Northern Eurasia (Pulliainen et al., 2017, Karelin et al.,
1886 2017, Rakitin et al., 2018, Skorokhod et al., 2017, Alekseychik et al. 2017). However, most of the results
1887 deal with atmospheric aerosol chemistry and physics in boreal and Arctic environments originating from
1888 measurements in the few flagship stations in Finland and Russia (Kerminen et al., 2018, Wiedensohler et al.,
1889 2019, Freud et al., 2017, Paasonen et al., 2018, Östrom et al., 2017, Kalogridis et al., 2018, Bondur et al.,
1890 2016, Bondur and Ginzburg 2016, Bondur et al. 2019 c,d, Bondur and Gordo, 2018; Mikhailov et al., 2017,
1891 Breider et al., 2017), indicating the need for a comprehensive station network in the PEEEX region. Black
1892 carbon emitted by the Siberian forest fires and some other sources, and its long range transport to the Arctic,
1893 are also widely discussed (Kalogridis et al., 2018, Bondur et al., 2016, Bondur and Ginzburg 2016,
1894 Mikhailov et al., 2017, Breider et al., 2017, Shevchenko et al., 2015, Konovalov et al., 2018, Marelle et al.,
1895 2018). In addition, measurements of ozone in the troposphere and stratosphere provide insight into
1896 atmospheric chemistry in urban environments (Skorokhod et al., 2017), UV radiation and human health
1897 (Chubarova et al., 2019). Environmental health, including the impacts of air quality and UV radiation, is
1898 foreseen as a high momentum research topic in the PEEEX domain, and further research is called for in this
1899 area.

1900
1901 Related to air pollution, we reported several new results on the dynamics between the haze pollution and
1902 boundary layer meteorology in enhancing air pollution in megacity environments (Zhao et al., 2017, Ding et

1903 al., 2016a, Wang et al., 2018b, Bai et al., 2018a, Ye et al., 2017). The long-term and comprehensive
 1904 measurements carried out especially at the SORPES station in Nanjing provide valuable data pools for such
 1905 studies (Ding et al., 2016a). However, the backbone of the recent progress has been the improved on-line
 1906 atmospheric measurements and the use of machine learning methods combined with different methodologies,
 1907 such as back trajectories together with the lidar and radiosonde data. In addition, improved models of
 1908 emission inventories together with the ECHAM-HAM and GAINS models have led to a better quantification
 1909 of aerosol number emissions. New knowledge has enabled the introduction of new theoretical arguments on
 1910 the feedbacks between high aerosol concentrations and the urban boundary layer (Petäjä et al. 2016). New
 1911 measurements have also been obtained from Siberian cities (Elansky et al., 2016, Chubarova et al., 2016a,
 1912 Mahura et al., 2018). However, we are still in the early phase of having a holistic picture on large-scale
 1913 feedbacks due to the lack of long-term, comprehensive measurements in these regions.

1914
 1915 Changes in the atmospheric dynamics in the North have potential impacts on short-term local/regional and
 1916 sub-seasonal to seasonal large-scale weather predictions, and on long-term projections on biogeochemical
 1917 systems. It is therefore crucial to understand changes in boundary-layer processes as well as synoptic- and
 1918 large-scale circulation in the Arctic and Northern Eurasia. Recent results show potential, but causally
 1919 arguable, connections between the alarming sea ice decline, evaporation, cloudiness, atmospheric circulation
 1920 and moisture transport as well as Arctic and European winter temperatures (Nygård et al., 2019, Rinke et al.,
 1921 2019, McCusker et al., 2016, Mori et al, 2014, Blackport et al., 2019; Cohen et al., 2020). Further
 1922 investigations are called for atmosphere-ice-ocean interactions, coupling between small-scale processes
 1923 (such as clouds and turbulence) and synoptic-scale weather, as well as for polar prediction and extreme
 1924 events. Furthermore, more quantitative knowledge is needed on pan-Arctic energy budgets (Spengler et al.,
 1925 2016). The urban heat island (UHI) phenomena taking place in Arctic cities has received an increasing
 1926 attention, and there is a special need for improved forecasting services for Arctic cities (Miles and Esau
 1927 2017, Konstantinov et al., 2018, Varentsov et al., 2018b).

1928
 1929 For the Water system, we discussed the Arctic sea ice dynamics and thermodynamics, snow depth and sea
 1930 ice thickness, sea ice research supporting navigation, and rare elements in the snow and the ocean sediments,
 1931 especially from the perspective of improvements in the observation and modelling methods (Q7, section
 1932 3.3.1.). New evidence on atmosphere-Arctic sea ice interactions have been provided by Lei et al. (2018), and
 1933 Jakobson et al. (2019). -Lei et al. (2018) analyzed how the climate warming would affect the winter growth
 1934 rate of thin and thick ice, and Jakobson et al. (2019) gave new insight into the relation between sea ice
 1935 concentration and the wind speed. Furthermore, advance has been made in understanding the
 1936 thermodynamics and metamorphosis of the snowpack on sea ice and their interactions with surface albedo
 1937 changes (Dou et al., 2019). Operational sea ice analysis is increasingly important for the Arctic shipping and
 1938 navigation (Lei et al., 2015, Karvonen et al., 2017). New results on rare elements, mineral composition and
 1939 CO₂ and methane fluxes associated with ocean sediments have been attained (Maslov, et al., 2018, Yasunaka
 1940 et al., 2018). This serves as an important information for mitigation plans, as well as for new estimates on the

1941 river runoff and discharge in Russian rivers into the Arctic seas (Grigoriev and Frolova 2018, Agafonova et
 1942 al., 2017).

1943
 1944 The marine Arctic ecosystems are under a progressive increase of anthropogenic impacts, the main issues
 1945 calling for better understanding being the integrated effect of Arctic warming, ice and snow melt, ocean
 1946 freshening, air quality and acidification of the Arctic marine ecosystems, primary production and carbon
 1947 cycle (Q8, section 3.3.2). Quantitative information about the CO₂ accumulation into the ocean is having a
 1948 high momentum. Marine organisms, such as coccolithoprip algae, are influencing the CO₂ flux exchange
 1949 (Kondrik, et al., 2018b, Pozdnyakov et al., 2017). In addition to changing marine environments, the Arctic –
 1950 boreal lakes and rivers may undergo changes in flooding, increasing the amount of fresh water and
 1951 allochthonous materials (Q9, section 3.3.3). In addition to the Arctic Ocean, the ice and snow conditions of
 1952 Northern lakes are under pressure. Lake Kilpisjärvi (Finland) (Arvola et al., 2017, Leppäranta et al., 2017)
 1953 and Lake Ladoga (Russia) (Karetnikov et al., 2017) have been under [an](#) intensive research, and the recent
 1954 results demonstrate changes in heat fluxes, ice cover periods and stratification. The browning of lakes and
 1955 lake sediments were discussed, and new results were attained from the Selenga River of the Baikal Lake.
 1956 Dramatic changes will be expected in the water runoff and in the amount of dissolved modes of metals, also
 1957 having serious impact on the environmental health (Chalov et al., 2015, 2016, 2017 a, 2017b, Karthe et al.,
 1958 2017 a, 2017b). As a comparison to the Northern high latitudes, we also discussed freezing lakes in Central
 1959 Asia, where the climate is cold and arid. There the ice is typically snow-free, or possesses only a thin snow
 1960 cover, allowing penetration of sunlight into the water body (Huang et al., 2019).

1961
 1962 For the Societal system, the anthropogenic impact has been addressed as one of the main themes (Q10). The
 1963 discussion on the mitigation and adaptation, including the urban infrastructure design (Juhola 2018) and risk
 1964 assessment, were addressed in this context (section 3.4.1). In social transformations, a special attention was
 1965 given to one of the most important local livelihoods in Lapland: reindeer grazing and how it interacts with
 1966 the environment (Q11 section 3.4.2). The adaptive capacity of the Northern societies rest on their
 1967 environment, demographic structure and economic activities (Q12). Referring to the earlier statement about
 1968 the future research needs for the Atmospheric system with respect to environmental health, here again we
 1969 would like to put an increasing attention to environmental health under changing climate, including the
 1970 spread of diseases and air pollution and their combined effects (section 3.4.3.).

1971
 1972 3.2 Feedback mechanisms under changing climate, cryosphere conditions and urbanization

1973
 1974 During the recent years, Kulmala et al. (2004, 2020) have focused on the quantification of the COntinental
 1975 Biosphere-Aerosol-Cloud-Climate (COBACC) feedback loop relevant to the boreal region in Northern
 1976 Eurasia. Previous results on the COBACC feedback loop addressed the role of BVOC emission dynamics
 1977 (Armeth et al., 2016). Both higher temperatures and increased CO₂ concentrations are (separately) expected
 1978 to increase emissions of biogenic volatile organic compounds (BVOCs) to the atmosphere. It also seems that

1979 the GPP is controlled by the BVOC effects on the clouds. Sporre et al. (2019) used an Earth System model to
 1980 estimate aerosol scattering due to enhanced BVOC emissions and estimated the associated negative direct
 1981 radiative effect (-0.06 W m^{-2}). The total global radiative effect associated with this feedback was estimated to
 1982 be -0.49 W m^{-2} (Sporre et al., 2019), indicating that it has the potential to offset about 13 % of the forcing
 1983 associated with a doubling of CO_2 . The direct effect of aerosol on GPP due to an increase in the fraction of
 1984 diffuse radiation was estimated between 6 and 14% increase in GPP at maximum observed aerosol loading
 1985 compared to low aerosol loading in Northern Eurasia forests (Ezhova et al., 2018b).

1986
 1987 The results from the Tibetan plateau demonstrate notable feedbacks between vegetation, BVOC emissions
 1988 and aerosol particles. The historical wetting of the TP region has increased the vegetation cover, allowing for
 1989 feedback processes via biogenic aerosol formation and aerosol-cloud-precipitation interactions. A significant
 1990 wetting trend since the early ~~1980s~~ 1980's in Tibetan Plateau is most conspicuous in central and eastern Asia.
 1991 Fang et al. (2019) hypothesized that the current warming may enhance emissions of biogenic volatile organic
 1992 compounds (BVOC), which can increase secondary organic aerosols concentrations, contributing to the
 1993 precipitation increase. The wetting trend can increase the vegetation cover and has a positive feedback on the
 1994 BVOC emissions. The simulations suggest a significant contribution of increased BVOC emissions to the
 1995 regional organic aerosol mass, and the simulated increase in BVOC emissions is significantly correlated with
 1996 the wetting trend in Tibetan Plateau.

1997
 1998 To estimate the net effects of various feedback mechanisms on land cover changes, photosynthetic activity,
 1999 GHG exchange, BVOC emissions, formation of aerosols and clouds, and radiative forcing (Q14) calls for
 2000 intensive collaboration and integration between the Arctic Ocean sciences and terrestrial sciences across the
 2001 Pan-Arctic domain and across the Arctic and high-latitude domain. The Arctic greening and browning
 2002 (section 3.1.3.) call for a multi-disciplinary scientific approach, improved modelling tools and new data to
 2003 deeply understand the biosphere-atmosphere-anthroposphere interactions and feedbacks. Petäjä et al. (2020a,
 2004 2020b) discussed the complexity of feedbacks, especially at the Arctic context, and the interplay between the
 2005 temperature, GHG, permafrost, land cover and water bodies and between photosynthetic activity, aerosols,
 2006 clouds and radiation budget. The current downturn of the arctic cryosphere (*section 3.1.2*), together with the
 2007 changes in sea ice dynamics and glaciers and the permafrost thawing, affect bot marine and terrestrial carbon
 2008 cycles in interconnected ways (section 3.3.1). Parmentier et al. (2017) discussed the changing arctic
 2009 cryosphere and how the processes in the ocean and on land are too often studied as separate systems,
 2010 although the sea ice decline connects the rapid warming of the Arctic, Arctic Ocean marine processes and
 2011 air-sea exchange of CO_2 . Thus, the future priorities would be on the development of our modelling tools
 2012 towards an all-scale modelling approach to cover the feedbacks, processes and interactions at the land-ocean
 2013 interface and also in urban environments in the Arctic region. We also need to support the further
 2014 development of the ground-based observation networks.

2015

3.3 Climate scenarios for the Arctic-boreal region

Climate scenarios set the urgency for the mitigation and adaptation actions for the Northern Eurasian region. The Arctic-boreal region combines an area of both amplified climate change (Arctic amplification) and large diversity in the model predictions (Collins et al., 2013; Hoegh-Guldberg et al., 2018). Under the “low-to-medium” RCP4.5 forcing scenario (van Vuuren et al., 2011), the CMIP5 multi-model mean temperature changes during the 21st century indicate the strongest winter-time warming of >5 °C in the Arctic Ocean, whereas the majority of the terrestrial region will warm by 2–4 °C (Fig. 12). Even during summertime, the continental warming over the region will generally exceed 2 °C. It is important to note that the diversity of model projections is accentuated over the Arctic and Northern Eurasian domain: the mechanisms behind the Arctic amplification are implemented in varying details in the distinct models, and the associated interactions and feedback processes provide a diverse picture of the future in the Arctic-boreal regions.

In addition to considerable trends in atmospheric temperatures, the models further indicate prominent changes in precipitation (Collins et al., 2013, Hoegh-Guldberg et al., 2018). For the Arctic boreal region, this is largely depicted as an increasing rainfall during both winter and summer, extending to 15-25% over most of the terrestrial domain over the winter and somewhat less during summer (Fig. 940). Contemporary warm Arctic temperatures and large sea ice deficits (75% volume loss) demonstrate climate states outside our previous experience. The modeled changes in the Arctic cryosphere demonstrate that even limiting the global temperature increase to 2 °C will leave the Arctic a much different environment by mid-century, with less snow and sea ice, melted permafrost, altered ecosystems, and a projected annual mean Arctic temperature increase of +4 °C. Even under ambitious emission reduction scenarios, high-latitude land ice melt, including Greenland, are foreseen to continue due to internal lags, leading to accelerating global sea level rise throughout the century (Overland et al., 2019).

4. CONCLUDING REMARKS

Only the integration of different observing networks and programs into an inter-operable and integrated observation system can provide data needed for understanding the mechanisms of the Arctic-boreal system. There is a fundamental need for an integrated, comprehensive network of the-state-of-the art *in situ* stations measuring Earth surface – atmosphere interactions (Kulmala et al., 2016a, 2018; Uttal et al., 2016; Hari et al., 2016; Alekseychik et al., 2016; Vihma et al. 2019). The results obtained in the Pan Eurasian Experiment (PEEX) programme in Russian and China introduced in this paper are based on a combination of long-term observations and campaign data. In addition, the Arctic marine regions require comprehensive observations and subsequent synthesis, as these regions are under a lot of environmental stresses. Therefore, we need more *in situ* observations of the Arctic system covering the marine atmosphere, sea ice and ocean. However, there are pronounced technological and logistical challenges to setup such continuous, marine *in situ* observations (e.g. Vihma et al. 2019). Furthermore, improved monitoring is needed for river discharge and

2054 associated fluxes of greenhouse gases and other key compounds and more research on the understanding of
 2055 coastal processes and atmospheric transport and specific regional socioeconomic issues and their interactions
 2056 with changing ~~environment~~environments (Vihma et al., 2019; Petäjä et al., ~~2020~~2020a).

2057
 2058 The international organizations and bodies like the Arctic Council (SAON's Roadmap for Arctic Observing
 2059 and Data Systems, ROADS), EU Horizon2020 (Blue Growth INTAROS and APPLICATE projects), GEO-
 2060 CRI (high Mountains and cold regions), the Belmont Forum COPERNICUS and WMO are coordinating
 2061 development of the Arctic data and services. New data products are expected from the large-scale MOSAiC
 2062 campaign and projects like ERA-PLANET iCUPE (Petäjä et al. 2020b) or ArcticFLUX to monitor the
 2063 interface between the marine Arctic and Eurasian continent. Also, national-based Arctic observations and
 2064 research programs like AC³ by German institutes play a significant role. Russia conducts extensive research
 2065 in the Arctic region, notably on the manned drifting ice stations. These Arctic observation activities are
 2066 coordinated and carried out by Roshydromet, universities and Russian Academy of Sciences' institutes.

2067
 2068 Concerning global energy markets, the Arctic region holds 25 % or more of the world's undiscovered oil and
 2069 gas ~~reservoirs~~reservoirs (Arctic Oil & Gas, 2008). The plans of China and Russia to build 'Ice Silk Road' along
 2070 Northern Sea linking the China and Russia to Europe is highlighting the ~~polar region's~~growing economic
 2071 and strategic ~~importance~~importances of the polar regions, and the increasing pressure on the Arctic
 2072 environment and local communities. In addition, wide ~~regions~~areas of the high latitudes and Arctic regions
 2073 are under the pressure of the changing economic activities of the Arctic, and ~~are~~also under a-high
 2074 ~~pressure~~pressures of the changing environment and climate. A comprehensive observation network
 2075 providing in-situ data in close coordination with satellite observations and ground-based remote sensing is
 2076 required to monitor the environmental impacts of the envisioned operations.

2077
 2078 Over the last few years, Earth system ~~science~~science is driven by the need to understand the scientific
 2079 processes of climate change and air quality, their -interrelations with ~~the~~ Earth system and their societal
 2080 impacts. The interplay between science, politics and business, and the analysis of the existing policies and
 2081 strategies, help us to recognize and analyze new and emerging trends of Arctic governance (e.g. protection
 2082 and resilience vis-a-vis economic activities), geopolitics (e.g. state sovereignty vis-a-vis internationalization),
 2083 geo-economics (e.g. tourism vis-à-vis reindeer herding), and science (e.g. climate change). The intensive
 2084 work towards the new Arctic observations and data systems, together with the intensive observations on the
 2085 land –atmosphere interactions taking place at the high latitudes, will provide the baseline for cross
 2086 disciplinary research era. PEEEX is aimed for these directions.

2087 2088 **ACKNOWLEDGEMENTS** 2089

2090 We thank the following funding agencies and projects: Academy of Finland contracts: No 280700, 294600,
 2091 296302 (Novel Assessment of Black Carbon in the Eurasian Arctic: From Historical Concentrations and

2092 Sources to Future Climate Impacts (NABCEA), 307331 (FCoE Atmospheric Sciences), 311932, 314798/99,
 2093 315203, 317999, 337549 (Atmosphere and Climate Competence Center (ACCC), Jane and Aatos Erkkö
 2094 Foundation, Russian Government megagrant project № 075-15-2021-574 "Megapolis - heat and pollution
 2095 island: interdisciplinary hydroclimatic, geochemical and ecological analysis", Russian Foundation for Basic
 2096 Research (RFBR) projects No. 17-29-05027 (Selenga-Baikal river system), 17-29-05102, 18-05-00306, 18-
 2097 05-60037, 18-05-60219 (Arctic river), 18-35-20031, 18-44-860017, 18-45-700015, 18-05-60083 (Storm
 2098 activity in the Barents Sea), 18-60084 (Dangerous impacts of large - scale industrial emissions on aerosol
 2099 pollution and Arctic ecosystem), 19-05-50088, 19-05-00352, 19-55-80021 (MOST and DST studies), the
 2100 IAO SB RAS supported by RFBR project No. 19-05-50024, Russian Science Foundation (RSF) projects;
 2101 RSF project 21-17-00181 (Monitoring at Lena River catchment)" No.17-17-01117, 18-17-00076 (Long-term
 2102 measurement of aerosol chemical composition in Central Siberia, 19-77-20109 (Black carbon emissions
 2103 from Siberian fires), 19-77-30004 (Moscow environment), 19-77-300-12 (Measurement networks and field
 2104 sites in Kola Peninsula), Yugra State University grant No.13-01-20/39, Ministry of Science and Higher
 2105 Education of Russia - Agreement No.13.1902.21.0003, State assignment No. 0148-2019-0006, Project
 2106 N75295423 launched by St. Petersburg State University, European Research Council (ERC) projects No.
 2107 742206 (ATM-GTP), No. 850614 (CHAPAs), EU Horizon 2020 projects No. 727890 (Integrated Arctic
 2108 Observing System, INTAROS), 689443 (Integrative and Comprehensive Understanding on Polar
 2109 Environments, iCUPE), 654109 (Aerosol Clouds and Trace Gases Research Infrastructure, ACTRIS-2),
 2110 EU7 FP MarcoPolo Grant No. 606953, Erasmus+ 561975-EPP-1-2015-1-FI-EPPKA2-CBHE-JP, Norwegian
 2111 Research Council and the Belmont Forum project SERUS, No. 311986, National Natural Science
 2112 Foundation of China Grant No. 41275137, ESA-MOST China Dragon Cooperation projects No. 10663 and
 2113 32771 (Dragon 3 and 4).

2114

2115 Our special thanks also to Mrs. Alla Borisova, INAR, University of Helsinki, for the technical editing of the
 2116 manuscript.

2117

2118 REFERENCES

- 2119 Andreae, M. O., Andreae, T. W., and Ditas, F.: How frequent is new particle formation in the boundary layer
 2120 over the remote temperate/boreal forest?, AGU Fall Meeting, San Francisco, USA,
 2121 doi:10.1002/essoar.10501148.1, 2019.
- 2122 Aalto, J., Porcar-Castell, A., Atherton, J., Kolari, P., Pohja, T., Hari, P., Nikinmaa, E., Petäjä, T., and Bäck,
 2123 J.: Onset of photosynthesis in spring speeds up monoterpene synthesis and leads to emission bursts, *Plant,*
 2124 *Cell and Environment.*, 38, 2299-2312, 2015.
- 2125 Agafonova, S. A., Frolova, N. L., Surkova, G. V., and Koltermann, K., P.: Modern characteristics of the ice
 2126 regime of Russian Arctic rivers and their possible changes in the 21st century, *Geogr. Environ. Sustain.*,
 2127 10(4), 4-15, doi:10.24057/2071-9388-2017-10-4-4-15, 2017.

- 2128 Alekseychik, P., Lappalainen, H.K., Petäjä, T., Zaitseva, N., Heimann, M., Laurila, T., Lihavainen, H., Asmi,
2129 E., Arshinov, M., Shevchenko, V., Makshtas, A., Dubtsov, S., Mikhailov, E., Lapshina, E., Kirpotin, S.,
2130 Kurbatova, Y., Ding, A., Guo, H., Park, S., Lavric, J.V., Reum, F., Panov, A., Prokushkin, A., and Kulmala,
2131 M.: Ground-based station network in Arctic and Subarctic Eurasia: An overview, *Geogr. Environ. Sustain.*,
2132 9(2), 75-88, doi:10.24057/2071-9388-2016-9-2-19-35, 2016.
- 2133 Alekseychik, P., Mammarella, I., Karpov, D., Dengel, S., Terentjeva, I., Sabrekov, A., Glagolev, M., and
2134 Lapshina, E.: Net ecosystem exchange and energy fluxes measured with the eddy covariance technique in a
2135 western Siberian bog, *Atmos. Chem. Phys.*, 17, 9333–9345, doi:10.5194/acp-17-9333-2017, 2017.
- 2136 AMAP, 2017: Arctic Pollution 2017. Arctic Monitoring and Assessment Programme (AMAP), Oslo,
2137 Norway.
- 2138 Andreae, M. O.: Emission of trace gases and aerosols from biomass burning – an updated assessment,
2139 *Atmos. Chem. Phys.*, 19, 8523-8546, doi:10.5194/acp-19-8523-2019, 2019.
- 2140 Arneth, A., Harrison, S., Zaehle, S., Tsigaridis, K., Menon, S., Bartlein, P. J., Feichter, J., Korhola, A.,
2141 Kulmala, M., O'Donnell, D., Schurgers, G., Sorvari, S., and Vesala, T.: Terrestrial biogeochemical feedbacks
2142 in the climate system. *Nature Geosci.*, 3, 525–532, <https://doi.org/10.1038/ngeo905>, 2010.
- 2143 Arneth, A., Makkonen, R., Olin, S., Paasonen, P., Holst, T., Kajos, M. K., Kulmala, M., Maximov, T.,
2144 Miller, P. A., and Schurgers, G.: Future vegetation–climate interactions in Eastern Siberia: an assessment of
2145 the competing effects of CO₂ and secondary organic aerosols, *Atmos. Chem. Phys.*, 16, 5243–5262,
2146 doi:10.5194/acp-16-5243-2016, 2016.
- 2147 Arnold, S. R., Law, K. S., Brock, C. A., Thomas, J. L., Starkweather, S. M., von Salzen, K., Stohl, A.,
2148 Sharma, S., Lund, M. T., Flanner, M. G., Petaja, T., Tanimoto, H., Gamble, J., Dibb J. E., Melamed M.,
2149 Johnson, N., Fidel, M., Tynkkynen, V.-P., Baklanov, A., Eckhardt, S., Monks, S. A., Browse, J., and Bozem,
2150 H.: Arctic air pollution: Challenges and opportunities for the next decade, *Elementa: Science of the*
2151 *Anthropocene*, 4:000104, <https://dx.doi.org/10.12952/journal.elementa.00010>. 2016.
- 2152 Arvola, L., Äijälä, C., and Leppäranta, M.: CDOM concentrations of large Finnish lakes relative to their
2153 landscape properties, *Hydrobiologia*, 780(1), 37-46, doi:10.1007/s10750-016-2906-4, 2016.
- 2154 Arvola, L., Leppäranta, M., and Äijälä, C.: CDOM variations in Finnish lakes and rivers between 1913 and
2155 2014, *Sci. Total Environ.*, 601, 1638-1648, doi:10.1016/j.scitotenv.2017.06.034, 2017.
- 2156 Asmi, E., Kondratyev, V., Brus, D., Laurila, T., Lihavainen, H., Backman, J., Vakkari, V., Aurela, M.,
2157 Hatakka, J., Viisanen, Y., Uttal, T., Ivakhov, V., and Makshtas, A.: Aerosol size distribution seasonal
2158 characteristics measured in Tiksi, Russian Arctic, *Atmos. Chem. Phys.*, 16, 1271–1287, doi:10.5194/acp-16-
2159 1271-2016, 2016.
- 2160 Backman, J., Schmeisser, L., Virkkula, A., Ogren, J. A., Asmi, E., Starkweather, S., Sharma, S.,
2161 Eleftheriadis, K., Uttal, T., Jefferson, A., Bergin, M., Makshtas, A., Tunved, P., and Fiebig, M.: On

- 2162 Aethalometer measurement uncertainties and an instrument correction factor for the Arctic, *Atmos. Meas.*
2163 *Tech.*, 10, 5039–5062, doi:10.5194/amt-10-5039-2017, 2017.
- 2164 Badina, S. V.: Socio-economic potential of municipalities in the context of natural risk (case study –
2165 Southern Siberian regions), *IOP Conference Series: Earth and Environmental Science*, 190,
2166 doi:10.1088/1755-1315/190/1/012001, 2018.
- 2167 Bai, J.H.: Estimation of the isoprene emission from the Inner Mongolia grassland, *Atmospheric Pollution*
2168 *Research*, 6, 406-414, doi: 10.5094/APR.2015.045, 2015.
- 2169 Bai, J.H.: UV extinction in the atmosphere and its spatial variation in North China, *Atmos. Environ.*, 154,
2170 318-330, doi:10.1016/j.atmosenv.2017.02.002, 2017a.
- 2171 Bai, J.H., Guenther, A., Turnipseed, A., Duhl, T., Greenberg J.: Seasonal and interannual variations in
2172 whole-ecosystem BVOC emissions from a subtropical plantation in China. *Atmospheric Environment*, 161,
2173 176-190. <http://dx.doi.org/10.1016/j.atmosenv.2017.05.002>, 2017b.
- 2174 Bai, J.H., de Leeuw, G., van der Ronald, A., De Smedt, I., Theys, N., Van Roozendael, M., Sogacheva, L.,
2175 and Chai, W. H.: Variations and photochemical transformations of atmospheric constituents in North China,
2176 *Atmos. Environ.*, 189, 213-226, doi:10.1016/j.atmosenv.2018.07.004, 2018a.
- 2177 Bai, Y., Zhang, J., Zhang, S., Yao, F., and Magliulo, V.: A remote sensing-based two-leaf canopy
2178 conductance model: Global optimization and applications in modeling gross primary productivity and
2179 evapotranspiration of crops, *Remote Sensing of Environment*, 215, 411-437, doi:10.1016/j.rse.2018.06.005,
2180 2018b.
- 2181 Bai, J. H.: A calibration method of solar radiometers, *Atmos. Pollut. Res.*, 10(4), 1365-1373,
2182 doi:10.1016/j.apr.2019.03.011, 2019.
- 2183 Bai, J. H.: O₃ Concentration and its relation with BVOC emissions in a subtropical plantation. *Atmosphere*,
2184 12, 711. <https://doi.org/10.3390/atmos12060711>, 2021.
- 2185 Baklanov, A., Mahura, A., Nazarenko, L., Tausnev, N., Kuchin, A., and Rigina, O.: *Atmospheric Pollution*
2186 *and Climate Change in Northern Latitudes*, Russ. Acad. Sci., Apatity, Russia, 2012.
- 2187 Baklanov, A. A., Penenko, V. V., Mahura, A. G., Vinogradova, A. A., Elansky, N. F., Tsvetova, E. A.,
2188 Rigina, O. Y., Maksimenkov, L. O., Nuterman, R. B., Pogarskii, F. A., and Zakey, A.: Aspects of
2189 Atmospheric Pollution in Siberia, in *Regional Environmental Changes in Siberia and Their Global*
2190 *Consequences*, edited by: Groisman P. Y., and Gutman, G., 303–346, Springer, Dordrecht, Netherlands,
2191 2013.
- 2192 Baklanov, A., Molina, L.T., and Gauss, M.: Megacities, air quality and climate, *Atmospheric Environment*,
2193 126, 235-249, <https://doi.org/10.1016/j.atmosenv.2015.11.059>, 2016.

- 2194 Baklanov, A., Smith Korsholm, U., Nuterman, R., Mahura, A., Nielsen, K. P., Sass, B. H., Rasmussen, A.,
2195 Zakey, A., Kaas, E., Kurganskiy, A., Sørensen, B., and González-Aparicio, I.: Enviro-HIRLAM online
2196 integrated meteorology–chemistry modelling system: strategy, methodology, developments and applications
2197 (v7.2), *Geosci. Model Dev.*, 10, 2971–2999, <https://doi.org/10.5194/gmd-10-2971-2017>, 2017.
- 2198 Baklanov, A., Brunner, D., Carmichael, G., Flemming, J., Freitas, S., Gauss, M., Hov, O., R. Mathur, R.,
2199 Schlünzen, K., Seigneur, C., and Vogel, B.: Key issues for seamless integrated chemistry-meteorology
2200 modeling, *Bull. Amer. Meteor. Soc.*, doi:10.1175/BAMS-D-15-00166.1., 2018.
- 2201 Balch, W. M., Bates, N. R., Lam, P. J., Twining, B. S., Rosengard, S. Z., Bowler, B. C., and Rauschenberg,
2202 S.: Factors regulating the Great Calcite Belt in the Southern Ocean, and its biogeochemical significance,
2203 *Global Biogeochem. Cycles*, 30(8), 1124–1144, doi:10.1002/2016GB005414, 2016.
- 2204 Balch, W. M.: The ecology, biogeochemistry, and optical properties of coccolithophores, *Ann. Rev. Mar.*
2205 *Sci.*, 109, 71–98, doi:10.1146/annurev-marine-121916-063319, 2018.
- 2206 Bartsch, A., Kumpula, T., Forbes, B.C. and Stammler F.: Detection of snow surface thawing and refreezing
2207 in the Eurasian Arctic with QuikSCAT: implications for reindeer herding, *Ecol Appl.*, 20, 2346–58., doi:
2208 10.1890/09-1927.1., 2010.
- 2209 Barreira, L. M. F., Duporté, G., Rönkkö, T., Parshintsev, J., Hartonen, K., Hyrsky, L., Heikkinen, E.,
2210 Kulmala, M., and Riekkola, M.-L.: Field measurements of biogenic volatile organic compounds in the
2211 atmosphere using solid-phase microextraction Arrow, *Atmos. Meas. Tech.*, 11, 881–893, 2018.
- 2212 Bashmachnikov, I.L., Yurova, A.Y., Bobylev, L.P., and Vesman, A. V.: Seasonal and Interannual Variations
2213 of Heat Fluxes in the Barents Sea Region, *Izv., Atmos. Ocean. Phys.*, 54, 213–222,
2214 doi:10.1134/S0001433818020032, 2018a.
- 2215 Bashmachnikov, I. L., Yurova, A.Y., Bobylev, L. P., Vesman, A.V.: Seasonal and interannual variations of
2216 the heat fluxes in the Barents Sea region, *Izv. Atmos. Ocean. Phys.*, 54(2), 239–249,
2217 doi:10.7868/S0003351518020149, 2018b.
- 2218 Beer, C., Reichstein, M., Tomelleri, E., Ciais, P., Jung, M., Carvalhais, N., Rödenbeck, C., Altaf Arain,
2219 A., Baldocchi, D., Bonan, G.B., Bondeau, A., Cescatti, A., Lasslop, G., Lindroth, A., Lomas, M.,
2220 Luysaert, S., Margolis, H., Oleson, K.W., Rouspard, O., Veenendaal, E., Viovy, N., Williams, C., F Ian
2221 Woodward, F.,I., and Papale, D.:Terrestrial gross carbon dioxide uptake: global distribution and covariation
2222 with climate. *Science*, 329, 834–838, doi: 10.1126/science.1184984, 2010.
- 2223 Belikov, D., Arshinov, M., Belan, B., Davydov, D., Fofonov, A., Sasakawa, M., Machida, T.: Analysis of the
2224 Diurnal, Weekly, and Seasonal Cycles and Annual Trends in Atmospheric CO₂ and CH₄ at Tower Network
2225 in Siberia from 2005 to 2016, *Atmosphere*, 10 (11), 689, doi: 10.3390/atmos10110689, 2019.
- 2226 Berchet, A., Bousquet, P., Pison, I., Locatelli, R., Chevallier, F., Paris, J.-D., Dlugokencky, E. J., Laurila, T.,
2227 Hatakka, J., Viisanen, Y., Worthy, D. E. J., Nisbet, E., Fisher, R., France, J., Lowry, D., Ivakhov, V., and

- 2228 Hermansen, O.: Atmospheric constraints on the methane emissions from the East Siberian Shelf, *Atmos. Chem. Phys.*, 16, 4147–4157, doi:10.5194/acp-16-4147-2016, 2016.
- 2230 Berezina, E., Moiseenko, K., Skorokhod, A., Elansky, N., Belikov, I., and Pankratova, N.: Isoprene and monoterpenes over Russia and their impacts in tropospheric ozone formation, *Geogr., Environ., Sustain.*, 12(1), 63-74, doi:10.24057/2071-9388-2017-24, 2019.
- 2233 Bezuglaya, E. Y., Ed.: Air quality in largest cities of Russia for 10 years (1988-1997), Hydrometeoizdat, St. Petersburg, Russia, 1999.
- 2235 Biskaborn, B. K., Smith, S. L., Noetzli, J., Matthes, H., Vieira, G., Streletskiy, D. A., Schoeneich, P., Romanovsky, V. E., Lewkowicz, A. G., Abramov, A., Allard, M., Boike, J., Cable, W. L., Christiansen, H., Delaloye, R., Diekmann, B., Drozdov, D., Etzelmüller, B., Grosse, G., ... and Lantuit, H.: Permafrost is warming at a global scale, *Nat. Commun.*, 10(1), 264, doi: 10.1038/s41467-018-08240-4, 2019.
- 2239 Blackport, R., Screen, J. A., van der Wiel, K., and Bintanja, R.: Minimal influence of reduced Arctic sea ice on coincident cold winters in mid-latitudes, *Nat. Clim. Change*, 9, 697–704, doi: 10.1038/s41558-019-0551-4, 2019.
- 2242 Bobylev, S.N., Chereshnya, O.Y., Kulmala, M., Lappalainen, H. K., Petäjä, T., Solov'eva, S.V., Tikunov, V.S., and Tynkkynen, V.-P.: Indicators for digitalization of sustainable development goals in PEEEX program, *J. Geogr. Sust.*, 11, 145-156, 2018.
- 2245 Boike, J., Nitzbon, J., Anders, K., Grigoriev, M., Bolshiyarov, D., Langer, M., Lange, S., Bornemann, N., Morgenstern, A., Schreiber, P., Wille, C., Chadburn, S., Gouttevin, I., Burke, E., and Kutzbach, L.: A 16-year record (2002–2017) of permafrost, active-layer, and meteorological conditions at the Samoylov Island Arctic permafrost research site, Lena River delta, northern Siberia: an opportunity to validate remote-sensing data and land surface, snow, and permafrost models, *Earth Syst. Sci. Data*, 11, 261–299, <https://doi.org/10.5194/essd-11-261-2019>, 2019.
- 2252 Bondur, G., and Vorobev, V. E.: Satellite Monitoring of Impact Arctic Regions, *Izv. Atmos. Ocean. Phys.*, 51, 949–968, doi: 10.1134/S0001433815090054, 2015.
- 2254 Bondur, V. G., and Ginzburg, A. S.: Emission of carbon-bearing gases and aerosols from natural fires on the territory of Russia based on space monitoring, *Dokl. Earth Sci.*, 466(2), 148-152, doi:10.1134/s1028334x16020045, 2016.
- 2257 Bondur, V. G.: Satellite monitoring of trace gas and aerosol emissions during wildfires in Russia. *Izv. Atmos. Ocean. Phys.*, 52(9), 1078-1091, doi:10.1134/s0001433816090103, 2016.
- 2259 Bondur, V. G., Gordo, K. A., and Kladoy, V. L.: Spacetime distributions of wildfire areas and emissions of carbon-containing gases and aerosols in northern Eurasia according to satellite-Monitoring Data, *Izv. Atmos. Ocean. Phys.*, 53(9), 859-874, doi:10.1134/s0001433817090055, 2017.

- 2262 Bondur, V. G. and Gordo, K. A.: Satellite Monitoring of Burned out Areas and Emissions of Harmful
 2263 Contaminants due to Forest and other Wildfires in Russia, *Izv., Atmos. Ocean. Phys.*, 54 (9),955–965, doi:
 2264 10.1134/S0001433818090104, 2018.
- 2265 Bondur V. G., Chimitdorzhiev T. N., Dmitriev A. V., and Dagurov P. N.: Otsenka prostranstvennoy
 2266 anizotropii neodnorodnostey lesnoy rastitelnosti pri razlichnykh azimutalnykh uglakh radarnogo
 2267 polyarimetricheskogo zondirovaniya (Spatial anisotropy assessment of the forest vegetation heterogeneity at
 2268 various azimuth angles of the radar polarimetric sensing), *Issledovanie Zemli iz kosmosa, Russia*, 3, 92-103,
 2269 doi:10.31857/S0205-96142019392-103, 2019a.
- 2270 Bondur, V. G., Chimitdorzhiev, T. N., Dmitriev, A. V., Dagurov, P. N., Zakharov, A. I., and Zakharova, L.
 2271 N.: Metody radarnoj polyarimetrii dlya issledovaniya izmenenij mekhanizmov obratnogo rasseyaniya v
 2272 zonah opolznei na primere obrusheniya sklona berega reki Bureya (Using radar polarimetry to monitor
 2273 changes in backscattering mechanisms in landslide zones for the case study of the Bureya river bank
 2274 collapse), *Issledovanie Zemli iz kosmosa.*, Russia, 4, 3-17, doi:10.31857/S0205-9614201943-17, 2019b.
- 2275 Bondur, V. G., Tsidilina, M. N., and Cherepanova, E.V.: Satellite Monitoring of Wildfire Impacts on The
 2276 Conditions of Various Types of Vegetation Cover in The Federal Districts of the Russian Federation, *Izv.*
 2277 *Atmos. Ocean. Phys.*, 55 (9), 1238–1253, doi:10.1134/s000143381909010X, 2019 (c).
- 2278 Bondur, V. G., Tsidilina, M. N., Kladov, V. L., and Gordo, K. A.: Irregular Variability of Spatiotemporal
 2279 Distributions of Wildfires and Emissions of Harmful Trace Gases in Europe Based on Satellite Monitoring
 2280 Data // *Doklady Earth Sciences*, Vol. 485, Part 2, pp. 461–464, doi: 10.1134/S1028334X19040202, 2019(d).
- 2281 Bondur, V. G., Zakharova, L. N., and Zakharov, A. I.: Monitoring of the landslide area state on Bureya river
 2282 in 2018-2019 according to radar and optical satellite images, *Issledovanie Zemli iz kosmosa, Russia*, No. 6,
 2283 26-35, doi:10.31857/S0205-96142019626-35, 2019(e).
- 2284 Bondur, V. G., Zakharova, L. N., Zakharov, A. I., Chimitdorzhiev, T. N., Dmitriev, A. V., and Dagurov,
 2285 P.N.: Monitoring of landslide processes by means of L-band radar interferometric observations: Bureya river
 2286 bank caving case // *Issledovanie Zemli iz kosmosa, Russia*, No. 5, 3-14, DOI:
 2287 <https://doi.org/10.31857/S0205-9614201953-14>. 2019 (f).
- 2288 Bondur, V. G., Tsidilina, M. N., and Kladov, V. L.: Irregular Variability of Spatiotemporal Distributions of
 2289 Wildfires and Emissions of Harmful Trace Gases in Europe Based on Satellite Monitoring Data, *Dokl. Earth*
 2290 *Sc.*, 485, 461–464, <https://doi.org/10.1134/S1028334X19040202>, 2019.
- 2291 Bondur, V. G., Mokhov, I. I., Voronova, O. S., and Sitnov, S. A.: Satellite Monitoring of Siberian Wildfires
 2292 and Their Effects: Features of 2019 Anomalies and Trends of 20-Year Changes, *Doklady Earth Sciences*,
 2293 492, 1, 370–375. doi: 10.1134/S1028334X20050049, 2020.
- 2294 Bormann, K. J., Brown, R. D., Derksen, C., and Painter, T. H.: Estimating snow-cover trends from space,
 2295 *Nat. Clim. Chang.*, 8, 924-928, 2018.

- 2296 Boy, M., Thomson, E. S., Acosta Navarro, J.-C., Arnalds, O., Batchvarova, E., Bäck, J., Berninger, F., Bilde,
 2297 M., Brasseur, Z., Dagsson-Waldhauserova, P., Castarède, D., Dalirian, M., de Leeuw, G., Dragosics, M.,
 2298 Duplissy, E.-M., Duplissy, J., Ekman, A. M. L., Fang, K., Gallet, J.-C., Glasius, M., Gryning, S.-E., Grythe,
 2299 H., Hansson, H.-C., Hansson, M., Isaksson, E., Iversen, T., Jonsdottir, I., Kasurinen, V., Kirkevåg, A.,
 2300 Korhola, A., Krejci, R., Kristjansson, J. E., Lappalainen, H. K., Lauri, A., Leppäranta, M., Lihavainen, H.,
 2301 Makkonen, R., Massling, A., Meinander, O., Nilsson, E. D., Olafsson, H., Pettersson, J. B. C., Prisle, N. L.,
 2302 Riipinen, I., Roldin, P., Ruppel, M., Salter, M., Sand, M., Seland, Ø., Seppä, H., Skov, H., Soares, J., Stohl,
 2303 A., Ström, J., Svensson, J., Swietlicki, E., Tabakova, K., Thorsteinsson, T., Virkkula, A., Weyhenmeyer, G.
 2304 A., Wu, Y., Zieger, P., and Kulmala, M.: Interactions between the atmosphere, cryosphere, and ecosystems
 2305 at northern high latitudes, *Atmos. Chem. Phys.*, 19, 2015–2061, <https://doi.org/10.5194/acp-19-2015-2019>,
 2306 2019.
- 2307 Breider, T.J., Mickley, L.J., Jacob, D.J., Ge, C., Wang, J., Sulprizio, M.P., Croft, B., Ridley, D.A.,
 2308 McConnell, J.R., Sharma, S., Husain, L., Dutkiewicz, V. A., Eleftheriadis, K., Skov, H., and Hopke, P. K.:
 2309 Multidecadal trends in aerosol radiative forcing over the Arctic: Contribution of changes in anthropogenic
 2310 aerosol to Arctic warming since 1980, *J. Geophys. Res.: Atmos.*, 122, 3573–3594,
 2311 <https://doi.org/10.1002/2016JD025321>, 2017.
- 2312 Burkhard, B., Kroll, F., Müller, F., and Windhorst, W. F., Landscapes' Capacities to Provide Ecosystem
 2313 Services – a Concept for Land-Cover Based Assessments, *Landscape Online* 15(1), 1-12, DOI:
 2314 10.3097/LO.200915, 2009.
- 2315 Chalov, S. R., Jarsjo, J., Kasimov, N. S., Romanchenko, A. O., Pietron, J., Thorslund, J., and Promakhova,
 2316 E. V.: Spatio-temporal variation of sediment transport in the Selenga River Basin, Mongolia and Russia,
 2317 *Environ. Earth Sci.*, 73(2), 663–680, doi:10.1007/s12665-014-3106-z, 2015.
- 2318 Chalov, S. R., Bazilova, V. O., and Tarasov, M. K.: Modelling suspended sediment distribution in the
 2319 Selenga River Delta using LandSat data, in *Integrating Monitoring and Modelling for Understanding,
 2320 Predicting and Managing Sediment Dynamics*, edited by: Collins, A., Stone, M., Horowitz, A., and Foster, I.,
 2321 Copernicus Gesellschaft, Gottingen, Germany, 375, 19-22, 2017a.
- 2322 Chalov, S., Thorslund, J., Kasimov, N., Aybullaev, D., Ilyicheva, E., Karthe, D., Kositsky, A., Lychagin,
 2323 M., Nittrouer, J., Pavlov, M., Pietron, J., Shinkareva, G., Tarasov, M., Garmaev, E., Akhtman, Y., and Jarsjö,
 2324 J.: The Selenga River delta: a geochemical barrier protecting Lake Baikal waters, *Regional Environ. Change*,
 2325 17, 2039–2053, doi: 10.1007/s10113-016-0996-1, 2017b.
- 2326 Chalov, S. R., Millionshchikova, T. D., and Moreido, V. M.: Multi-Model Approach to Quantify Future
 2327 Sediment and Pollutant Loads and Ecosystem Change in Selenga River System, *Water Resour.*, 45, S22-S34,
 2328 doi:10.1134/s0097807818060210, 2018.

- 2329 Che, Y., Xue, Y., Mei, L., Guang, J., She, L., Guo, J., Hu, Y., Xu, H., He, X., Di, A., and Fan, C.: Technical
 2330 note: Intercomparison of three AATSR Level 2 (L2) AOD products over China, *Atmos. Chem. Phys.*, 16,
 2331 9655–9674, <https://doi.org/10.5194/acp-16-9655-2016>, 2016.
- 2332 Cheng, Y., Cheng, B., Zheng, F., Vihma, T., Kontu, A., Yang, Q. and Liao, Z.: Air/snow, snow/ice and
 2333 ice/water interfaces detection from high-resolution vertical temperature profiles measured by ice mass-
 2334 balance buoys on an Arctic lake. *Annals of Glaciology*, accepted (2020).
- 2335 Chernokulsky, A. V., Esau, I., Bulygina, O. N., Davy, R., Mokhov, II, Outten, S., and Semenov, V. A.:
 2336 Climatology and interannual variability of cloudiness in the Atlantic Arctic from surface observations since
 2337 the late nineteenth century, *J. Clim.*, 30(6), 2103–2120, doi:10.1175/jcli-d-16-0329.1, 2017.
- 2338 Chernokulsky, A., and Esau, I.: Cloud cover and cloud types in the Eurasian Arctic in 1936–2012. *Int. J.*
 2339 *Climatol.*, 39(15), 5771–5790, <https://doi.org/10.1002/joc.6187>, 2019
- 2340 Chu, B., Kerminen, V.-M., Bianchi, F., Yan, C., Petäjä, T. and Kulmala, M.: Atmospheric new particle
 2341 formation in China, *Atmos. Chem. Phys.*, 19, 115–138, 2019.
- 2342 Chubarova, N. Y., Poliukhov, A. A., and Gorlova, I. D.: Long-term variability of aerosol optical thickness in
 2343 Eastern Europe over 2001–2014 according to the measurements at the Moscow MSU MO AERONET site
 2344 with additional cloud and NO2 correction, *Atmos. Meas. Tech.*, 9, 313–334, [https://doi.org/10.5194/amt-9-](https://doi.org/10.5194/amt-9-313-2016)
 2345 313-2016, 2016a.
- 2346 Chubarova, N., Zhdanova, Y., and Nezval, Y.: A new parameterization of the UV irradiance altitude
 2347 dependence for clear-sky conditions and its application in the on-line UV tool over Northern Eurasia, *Atmos.*
 2348 *Chem. Phys.*, 16, 11867–11881, <https://doi.org/10.5194/acp-16-11867-2016>, 2016b.
- 2349 Chubarova, N. E., Pastukhova, A. S., and Galin, V. Y.: Long-Term Variability of UV Irradiance in the
 2350 Moscow Region according to Measurement and Modeling Data, *Izv. Atmos. Ocean. Phys.*, 54, 139–146,
 2351 <https://doi.org/10.1134/S0001433818020056>, 2018.
- 2352 Chubarova, N. E., Androsova, E. E., Kirsanov, A. A., Vogel, B., Vogel, H., Popovicheva, O. B., and Rivin,
 2353 G. S.: Aerosol and Its Radiative Effects during the Aeroradcity 2018 Moscow Experiment, *Geography,*
 2354 *Environment, Sustainability*, 12, 114–131, <https://doi.org/10.24057/2071-9388-2019-72> 2019a.
- 2355 Chubarova, N. E., Timofeev, Y. M., Virolainen, Y. A., and Polyakov, A. V.: Estimates of UV indices during
 2356 the periods of reduced ozone content over Siberia in Winter-Spring 2016, *Atmos. Oceanic Opt.*, 32, 177–179,
 2357 doi:10.1134/s1024856019020040, 2019b.
- 2358 Chubarova, N. E., Pastukhova, A.S., Zhdanova, E.Y., Volpert, E.V., Smyshlyaev and S.P., and Galin, V.Y.:
 2359 Effects of Ozone and Clouds on Temporal Variability of Surface UV Radiation and UV Resources over
 2360 Northern Eurasia Derived from Measurements and Modeling., *Atmosphere*, 11, 59, 2020.
- 2361 Cohen, J., X. Zhang, T., Jung, R. Kwok, J., Overland, T., Ballinger, U.S., Bhatt, H. W., Chen, D., Coumou,
 2362 S., Feldstein, H., Gu, D., Handorf, G., Henderson, M., Ionita, M., Kretschmer, F., Laliberte, S., Lee, H. W.,

Formatted: German (Germany)

- 2363 Linderholm, W., Maslowski, Y., Peings, K., Pfeiffer, I., Rigor, T., Semmler, J., Stroeve, P.C., Taylor, S.,
 2364 Vavrus, T., Vihma, S., Wang, M., Wendisch, Y., Wu, and Yoon, J.: Divergent consensus on Arctic
 2365 amplification influence on midlatitude severe winter weather. *Nature Climate Change*, 10, 20-29,
 2366 doi:10.1038/s41558-019-0662-y, 2020.
- 2367 Collins, M., Knutti, R., Arblaster, J., Dufresne, J.-L., Fichet, T., Friedlingstein, P., Gao, X., Gutowski,
 2368 W.J., Johns, T., Krinner, G., Shongwe, M., Tebaldi, C., Weaver, A.J., and Wehner, M.: Long-term climate
 2369 change: Projections, commitments and irreversibility, in *Climate Change 2013: The Physical Science Basis*.
 2370 Contribution of Working Group I to the Fifth Assessment Report of the Intergovernmental Panel on Climate
 2371 Change, edited by: Stocker, T.F., Qin, D., Plattner, G.-K., Tignor, M., Allen, S.K., Doschung, J., Nauels,
 2372 A., Xia, Y., Bex, V., and Midgley, P.M., Cambridge University Press, Cambridge, United-Kingdom, 1029-
 2373 1136, doi:10.1017/CBO9781107415324.024, 2013.
- 2374 Commane, R., Lindaas, J., Benmergui, J., Luus, K. A., Chang, R. Y.-W., Daube, B. C., Euskirchen, E. S.,
 2375 Henderson, J. M., Karion, A., Miller, J. B., Miller, S. M., Parazoo, N. C., Randerson, J. T., Sweeney, C.,
 2376 Tans, P., Thoning, K., Veraverbeke, S., Miller, C. E., and Wofsy, S. C.: Carbon dioxide sources from Alaska
 2377 driven by increasing early winter respiration from Arctic tundra, *PNAS*, 114(21), 5361-5366, 2017.
- 2378 Coumou, C., Petoukhov, V., Rahmstorf, S., Petri, S., and Schellnhuber, H.-J.: Quasi-resonant circulation
 2379 regimes and hemispheric synchronization of extreme weather in boreal summer, *Proc. Natl. Acad. Sci.*, 111,
 2380 12 331–12336, <https://doi.org/10.1073/pnas.1412797111>, 2014.
- 2381 Dada, L., Paasonen, P., Nieminen, T., Buenrostro Mazon, S., Kontkanen, J., Peräkylä, O., Lehtipalo, K.,
 2382 Hussein, T., Petäjä, T., Kerminen, V.-M., Bäck, J. and Kulmala, M.: Long-term analysis of clear-sky new
 2383 particle formation events and nonevents in Hyytiälä, *Atmos. Chem. Phys.*, 17, 6227-6241, 2017.
- 2384 Dada, L., Chellapermal, R., Buenrostro Mazon, S., Paasonen, P., Lampilahti, J., Manninen, H. E., Junninen,
 2385 H., Petäjä, T., Kerminen, V.-M., and Kulmala, M.: Refined classification and characterization of atmospheric
 2386 new-particle formation events using air ions, *Atmos. Chem. Phys.*, 18, 17883–17893,
 2387 <https://doi.org/10.5194/acp-18-17883-2018>, 2018.
- 2388 Dagsson-Waldhauserova, P., Meinander, O.: Atmosphere-cryosphere interaction in the Arctic, at high
 2389 latitudes and mountains with focus on transport, deposition and effects of dust, black carbon, and other
 2390 aerosols., *Front. Earth Sci.*, 7, 337, <https://www.frontiersin.org/articles/10.3389/feart.2019.00337/full>, 2019.
- 2391 Dave, B., and Kobayashi, Y.: China's silk road economic belt initiative in Central Asia: economic and
 2392 security implications, *Asia Europe Journal*, 16, 1-15. doi:10.1007/s10308-018-0513-x, 2018.
- 2393 Davy, R., and Esau, I.: Differences in the efficacy of climate forcings explained by variations in atmospheric
 2394 boundary layer depth, *Nat. Commun.*, 7, 8, doi:10.1038/ncomms11690, 2016.
- 2395 Davy, R., Esau, I., Chernokulsky, A., Outten, S., and Zilitinkevich, S.: Diurnal asymmetry to the observed
 2396 global warming, *Int. J. Climatol.*, 37, 79-93, doi:10.1002/joc.4688, 2017.

- 2397 Dean, J. F., Middelburg, J. J., Röckmann, T., Aerts, R., Blauw, L. G., Egger, M., Jetten, M. S. M., de Jong,
2398 A. E. E., Meisel, O. H., Rasigraf, O., Slomp, C. P., in't Zandt, M. H., and Dolman, A. J.: Methane feedbacks
2399 to the global climate system in a warmer world, *Rev. Geophys.*, 56(1), 207-250,
2400 <https://doi.org/10.1002/2017RG00055>, 2018.
- 2401 Derksen, C., and Brown, R.: Spring snow cover extent reductions in the 2008-2012 period exceeding climate
2402 model predictions, *Geophys. Res. Lett.*, 39, L19504, 2012.
- 2403 Derome, J., and Lukina, N.: Interaction between environmental pollution and land-cover/land-use change in
2404 Arctic areas, in: *Eurasian Arctic Land Cover and Land Use in a Changing Climate*, edited by: Gutman, G.,
2405 and Reissell, A., 6, 269–290, Springer, Amsterdam, Netherlands, 2011.
- 2406 Ding, A. J., Huang, X., Nie, W., Sun, J. N., Kerminen, V.-M., Petäjä, T., Su, H., Chen, Y. F., Yang, X.-Q.,
2407 Wang, M. H., Chi, X. G., Wang, J. P., Virkkula, A., Guo, W. D., Yuan, J., Wang, S. Y., Zhang, R. J., Wu, Y.
2408 F., Song, Y. Zhu, T., Zilitinkevich, S., Kulmala, M., and Fu, C. B.: Enhanced haze pollution by black carbon
2409 in megacities in China, *Geophys. Res. Lett.*, 43, 2873-2879, doi:10.1002/2016GL067745, 2016a.
- 2410 Ding, A. J., Nie, W., Huang, X., Chi, X., Sun, J., Kerminen, V.-M., Xu, Z., Guo, W., Petäjä, T., Yang, X.,
2411 Kulmala, M., and Fu, G.: Long-term observation of pollution-weather/climate interactions at the SORPES
2412 station: a review and outlook, *Front. Environ. Sci. Eng.*, 10, doi:10.1007/s11783-016-0877-3, 2016b.
- 2413 Dou, T., Xiao, C., Liu, J., Han, W., Du, Z., Mahoney, A. R., Jones, J., and Eicken, H.: A key factor initiating
2414 surface ablation of Arctic sea ice: earlier and increasing liquid precipitation, *The Cryosphere*, 13, 1233–
2415 1246, <https://doi.org/10.5194/tc-13-1233-2019>, 2019.
- 2416 Dragosics, M., Meinander, O., Jonsdottir, T., Durig, T., De Leeuw, G., Palsson, F., Dagsson-Waldhauserová,
2417 P., and Thorsteinsson, T.: Insulation effects of Icelandic dust and volcanic ash on snow and ice, *Arab. J.*
2418 *Geosci.*, 9, 126, DOI:10.1007/s12517-015-2224-6, 2016.
- 2419 Duporte, G., Parshintsev, J., Barreira, L. M. F., Hartonen, K., Kulmala, M., and Riekkola, M. L.: Nitrogen-
2420 containing low volatile compounds from pinonaldehyde-dimethylamine reaction in the atmosphere: a
2421 laboratory and field study, *Environ. Sci. Technol.*, 50(9), 4693-4700, doi:10.1021/acs.est.6b00270, 2016.
- 2422 Durairaj, P., Sarangi, R., Ramalingam, S., Thirunavukarassu, T., and Chauhan, P.: Seasonal nitrate
2423 algorithms for nitrate retrieval using OCEANSAT-2 and MODIS-AQUA satellite data, *Environ. Monit.*
2424 *Assess.*, 187, 176-189, doi: 10.1007/s10661-015-4340-x, 2015.
- 2425 Dyukarev, E.A., Godovnikov, E.A., Karpov, D.V., Kurakov, S.A., Lapshina, E.D., Filippov, I.V., Filippova,
2426 N.V., and Zarov, E.A.: Net ecosystem exchange, gross primary production and ecosystem respiration in
2427 ridge-hollow complex at Mukhrino Bog, *Geography, Environment, Sustainability*, 12(2), 227-244,
2428 doi:10.24057/2071-9388-2018-77, 2019.
- 2429 Elansky, N. F., Lavrova, O. V., Skorokhod, A. I., and Belikov, I. B.: Trace gases in the atmosphere over
2430 Russian cities, *Atmos. Environ.*, 143, 108-119, doi:10.1016/j.atmosenv.2016.08.046, 2016.

- 2431 Esau, I., Miles, V. V., Davy, R., Miles, M. W., and Kurchatova, A.: Trends in normalized difference
2432 vegetation index (NDVI) associated with urban development in northern West Siberia, *Atmos. Chem. Phys.*,
2433 16, 9563–9577, <https://doi.org/10.5194/acp-16-9563-2016>, 2016.
- 2434 Esau, I., Varentsov, M., Laruelle, M., Miles, M. W., Konstantinov, P., Soromotin, A., Baklanov, A. A., and
2435 Miles, V. V.: Warmer Climate of Arctic Cities, Chapter 3 in the monography “The Arctic: Current Issues and
2436 Challenges”, Edited by: Pokrovsky, O., NOVA Publishers, ISBN: 978-1-53617-306-2,
2437 <https://novapublishers.com/shop/the-arctic-current-issues-and-challenges/>, 2020.
- 2438 Euskirchen, E. S., Bret-Harte, M. S., Shaver, G. R., Edgar, C. W., and Romanovsky, V. E.: Long-term
2439 release of carbon dioxide from arctic tundra ecosystems in northern Alaska, *Ecosystems*, 1–15, 2017.
- 2440 Evangeliou, N., Shevchenko, V. P., Yttri, K. E., Eckhardt, S., Sollum, E., Pokrovsky, O. S., Kobelev, V. O.,
2441 Korobov, V. B., Lobanov, A. A., Starodymova, D. P., Vorobiev, S. N., Thompson, R. L., and Stohl, A.:
2442 Origin of elemental carbon in snow from western Siberia and northwestern European Russia during winter–
2443 spring 2014, 2015 and 2016, *Atmos. Chem. Phys.*, 18, 963–977, <https://doi.org/10.5194/acp-18-963-2018>,
2444 2018.
- 2445 Ezhova, E., Orlov, D., Suhonen, E., Kaverin, D., Mahura, A., Gennadinik, V., Kukkonen, I., Drozdov, D.,
2446 Lappalainen, H. K., Melnikov, V., Petäjä, T., Kerminen, V.-M., Zilitinkevich, S., Malkhazova, S. M.,
2447 Christensen, T. R., and Kulmala, M.: Climatic Factors Influencing the Anthrax Outbreak of 2016 in Siberia,
2448 Russia. *EcoHealth*, <https://doi.org/10.1007/s10393-021-01549-5>, 2021.
- 2449 Ezhova, E., Kerminen, V.-M., Lehtinen, K. E. J., and Kulmala, M.: A simple model for the time evolution of
2450 the condensation sink in the atmosphere for intermediate Knudsen numbers, *Atmos. Chem. Phys.*, 18, 2431–
2451 2442, <https://doi.org/10.5194/acp-18-2431-2018>, 2018a.
- 2452 Ezhova, E., Ylivinkka, I., Kuusk, J., Komsaare, K., Vana, M., Krasnova, A., Noe, S., Arshinov, M., Belan,
2453 B., Park, S.-B., Lavrič, J. V., Heimann, M., Petäjä, T., Vesala, T., Mammarella, I., Kolari, P., Bäck, J.,
2454 Rannik, Ü., Kerminen, V.-M., and Kulmala, M.: Direct effect of aerosols on solar radiation and gross
2455 primary production in boreal and hemiboreal forests, *Atmos. Chem. Phys.*, 18, 17863–17881,
2456 <https://doi.org/10.5194/acp-18-17863-2018>, 2018b.
- 2457 Fang, K., Makkonen, R., Guo, Z., and Seppä, H.: An increase in the biogenic aerosol concentration as a
2458 contributing factor to the recent wetting trend in Tibetan Plateau. *Sci Rep* 5, 14628,
2459 <https://doi.org/10.1038/srep14628>, 2015.
- 2460 Fang, Y., Changyou, L., Leppäranta, M., Xiaonghong, S., Shengnan, Z., and Chengfu, Z.: Notable increases
2461 in nutrient concentrations in a shallow lake during seasonal ice growth, *Water Science and Technology*,
2462 74(12), 2773–2783, 2016.

- 2463 Fang, K. , Makkonen, R. , Guo, Z., Zhao , Y., and Seppä, H.: An increase in the biogenic aerosol
 2464 concentration as a contributing factor to the recent wetting trend in Tibetan Plateau, *Scientific Reports* , 5 ,
 2465 14628, DOI: 10.1038/srep14628, 2015.
- 2466 Fletcher, S. E. M., and Schaefer, H.: Rising methane: a new climate challenge, *Science*, 364, 932-933, 2019.
- 2467 Franz, D., Mammarella, I., Boike, J., Kirillin, G., Vesala, T., Bornemann, N., Larmanou, E., Langer, M., and
 2468 Sachs, T.: Lake-Atmosphere Heat Flux Dynamics of a Thermokarst Lake in Arctic Siberia, *J. Geophys. Res.:*
 2469 *Atmos.*, 123(10), 5222-5239, doi:10.1029/2017jd027751, 2018.
- 2470 Freud, E., Krejci, R., Tunved, P., Leaitch, R., Nguyen, Q. T., Massling, A., Skov, H., and Barrie, L.: Pan-
 2471 Arctic aerosol number size distributions: seasonality and transport patterns, *Atmos. Chem. Phys.*, 17, 8101–
 2472 8128, <https://doi.org/10.5194/acp-17-8101-2017>, 2017.
- 2473 Frolova, N.L., Belyakova, P.A., Grigoriev, V.Y. *et al.* : Runoff fluctuations in the Selenga River Basin, *Reg*
 2474 *Environ Change*, 17, 1965–1976, doi.org/10.1007/s10113-017-1199-0, 2017.
- 2475
- 2476 Fu, B. J., and Forsius, M.: Ecosystem services modeling in contrasting landscapes, *Landscape Ecol.*, 30(3),
 2477 375-379, doi:10.1007/s10980-015-0176-6, 2015.
- 2478 Garmaev, E. Z., Kulikov, A. I., Tsydypov, B. Z., Sodnomov, B. V., and Ayurzhanayev, A. A.: Environmental
 2479 Conditions Of Zakamensk Town (Dzhida River Basin Hotspot), *Geography, Environment,*
 2480 *Sustainability*, 12(3), 224-239, <https://doi.org/10.24057/2071-9388-2019-32>, 2019.
- 2481 Georgiadi, A. G., Koronkevich, N. I., Milyukova, I. P., and Barabanova, E. A.: Integrated projection for
 2482 runoff changes in large Russian river basins in the XXI Century, *Geography, Environment, Sustainability,*
 2483 9(2), 38-46, 2016.
- 2484 GGO: Air quality in cities of Russia during the year 2015, St. Petersburg, Voeikov Main Geophysical
 2485 Observatory, RosHydroMet, 2016.
- 2486 Giamarelou, M., Eleftheriadis, K., Nyeki, S., Tunved, P., Tørseth, K., and Biskos, G.: Indirect evidence of
 2487 the composition of nucleation mode atmospheric particles in the high Arctic, *J. Geophys. Res.: Atmos.*,
 2488 121(2), 965-975, doi:10.1002/2015jd023646, 2016.
- 2489 Gil, J., Pérez, T., Boering, K., Martikainen, P. J., and Biasi, C.: Mechanisms responsible for high N₂O
 2490 emissions from subarctic permafrost peatlands studied via stable isotope techniques, *Global Biogeochem.*
 2491 *Cycles*, 31(1), 172, doi:10.1002/2015GB005370, 2017.
- 2492 Glagolev, M.V., Ilyasov, D. V. I., Terentieva, E., Sabrekov, A. F., Yu Mochenov, S., and Maksutov, S. S.:
 2493 Methane and carbon dioxide fluxes in the waterlogged forests of south and middle taiga of Western Siberia,
 2494 *IOP Conf. Ser.: Earth Environ. Sci.*, 138 012005, 2018.

- 2495 Gnatiuk, N., Radchenko, I., Davy, R., Morozov E., and Bobylev, L.: Simulation of factors affecting
2496 *Emiliania huxleyi* blooms in Arctic and sub-Arctic seas by CMIP5 climate models: model validation and
2497 selection, *Biogeosciences*, 17, 1199–1212. doi: 10.5194/bg-17-1199-2020, 2020.
- 2498 Godrijan, J., Drapeau, D., and Balch, W. M.: Mixotrophic uptake of organic compounds by coccolithophores,
2499 *Limnol. Ocean.*, Early bird publication, <https://doi.org/10.1002/lno.11396>, 2020.
- 2500 Gordov, E.P., Okladnikov, I.G., Titov, A.G., Voropay N.N., Ryazanova A.A., and Lykosov V.N.:
2501 Development of Information-computational Infrastructure for Modern Climatology, *Russ. Meteorol. Hydrol.*,
2502 43, 722–728, <https://doi.org/10.3103/S106837391811002X>, 2018.
- 2503 Granath, G., Rydin, H., Baltzer, J. L., Bengtsson, F., Boncek, N., Bragazza, L., Bu, Z.-J., Caporn, S. J. M.,
2504 Dorrepaal, E., Galanina, O., Gałka, M., Ganeva, A., Gillikin, D. P., Goia, I., Goncharova, N., Hájek, M.,
2505 Haraguchi, A., Harris, L. I., Humphreys, E., Jiroušek, M., Kajukalo, K., Karofeld, E., Koronatova, N. G.,
2506 Kosykh, N. P., Lamentowicz, M., Lapshina, E., Limpens, J., Linkosalmi, M., Ma, J.-Z., Mauritz, M., Munir,
2507 T. M., Natali, S. M., Natcheva, R., Noskova, M., Payne, R. J., Pilkington, K., Robinson, S., Robroek, B. J.
2508 M., Rochefort, L., Singer, D., Stenøien, H. K., Tuittila, E.-S., Vellak, K., Verheyden, A., Waddington, J. M.,
2509 and Rice, S. K.: Environmental and taxonomic controls of carbon and oxygen stable isotope composition in
2510 *Sphagnum* across broad climatic and geographic ranges, *Biogeosciences*, 15, 5189–5202,
2511 <https://doi.org/10.5194/bg-15-5189-2018>, 2018.
- 2512 Grigoriev, V.Y., and Frolova, N.L.: Terrestrial water storage change of European Russia and its impact on
2513 water balance, *Geography, Environment, Sustainability*, 11(1), 38-50. [https://doi.org/10.24057/2071-9388-](https://doi.org/10.24057/2071-9388-2018-11-1-38-50)
2514 2018-11-1-38-50, 2018.
- 2515 Groundstroem, F., and Juhola, S.: A framework for identifying cross-border impacts of climate change on
2516 the energy sector, *Environment Systems and Decisions*, 39(1), 3-15, doi:10.1007/s10669-018-9697-2, 2019.
- 2517 Gunchin, G., Manousakas, M., Osan, J., Karydas, A. G., Eleftheriadis, K., Lodoysamba, S., Shagjjamba, D.,
2518 Migliori, A., Padilla-Alvarez, R., Strelí, C., and Darby, I.: Three-year long source apportionment study of
2519 airborne particles in Ulaanbaatar using x-ray fluorescence and positive matrix factorization, *Aerosol and Air*
2520 *Quality Research*, 19(5), 1056-1067, doi:10.4209/aaqr.2018.09.0351, 2019.
- 2521 Guo, Y., Yan, C., Li, C., Feng, Z., Zhou, Y., Lin, Z., Dada, L., Stolzenburg, D., Yin, R., Kontkanen, J.,
2522 Daellenbach, K. R., Kangasluoma, J., Yao, L., Chu, B., Wang, Y., Cai, R., Bianchi, F., Liu, Y., and Kulmala,
2523 M.: Formation of Nighttime Sulfuric Acid from the Ozonolysis of Alkenes in Beijing, *Atmos. Chem. Phys.*
2524 *Discuss.*, <https://doi.org/10.5194/acp-2019-1111>, in review, 2020.
- 2525 Gurchenkov, A. A., Murynin, A. B., Trekin, A. N., and Ignatyev, V. Y.: Object-oriented classification of
2526 substrate surface objects in Arctic impact regions aerospace monitoring, *Herald of the Bauman Moscow*
2527 *State Technical University*, 135-146. doi:10.18698/1812-3368-2017-3-135-146, 2017.

- 2528 Göckede, M., Kittler, F., Kwon, M. J., Burjack, I., Heimann, M., Kolle, O., Zimov, N., and Zimov, S.:
2529 Shifted energy fluxes, increased Bowen ratios, and reduced thaw depths linked with drainage-induced
2530 changes in permafrost ecosystem structure, *The Cryosphere*, 11, 2975–2996, [https://doi.org/10.5194/tc-11-](https://doi.org/10.5194/tc-11-2975-2017)
2531 2975-2017, 2017.
- 2532 Göckede, M., Kwon, M. J., Kittler, F., Heimann, M., Zimov, N., and Zimov, S.: Negative feedback processes
2533 following drainage slow down permafrost degradation, *Glob. Change Biol.*, 25, 3254– 3266,
2534 <https://doi.org/10.1111/gcb.14744>, 2019.
- 2535 Hao, L., Garmash, O., Ehn, M., Miettinen, P., Massoli, P., Mikkonen, S., Jokinen, T., Roldin, P., Aalto, P.,
2536 Yli-Juuti, T., Joutsensaari, J., Petäjä, T., Kulmala, M., Lehtinen, K. E. J., Worsnop, D. R., and Virtanen, A.:
2537 Combined effects of boundary layer dynamics and atmospheric chemistry on aerosol composition during
2538 new particle formation periods, *Atmospheric Chemistry and Physics*, 18(23), 17705-17716. doi:10.5194/acp-
2539 18-17705-2018, 2018.
- 2540 Hari, P. & Kulmala, M.: Station for Measuring Ecosystem–Atmosphere Relations (SMEAR II). *Boreal Env.*
2541 *Res.* 10: 315–322, 2005.
- 2542
- 2543 Hari, P., Andreae M., Kabat P., and Kulmala M.: A comprehensive network of measuring stations to
2544 monitor climate change. *Boreal Env. Res.* 14: 442-446, 2009.
- 2545
- 2546 Hari, P., Petäjä, T., Bäck, J., Kerminen, V.-M., Lappalainen, H. K., Vihma, T., Laurila, T., Viisanen, Y.,
2547 Vesala, T., and Kulmala, M.: Conceptual design of a measurement network of the global change, *Atmos.*
2548 *Chem. Phys.*, 16, 1017-1028, doi:10.5194/acp-16-1017-2016, 2016.
- 2549 Hari, P., Kerminen, V.-M., Kulmala, L., Kulmala, M., Noe, S., Petäjä, T., Vanhatalo, A., and Bäck, J.:
2550 Annual cycle of Scots pine photosynthesis, *Atmos. Chem. Phys.*, 17, 15045–15053, doi:10.5194/acp-17-
2551 15045-2017, 2017.
- 2552 Heikkilä, A., Makelä, J. S., Lakkala, K., Meinander, O., Kaurola, J., Koskela, T., Karhu, J. M., Karppinen,
2553 T., Kyro, E., and De Leeuw, G.: In search of traceability: two decades of calibrated Brewer UV
2554 measurements in Sodankyla and Jokioinen, *Geoscientific Instrumentation, Methods and Data Systems*, 5(2),
2555 531-540, doi:10.5194/gi-5-531-2016, 2016.
- 2556 Heintzenberg, J., Tunved, P., Galí, M., and Leck, C.: New particle formation in the Svalbard region 2006–
2557 2015, *Atmos. Chem. Phys.*, 17, 6153–6175, doi:10.5194/acp-17-6153-2017, 2017.
- 2558 Helin, A., Sietiö, O.-M., Heinonsalo, J., Bäck, J., Riekkola, M.-L., and Parshintsev, J.: Characterization of
2559 free amino acids, bacteria and fungi in size-segregated atmospheric aerosols in boreal forest: seasonal
2560 patterns, abundances and size distributions, *Atmos. Chem. Phys.*, 17, 13089–13101, doi.org/10.5194/acp-17-
2561 13089-2017, 2017.

- 2562 Hellén, H., Praplan, A. P., Tykkä, T., Ylivinkka, I., Vakkari, V., Bäck, J., Petäjä, T., Kulmala, M., and
2563 Hakola, H.: Long-term measurements of volatile organic compounds highlight the importance of
2564 sesquiterpenes for the atmospheric chemistry of a boreal forest, *Atmos. Chem. Phys.*, 18, 13839–13863,
2565 <https://doi.org/10.5194/acp-18-13839-2018>, 2018.
- 2566 Hinzman, L.D., Bettez, N.D., Bolton, W.R. et al. :Evidence and Implications of Recent Climate Change in
2567 Northern Alaska and Other Arctic Regions, *Climatic Change*, 72, 251–298, [doi.org/10.1007/s10584-005-](https://doi.org/10.1007/s10584-005-5352-2)
2568 [5352-2](https://doi.org/10.1007/s10584-005-5352-2), 2005.
- 2569 Hoegh-Guldberg, O., Jacob, D., Taylor, M., Bindi, M., Brown, S., Camilloni, I., Diedhiou, A.,
2570 Djalante, R., Ebi, K. L., Engelbrecht, F., Guiot, J., Hijioka, Y., Mehrotra, S., Payne, A., Seneviratne, S. I.,
2571 Thomas, A., Warren, R., and Zhou, G.: Impacts of 1.5°C Global Warming on Natural and Human Systems,
2572 in: *Global Warming of 1.5°C: An IPCC Special Report on the impacts of global warming of 1.5°C above*
2573 *pre-industrial levels and related global greenhouse gas emission pathways, in the context of*
2574 *strengthening the global response to the threat of climate change, sustainable development, and efforts to*
2575 *eradicate poverty*, edited by: Masson-Delmotte, V., Zhai, P., Pörtner, H.-O., Roberts, D., Skea, J., Shukla, P.
2576 R., Pirani, A., Moufouma-Okia, W., Péan, C., Pidcock, R., Connors, S., Matthews, J. B. R., Chen, Y., Zhou,
2577 X., Gomis, M. I., Lonnoy, E., Maycock, T., Tignor, M., and Waterfield, T., WMO, Geneva, Switzerland,
2578 2018.
- 2579 Hong, J., Kim, J., Nieminen, T., Duplissy, J., Ehn, M., Äijälä, M., Hao, L. Q., Nie, W., Sarnela, N., Prisle, N.
2580 L., Kulmala, M., Virtanen, A., Petäjä, T., and Kerminen, V.-M.: Relating the hygroscopic properties of
2581 submicron aerosol to both gas- and particle-phase chemical composition in a boreal forest environment,
2582 *Atmos. Chem. Phys.*, 15, 11999–12009, <https://doi.org/10.5194/acp-15-11999-2015>, 2015.
- 2583 Huang, W., Cheng, B., Zhang, J., Zhang, Z., Vihma, T., Li, Z., and Niu, F.: Modeling experiments on
2584 seasonal lake ice mass and energy balance in the Qinghai–Tibet Plateau: a case study, *Hydrol. Earth Syst.*
2585 *Sci.*, 23, 2173–2186, 2019a.
- 2586 Huang, W., Zhang, J., Leppäranta, M., Li, Z., Cheng, B. and Lin, Z. 2019b. Thermal structure and water-ice
2587 heat transfer in a shallow ice-covered thermokarst lake in central Qinghai-Tibet Plateau, *Journal of*
2588 *Hydrology*, 578, [124122], 2019b.
- 2589 Hölttä, T., Lintunen, A., Chan, T., Mäkelä, A., and Nikinmaa, E.: A steady state stomatal model of balanced
2590 leaf gas exchange, hydraulics and maximal source-sink flux, *Tree Physiology*, 37, 851–868, doi:
2591 [10.1093/treephys/tpx011](https://doi.org/10.1093/treephys/tpx011), 2017.
- 2592 IPCC: Special Report on the Ocean and Cryosphere in a Changing Climate, edited by Pörtner, H.-O.,
2593 Roberts, D.C., Masson-Delmotte, V., Zhai, P., Tignor, M., Poloczanska, E., Mintenbeck, K., Alegría, A.,
2594 Nicolai, M., Okem, A., Petzold, J., Rama, B., and Weyer, N. M., 2019.
- 2595 IPCC, 2021: Climate Change 2021: The Physical Science Basis. Contribution of Working Group I to the
2596 Sixth Assessment Report of the Intergovernmental Panel on Climate Change [Masson-Delmotte, V., P. Zhai,

- 2597 A. Pirani, S. L. Connors, C. Péan, S. Berger, N. Caud, Y. Chen, L. Goldfarb, M. I. Gomis, M. Huang, K.
2598 Leitzell, E. Lonnoy, J.B.R. Matthews, T. K. Maycock, T. Waterfield, O. Yelekçi, R. Yu and B. Zhou (eds.)].
2599 Cambridge University Press. In Press. Summary for Policymakers IPCC, 2021: Summary for Policymakers.
2600 In: Climate Change 2021: The Physical Science Basis. Contribution of Working Group I to the Sixth
2601 Assessment Report of the Intergovernmental Panel on Climate Change [Masson-Delmotte, V., P. Zhai, A.
2602 Pirani, S. L. Connors, C. Péan, S. Berger, N. Caud, Y. Chen, L. Goldfarb, M. I. Gomis, M. Huang, K.
2603 Leitzell, E. Lonnoy, J.B.R. Matthews, T. K. Maycock, T. Waterfield, O. Yelekçi, R. Yu and B. Zhou (eds.)].
2604 Cambridge University Press. In Press.
- 2605 Ivakhov, V. M., Paramonova, N. N., Privalov, V. I., Zinchenko, A. V., Loskutova, M. A., Makshtas, A. P.,
2606 Kustov, V. Y., Laurila, T., Aurela, M., and Asmi, E.: Atmospheric Concentration of Carbon Dioxide at Tiksi
2607 and Cape Baranov Stations in 2010-2017, *Russ. Meteorol. Hydrol.*, 44, 291–299,
2608 doi:10.3103/s1068373919040095, 2019.
- 2609 Jaffe, D., Bertschi, I., Jaegle, L., Novelli, P., Reid, J. S., Tanimoto, H., Vingarzan, R. and Westphal, D. L.:
2610 Long-range transport of Siberian biomass burning emissions and impact on surface ozone in western North
2611 America, *Geophys. Res. Lett.*, 31(16), L16106, doi:10.1029/2004GL020093, 2004.
- 2612 Jakobson, L., T. Vihma, and E. Jakobson,: Relationships between Sea Ice Concentration and Wind Speed
2613 over the Arctic Ocean during 1979–2015., *J. Climate*, 32, 7783–7796, [https://doi.org/10.1175/JCLI-D-19-](https://doi.org/10.1175/JCLI-D-19-0271.1)
2614 [0271.1](https://doi.org/10.1175/JCLI-D-19-0271.1), 2019.
- 2615 Juhola, S.: Planning for a green city: The Green Factor tool, *Urban Forestry and Urban Greening*, 34, 254-
2616 258, doi:10.1016/j.ufug.2018.07.019, 2018.
- 2617 Juutinen, S., Virtanen, T., Kondratyev, V., Laurila, T., Linkosalmi, M., Mikola, J., Nyman, J., Räsänen, A.,
2618 Tuovinen, J.-P., and Aurela, M.: Spatial variation and seasonal dynamics of leaf-area index in the arctic
2619 tundra-implications for linking ground observations and satellite images, *Environ. Res. Lett.*, 12(9), 10,
2620 doi:10.1088/1748-9326/aa7f85, 2017.
- 2621 Kalogridis, A.C., Popovicheva, O.B., Engling, G., Diapouli, E., Kawamura, K., Tachibana, E., Ono, K.,
2622 Kozlov, V.S., and Eleftheriadis, K.: Smoke aerosol chemistry and aging of Siberian biomass burning
2623 emissions in a large aerosol chamber, *Atmos. Environ.*, 185, 15-28, 2018.
- 2624 Kangasluoma, J., Ahonen, L. R., Laurila, T., Cai, R., Enroth, J., Mazon, S., Korhonen, F., Aalto, P.,
2625 Kulmala, M., Attoui, M. and Petäjä, T.: Laboratory verification of a new high flow differential mobility
2626 particle sizer, and field measurements in Hyytiälä, *J Aerosol Sci*, 124, 1-9, 2018.
- 2627 Karelin, D. V., Goryachkin, S. V., Zamolodchikov, D. G., Dolgikh, A. V., Zazovskaya, E. P., Shishkov, V.
2628 A., and Kraev, G. N.: Human footprints on greenhouse gas fluxes in cryogenic ecosystems, *Dokl. Earth Sc.*,
2629 477, 1467–1469, doi:10.1134/S1028334X17120133, 2017.

- 2630 Karetnikov, S., Leppäranta, M., and Montonen, A.: A time series of over 100 years of ice seasons on Lake
2631 Ladoga, *Journal of Great Lakes Research*, 43(6), 979-988, doi:10.1016/j.jglr.2017.08.010, 2017.
- 2632 Karthe, D., Abdullaev, I., Boldgiv, B., Borchardt, D., Chalov, S., Jarsjö, J., Li, L., and Nittrouer, J.A.: Water
2633 in Central Asia: an integrated assessment for science-based management, *Environmental Earth Sciences*,
2634 76(20), 15, doi:10.1007/s12665-017-6994-x, 2017a.
- 2635 Karthe, D., Chalov, S., Moreido, V., Pashkina, M., Romanchenko, A., Batbayar, G., Kalugin, A., Westphal,
2636 K., Malsy, M., and Flörke, M.: Assessment of runoff, water and sediment quality in the Selenga River basin
2637 aided by a web-based geoservice, *Water Resources*, 44(3), 399-416, 2017b.
- 2638 Karthe D., Chalov S., Gradel A., and Kusbach A.: Special issue: Environment change on the Mongolian
2639 plateau: atmosphere, forests, soils and water, *Geography, Environment, Sustainability*, 12(3), 60-65,
2640 doi:10.24057/2071-9388-2019-1411, 2019.
- 2641 Karvonen, J., Shi, L., Cheng, B., Similä, M., Mäkynen, M., and Vihma, T.: Bohai Sea ice parameter
2642 estimation based on thermodynamic ice model and Earth observation data, *Remote Sensing*, 9, 234,
2643 doi:10.3390/rs9030234, 2017.
- 2644 Kasimov, N., Karthe, D., and Chalov, S.: Environmental change in the Selenga River—Lake Baikal Basin,
2645 *Reg. Environ. Chang.*, 17, 1945–1949, 2017a.
- 2646 Kasimov, N. S., Kosheleva, N. E., Nikiforova, E. M., and Vlasov, D. V.: Benzo a pyrene in urban
2647 environments of eastern Moscow: pollution levels and critical loads, *Atmos. Chem. Phys.*, 17(3), 2217-2227,
2648 doi:10.5194/acp-17-2217-2017, 2017b.
- 2649 Kasimov, N., Shinkareva, G., Lychagin, M., Kosheleva, N., Chalov, S., Pashkina, M., Thorslund, J., and
2650 Jarsjö, J.: River water quality of the selenga-baikal basin: Part i—spatio-temporal patterns of dissolved and
2651 suspended metals, *Water*, 12(8), 2137, 2020a.
- 2652
- 2653 Kasimov, N., Shinkareva, G., Lychagin, M., Chalov, S., Pashkina, M., Thorslund, J., and Jarsjö, J.: River
2654 water quality of the selenga-baikal basin: part ii — metal partitioning under different hydroclimatic
2655 conditions, *Water*, 12(9), 2392, 2020b.
- 2656
- 2657 Kaus, A., Schäffer, M., Karthe, D., Büttner, O., von Tümpling, W., and Borchardt, D.: Regional patterns of
2658 heavy metal exposure and contamination in the fish fauna of the Kharaa River basin, Mongolia, *Reg.*
2659 *Environ. Change*, 17, 2023–2037, doi: 10.1007/s10113-016-0969-4, 2017.
- 2660 Kazakov, E., Kondrik, D., and Pozdnyakov, D.: A synthetic satellite dataset of the spatio-temporal
2661 distributions of *Emiliania huxleyi* blooms and their impacts on Arctic and sub-Arctic marine environments
2662 (1998–2016), *Earth Systems Science Data*, 11, 119–128, doi: 10.5194/essd-11-119-2019, 2019.

- 2663 Kecorius, S., Vogl, T., Paasonen, P., Lampilahti, J., Rothenberg, D., Wex, H., Zeppenfeld, S., van Pinxteren,
2664 M., Hartmann, M., Henning, S., Gong, X., Welti, A., Kulmala, M., Stratmann, F., Herrmann, H., and
2665 Wiedensohler, A.: New particle formation and its effect on cloud condensation nuclei abundance in the
2666 summer Arctic: a case study in the Fram Strait and Barents Sea, *Atmos. Chem. Phys.*, 19, 14339–14364, doi:
2667 10.5194/acp-19-14339-2019, 2019.
- 2668 Kerminen, V.-M., Chen, X., Vakkari, V., Petäjä, T., Kulmala, M., and Bianchi, F.: Atmospheric new particle
2669 formation and growth: review of field observations, *Environ. Res. Lett.*, 13, 103003, doi: 10.1088/1748-
2670 9326/aadf3c, 2018.
- 2671 Kim, J., Kim, H. M., Cho, C.-H., Boo, K.-O., Jacobson, A. R., Sasakawa, M., Machida, T., Arshinov, M.,
2672 and Fedoseev, N.: Impact of Siberian observations on the optimization of surface CO₂ flux, *Atmos. Chem.*
2673 *Phys.*, 17, 2881–2899, <https://doi.org/10.5194/acp-17-2881-2017>, 2017.
- 2674 Kirillin, G., Leppäranta, M., Terzhevik, A., Bernhardt, J., Engelhardt, C., Granin, N., Golosov, S., Efremova,
2675 T., Palshin, N., Sherstyankin, P., Zdorovenova, G., and Zdorovenov, R.: Physics of seasonally ice-covered
2676 lakes: major drivers and temporal/spatial scales, *Aquatic Ecol.*, 74, 659–682, 2012.
- 2677 Kirillin, G., Aslamov, I., Leppäranta, M., and Lindgren, E.: Turbulent mixing and heat fluxes under lake ice:
2678 the role of seiche oscillations, *Hydrology of Earth System Sciences*, 22(12), 6493–6504, doi:10.5194/hess-
2679 22-6493-2018, 2018.
- 2680 Kirschke, S., Bousquet, P., Ciais, P., Saunio, M., Canadell, J. G., Dlugokencky, E. J., Bergamaschi, P.,
2681 Bergmann, D., Blake, D. R., Bruhwiler, L., Cameron-Smith, P., Castaldi, S., Chevallier, F., Feng, L., Fraser,
2682 A., Heimann, M., Hodson, E. L., Houweling, S., Josse, B., Fraser, P. J., Krummel, P. B., Lamarque, J.-F.,
2683 Langenfelds, R. L., Le Quere, C., Naik, V., O’Doherty, S., Palmer, P. I., Pison, I., Plummer, D., Poulter, B.,
2684 Prinn, R. G., Rigby, M., Ringeval, B., Santini, M., Schmidt, M., Shindell, D. T., Simpson, I. J., Spahni, R.,
2685 Steele, L. P., Strode, S. A., Sudo, K., Szopa, S., van der Werf, G.R., Voulgarakis, A., van Weele, M., Weiss,
2686 R. F., Williams, J. E., and Zeng, G.: Three decades of global methane sources and sinks, *Nature Geoscience*,
2687 6(10), 813–823, doi: 10.1038/ngeo1955, 2013.
- 2688 Kiselev, M. V., Voropay, N. N., and Cherkashina, A. A.: influence of anthropogenic activities on the
2689 temperature regime of soils of the South-Western Baikal region, *IOP Conf. Ser.: Earth Environ. Sci.*, 381,
2690 012043, doi: 10.1088/1755-1315/381/1/012043, 2019.
- 2691 Kittler, F., Heimann, M., Kolle, O., Zimov, N., Zimov, S., and Göckede, M.: Long-term drainage reduces
2692 CO₂ uptake and CH₄ emissions in a Siberian permafrost ecosystem, *Global Biogeochemical Cycles*, 31,
2693 1704–1717. doi: 10.1002/2017GB005774, 2017.
- 2694 Kiuru, P., Ojala, A., Mammarella, I., Heiskanen, J., Kämäräinen, M., Vesala, T. and Huttula, T.: Effects of
2695 Climate Change on CO₂ Concentration and Efflux in a Humic Boreal Lake: A Modeling Study, *Journal of*
2696 *Geophysical Research, Biogeosciences*, 123, 7, 2212–2233, 2018.

- 2697 Kondrik, D., Pozdnyakov, D., and Pettersson, L.: Particulate inorganic carbon production within *E. huxleyi*
2698 blooms in subpolar and polar seas: a satellite time series study (1998–2013), *International Journal of Remote*
2699 *Sensing*, 38:22, 6179–6205, doi: 10.1080/01431161.2017.1350304, 2017.
- 2700 Kondrik, D. V., Pozdnyakov, D. V., and Johannessen, O. M.: Satellite evidence that *E. huxleyi*
2701 phytoplankton blooms weaken marine carbon sinks, *Geophys. Res. Lett.*, 5, 846–854. doi:
2702 10.1002/2017GL076240, 2018a.
- 2703 Kondrik, D. V., Pozdnyakov, D. V., and Pettersson, L. H.: Tendencies in Coccolithophorid Blooms in Some
2704 Marine Environments of the Northern Hemisphere according to the Data of Satellite Observations in 1998–
2705 2013. *Izv. Atmos. Ocean. Phys.*, 53, 955–964, doi: 10.1134/S000143381709016X, 2018b.
- 2706 Kondrik, D. V., Kazakov, E. E., Pozdnyakov, D. V., and Johannessen, O. M.: Satellite evidence for
2707 enhancement of the column mixing ratio of atmospheric CO₂ over *E. huxleyi* blooms, *Transactions of the*
2708 *Karelian Research Centre of the Russian Academy of Sciences, Limnologoia i Oceanologia series*, 9, 1–11,
2709 doi: 10/17076/lim1107, 2019.
- 2710 Konovalov, I. B., Lvova, D. A., Beekmann, M., Jethva, H., Mikhailov, E. F., Paris, J.-D., Belan, B. D.,
2711 Kozlov, V. S., Ciais, P., and Andreae, M. O.: Estimation of black carbon emissions from Siberian fires using
2712 satellite observations of absorption and extinction optical depths, *Atmos. Chem. Phys.*, 18, 14889–14924,
2713 doi: 10.5194/acp-18-14889-2018, 2018.
- 2714 Konovalov V., Rets E., and Pimankina N.: Interrelation between glacier summer mass balance and runoff in
2715 mountain river basins, *Geography, Environment, Sustainability*, 12(1), 23–33, doi: 10.24057/2071-9388-
2716 2018-26, 2019.
- 2717 Konstantinov, P. I., Grishchenko, M. Y., and Varentsov, M. I.: Mapping urban heat islands of arctic cities
2718 using combined data on field measurements and satellite images based on the example of the city of Apatity
2719 (Murmansk Oblast), *Izv. Atmos. Ocean. Phys.*, 51(9), 992–998, doi:10.1134/s000143381509011x, 2015.
- 2720 Konstantinov, P., Varentsov, M., and Esau, I.: A high density urban temperature network deployed in several
2721 cities of Eurasian Arctic, *Environ. Res. Lett.*, 13(7), 12, doi:10.1088/1748-9326/aac84, 2018.
- 2722 Kontkanen, J., Paasonen, P., Aalto, J., Back, J., Rantala, P., Petäjä, T., and Kulmala, M.: Simple proxies for
2723 estimating the concentrations of monoterpenes and their oxidation products at a boreal forest site, *Atmos.*
2724 *Chem. Phys.*, 16(20), 13291–13307, doi:10.5194/acp-16-13291-2016, 2016.
- 2725 Kontkanen, J., Deng, C., Fu, Y., Dada, L., Zhou, Y., Cai, J., Daellenbach, K.R., Hakala, S., Kokkonen, T.V.,
2726 Lin, Z., Liu, Y., Wang, Y., Yan, C., Petäjä, T., Jiang, J., Kulmala, M. and Paasonen, P. : Size-resolved
2727 particle number emissions in Beijing determined from measured particle size distributions, *Atmos. Chem.*
2728 *Phys.* 20, 11329–11348, 2020.

- 2729 Kooijmans, L. M. J., Sun, W., Aalto, J., Erkkilä, K.M., Maseyk, K., Seibt, U., Vesala, T., Mammarella, I.,
2730 and Chen, H.: Influences of light and humidity on carbonyl sulfide-based estimates of photosynthesis,
2731 *Proceedings of the National Academy of Sciences*, 116 (7), 2470-2475, doi:10.1073/pnas.1807600116, 2019.
- 2732 Korneykova, M. V., and Evdokimova, G. A.: Microbiota of the ground air layers in natural and industrial
2733 zones of the Kola Arctic, *J Environ. Sci. Health A*, 53(3), 271-277, doi:10.1080/10934529.2017.1397444,
2734 2018a.
- 2735 Korneikova, M. V., Redkina, V. V., and Shalygina, R. R.: Algological and mycological characterization of
2736 soils under pine and birch forests in the Pasvik Reserve, *Eurasian Soil Science*, 51(2), 211-220,
2737 doi:10.1134/s1064229318020047, 2018b.
- 2738 Koronatova, N. G., & Milyaeva, E. V.: Plant community succession in post-mined quarries in the northern-
2739 taiga zone of West Siberia. *Contemporary Problems of Ecology*, 4(5), 513–518, 2011.
- 2740 Kukkonen, I., Ezhova, E., Suhonen, E. A. J., Lappalainen, H. K., Gennadinik, V., Ponomareva, O., Gravis,
2741 A., Miles, V., Kulmala, M., Melnikov, V., and Drozdov, D.: Observations and modelling of ground
2742 temperature evolution in the discontinuous permafrost zone in Nadym, North-West Siberia, *Permafrost and*
2743 *Periglacial Processes*, 1– 17, doi:10.1002/ppp.2040, 2020.
- 2744 Kulmala, M., Vehkamäki, H., Petäjä, T., Dal Maso, M., Lauri, A., Kerminen, V.-M., Birmili, W., and
2745 McMurry, P.H.: Formation and growth rates of ultrafine atmospheric particles: a review of observations,
2746 *Journal of Aerosol Science*, 35, 143-176, doi:10.1134/S1995425511050, 2004.
- 2747 Kulmala, M.: Atmospheric chemistry: China's choking cocktail, *Nature*, 526, 497-499,
2748 doi:10.1038/526497a, 2015a.
- 2749 Kulmala, M., Lappalainen, H. K., Petäjä, T., Kurten, T., Kerminen, V.-M., Viisanen, Y., Hari, P., Sorvari, S.,
2750 Bäck, J., Bondur, V., Kasimov, N., Kotlyakov, V., Matvienko, G., Baklanov, A., Guo, H. D., Ding, A.,
2751 Hansson, H.-C., and Zilitinkevich, S.: Introduction: The Pan-Eurasian Experiment (PEEX) –
2752 multidisciplinary, multiscale and multicomponent research and capacity-building initiative, *Atmos. Chem.*
2753 *Phys.*, 15, 13085-13096, doi:10.5194/acp-15-13085-2015, 2015b.
- 2754 Kulmala, M., Lappalainen, H. K., Petäjä, T., Kerminen, V.-M., Viisanen, Y., Matvienko, G., Melnikov, V.,
2755 Baklanov, A., Bondur, V., Kasimov, N., and Zilitinkevich, S.: Pan-Eurasian Experiment (PEEX) Program:
2756 Grant Challenges in the Arctic-boreal context, *J. Geography Environment Sustainability*, 2, 5–18, 2016a.
- 2757 Kulmala, M., Petäjä, T., Kerminen, V. M., Kujansuu, J., Ruuskanen, T., Ding, A., Nie, W., Hu, M., Wang,
2758 Z., Wu, Z., and Wang, L.: On secondary new particle formation in China, *Front. Environ. Sci. Eng.*, 10, 8,
2759 doi:10.1007/s11783-016-0850-1, 2016b.
- 2760 Kulmala, M., Kerminen, V.-M., Petäjä, T., Ding, A. J., and Wang L.: Atmospheric gas-to-particle
2761 conversion: why NPF events are observed in megacities?, *Faraday Discuss.*, 200, 271-288,
2762 doi:10.1039/c6fd00257a, 2017.

- 2763 Kulmala, M.: Build a global Earth observatory, *Nature*, 553, 21-23, doi: 10.1038/d41586-017-08967-y, 2018.
- 2764 Kulmala, L., Pumpanen, J., Kolari, P., Dengel, S., Berninger, F., Köster, K., Matkala, L., Vanhatalo, A.,
2765 Vesala, T., and Bäck, J.: Inter- and intra-annual dynamics of photosynthesis differ between forest floor
2766 vegetation and tree canopy in a subarctic Scots pine stand, *Agricultural and Forest Meteorology*, 271, 1-11,
2767 doi: 10.1016/j.agrformet.2019.02.029, 2019.
- 2768 Kulmala, M., Dada, L., Daellenbach, K. R., Yan, C., Stolzenburg, D., Kontkanen, J., Ezhova, E., Hakala, S.,
2769 Tuovinen, S., Kokkonen, T. V., Kurppa, M., Cai, R., Zhou, Y., Yin, R., Baalbaki, R., Chan, T., Chu, B.,
2770 Deng, C., Fu, Y., Ge, M., He, H., Heikkinen, L., Junninen, H., Liu, Y., Lu, Y., Nie, W., Rusanen, A.,
2771 Vakkari, V., Wang, V., Yang, G., Yao, L., Zheng, J., Kujansuu, J., Kangasluoma, J., Petäjä, T., Paasonen, P.,
2772 Järvi, L., Worsnop, D., Ding, A., Liu, Y., Wang, L., Jiang, J., Bianchi, F., and Kerminen, V.-M.: Is reducing
2773 new particle formation a plausible solution to mitigate particulate air pollution in Beijing and other Chinese
2774 megacities?, *Faraday Discussions*, doi: 10.1039/D0FD00078G.2021.
- 2775 Kwon, M. J., Beulig, F., Ilie, I., Wildner, M., Küsel, K., Merbold, L., Mahecha, M. D., Zimov, N., Zimov, S.
2776 A., Heimann, M., Schuur, E. A. G., Kostka, J. E., Kolle, O., Hilke, I. and Göckede, M.: Plants,
2777 microorganisms, and soil temperatures contribute to a decrease in methane fluxes on a drained Arctic
2778 floodplain, *Glob. Change Biol.*, 23, 2396-2412, doi:10.1111/gcb.13558, 2017.
- 2779 Kwon, M. J., Natali, S. M., Hicks Pries, C. E., Schuur, E. A., Steinhof, A., Crummer, K. G., Zimov, N.,
2780 Zimov, S. A., Heimann, M., Kolle, O., and Göckede, M.: Drainage enhances modern soil carbon contribution
2781 but reduces old soil carbon contribution to ecosystem respiration in tundra ecosystems, *Glob. Change Biol.*,
2782 25, 1315– 1325, doi: 10.1111/gcb.14578, 2019.
- 2783 Kühn, T., Kupiainen, K., Miinalainen, T., Kokkola, H., Paunu, V.-V., Laakso, A., Tonttila, J., Van
2784 Dingenen, R., Kulovesi, K., Karvosenoja, N., and Lehtinen, K. E. J.: Effects of black carbon mitigation on
2785 Arctic climate, *Atmos. Chem. Phys.*, 20, 5527–5546, doi: 10.5194/acp-20-5527-2020, 2020.
- 2786 Köster, E., Köster, K., Berninger, F., and Pumpanen, J.: Carbon dioxide, methane and nitrous oxide fluxes
2787 from podzols of a fire chronosequence in the boreal forests in Värriö, Finnish Lapland, *Geoderma Regional*,
2788 5, 181-187, doi:10.1016/j.geodrs.2015.07.001, 2015.
- 2789 Köster, E., Köster, K., Berninger, F., Prokushkin, A., Aaltonen, H., Zhou, X., and Pumpanen, J.: Changes in
2790 fluxes of carbon dioxide and methane caused by fire in Siberian boreal forest with continuous permafrost,
2791 *Journal of Environmental Management*, 228, 405-415, doi:10.1016/j.jenvman.2018.09.051, 2018.
- 2792 Köster, K., Berninger, F., Köster, E., and Pumpanen, J.: Influences of reindeer grazing on above- and
2793 belowground biomass and soil carbon dynamics, *Arctic Antarctic and Alpine Res.*, 47(3), 495-503,
2794 doi:10.1657/aaar0014-062, 2015.

- 2795 Köster, K., Berninger, F., Heinonsalo, J., Lindén, A., Köster, E., Ilvesniemi, H., and Pumpanen J.: The long-
 2796 term impact of low-intensity surface fires on litter decomposition and enzyme activities in boreal coniferous
 2797 forests, *Int. J Wildland Fire*, 25(2), 213-223, doi:10.1071/wf14217_co, 2016.
- 2798 Köster, K., Koster, E., Berninger, F., Heinonsalo, J., and Pumpanen, J.: Contrasting effects of reindeer
 2799 grazing on CO₂, CH₄, and N₂O fluxes originating from the northern boreal forest floor. *Land Degradation
 2800 and Development*, 29(2), 374-381, doi:10.1002/ldr.2868, 2018.
- 2801 Köster, K., Koster, E., Kulmala, L., Berninger, F., and Pumpanen, J.: Are the climatic factors combined with
 2802 reindeer grazing affecting the soil CO₂ emissions in subarctic boreal pine forest? *Catena*, 149, 616-622,
 2803 doi:10.1016/j.catena.2016.06.011, 2017.
- 2804 Lan, H., Holopainen, J., Hartonen, K., Jussila, M., Ritala, M. and Riekkola, M.-L.: Fully automated online
 2805 dynamic in-tube extraction for continuous sampling of volatile organic compounds in air, *Anal. Chem.*, 91,
 2806 8507, 2019.
- 2807 Lappalainen, H.K., Kulmala, M. and Zilitinkevich, S. (Eds.): Pan Eurasian Experiment (PEEX) Science Plan,
 2808 web: www.atm.helsinki.fi/peex, ISBN 978-951-51-0587-5 (printed), ISBN 978-951-51-0588-2 (online),
 2809 2015.
- 2810 Lappalainen H.K., Petäjä T., Kujansuu J., Kerminen V., Shvidenko A., Bäck J., Vesala T., Vihma T., De
 2811 Leeuw G., Lauri A., Ruuskanen T., Lapshin V.B., Zaitseva N., Glezer O., Arshinov M., Spracklen D.V.,
 2812 Arnold S.R., Juhola S., Lihavainen H., Viisanen Y., Chubarova N., Chalov S., Filatov N., Skorokhod A.,
 2813 Elansky N., Dyukarev E., Esau I., Hari P., Kotlyakov V., Kasimov N., Bondur V., Matvienko G., Baklanov
 2814 A., Mareev E., Troitskaya Y., Ding A., Guo H., Zilitinkevich S., and Kulmala M.: Pan-Eurasian Experiment
 2815 (PEEX) –a research initiative meeting the grand challenges of the changing environment of the northern Pan-
 2816 Eurasian arctic-boreal areas, *J. Geography Environment Sustainability*, 2(7), 13-48, doi:10.24057/2071-
 2817 9388-2014-7-2-13-48, 2014.
- 2818 Lappalainen, H. K., Kerminen, V.-M., Petäjä, T., Kurten, T., Baklanov, A., Shvidenko, A., Bäck, J., Vihma,
 2819 T., Alekseychik, P., Andreae, M. O., Arnold, S. R., Arshinov, M., Asmi, E., Belan, B., Bobylev, L., Chalov,
 2820 S., Cheng, Y., Chubarova, N., de Leeuw, G., Ding, A., Dobrolyubov, S., Dubtsov, S., Dyukarev, E., Elansky,
 2821 N., Eleftheriadis, K., Esau, I., Filatov, N., Flint, M., Fu, C., Glezer, O., Gliko, A., Heimann, M., Holtslag, A.
 2822 A. M., Hörrak, U., Janhunen, J., Juhola, S., Järvi, L., Järvinen, H., Kanukhina, A., Konstantinov, P.,
 2823 Kotlyakov, V., Kieloaho, A.-J., Komarov, A. S., Kujansuu, J., Kukkonen, I., Duplissy, E.-M., Laaksonen, A.,
 2824 Laurila, T., Lihavainen, H., Lisitzin, A., Mahura, A., Makshtas, A., Mareev, E., Mazon, S., Matishov, D.,
 2825 Melnikov, V., Mikhailov, E., Moisseev, D., Nigmatulin, R., Noe, S. M., Ojala, A., Pihlatie, M., Popovicheva,
 2826 O., Pumpanen, J., Regerand, T., Repina, I., Shcherbinin, A., Shevchenko, V., Sipilä, M., Skorokhod, A.,
 2827 Spracklen, D. V., Su, H., Subetto, D. A., Sun, J., Terzhevik, A. Y., Timofeyev, Y., Troitskaya, Y.,
 2828 Tynkkynen, V.-P., Kharuk, V. I., Zaytseva, N., Zhang, J., Viisanen, Y., Vesala, T., Hari, P., Hansson, H. C.,
 2829 Matvienko, G. G., Kasimov, N. S., Guo, H., Bondur, V., Zilitinkevich, S., and Kulmala, M.: Pan-Eurasian
 2830 Experiment (PEEX): towards a holistic understanding of the feedbacks and interactions in the land–

- 2831 atmosphere–ocean–society continuum in the northern Eurasian region, *Atmos. Chem. Phys.*, 16, 14421–
2832 14461, <https://doi.org/10.5194/acp-16-14421-2016>, 2016.
- 2833 Lappalainen, H.K., Kulmala, M., Kujansuu, J., Petäjä, T., Mahura, A., de Leeuw, G., Zilitinkevich, S.,
2834 Juustila, M., Kerminen, V.M., Bornstein, B. and Jiahua, Z.: The Silk Road agenda of the Pan-Eurasian
2835 Experiment (PEEX) program, *Big Earth Data*, 2(1), 8-35, doi:10.1080/20964471.2018.1437704, 2018.
- 2836 Lei, R. B., Xie, H. J., Wang, J., Leppäranta, M., Jonsdóttir, I., and Zhang, Z. H.: Changes in sea ice
2837 conditions along the Arctic Northeast Passage from 1979 to 2012, *Cold Regions Science and Technology*,
2838 119, 132-144. doi:10.1016/j.coldregions.2015.08.004, 2015.
- 2839 Lei, R., Tian-Kunze, X., Leppäranta, M., Wang, J., Kaleschke, L., and Zhang, Z.: Changes in summer sea
2840 ice, albedo, and partitioning of surface solar radiation in the Pacific sector of Arctic Ocean during 1982-2009,
2841 *J. Geophys. Res.: Oceans*, 121(8), 5470-5486, doi:10.1002/2016jc011831, 2016.
- 2842 Lei, R. B., Cheng, B., Heil, P., Vihma, T., Wang, J., Ji, Q., and Zhang, Z. H.: Seasonal and interannual
2843 variations of sea ice mass balance from the Central Arctic to the Greenland Sea, *J. Geophys. Res.: Oceans*,
2844 123(4), 2422-2439, doi:10.1002/2017jc013548, 2018.
- 2845 Leino, K., Nieminen, T., Manninen, H. E., Petäjä, T., Kerminen, V.-M., and Kulmala, M.: Intermediate ions
2846 as a strong indicator of new particle formation bursts in a boreal forest, *Boreal Environ. Res.*, 21(3-4), 274-
2847 286, 2016.
- 2848 Leppäranta, M.: Structure and properties of lake ice. *Freezing of Lakes and the Evolution of their Ice Cover*,
2849 Springer, Berlin/Heidelberg, Germany, 51–90. doi: 10.1007/978-3-642-29081-7_3, 2015.
- 2850 Leppäranta, M., Lindgren, E., and Shirasawa, K.: The heat budget of Lake Kilpisjärvi in the Arctic tundra,
2851 *Hydrol. Res.*, 48(4), 969-980, doi:10.2166/nh.2016.171, 2017.
- 2852 Leppäranta, M., Lewis, J. E., Heini, A., and Arvola, L.: Spatial statistics of hydrography and water chemistry
2853 in a eutrophic boreal lake based on sounding and water samples, *Environ. Monit. Assess.*, 190(7), 378,
2854 doi:10.1007/s10661-018-6742-z, 2018.
- 2855 Leppäranta, M., Lindgren, E., Wen, L. and Kirillin, G.: Ice cover decay and heat balance in Lake Kilpisjärvi
2856 in Arctic tundra, *Journal of Limnology*, 78(2). doi: 10.4081/jlimnol.2019.1879, 2019.
- 2857 Leppäranta, M., Meleshko, V., Uotila, P., and Pavlova, T.: Sea ice modelling, 315-387, *Sea Ice in the Arctic*
2858 (Springer, Cham), 2020.
- 2859 Li, H., Väiliranta, M., Mäki, M., Kohl, L., Sannel, B., Pumpanen, J., Koskinen, M., Bäck, J. and Bianchi, F.:
2860 Overlooked organic vapor emissions from thawing Arctic permafrost, *Environmental Research Letters* 15,
2861 Issue 10, id.104097, 12 pp., 2020a.
- 2862 Li, M., Wang, L., Liu, J., Gao, W., Song, T., Sun, Y., Li, L., Li, X., Wang, Y., Liu, L. and Daellenbach,
2863 K.R., Paasonen, P.J., Kerminen, V.-M., Kulmala, M., and Wang Y.: Exploring the regional pollution

- 2864 characteristics and meteorological formation mechanism of PM_{2.5} in North China during 2013–2017,
2865 *Environment international*, 134, 105283, 2020b.
- 2866 Liao, Z., Cheng, B., Zhao, J., Vihma, T., Jackson, K., Yang, Q., Yang, Y., Zhang, L., Li, Z., Qiu, Y., and
2867 Cheng, X.: Snow depth and ice thickness derived from SIMBA ice mass balance buoy data using an
2868 automated algorithm, *Int. J. Digital Earth*, 12(8), 962-979, doi:10.1080/17538947.2018.1545877, 2018.
- 2869 Lin, X., Rogers, B. M., Sweeney, C., Chevallier, F., Arshinov, M., Dlugokencky, E., Machida, T., Motoki
2870 Sasakawa, Tans, P., Keppel-Aleks, G.: Siberian and temperate ecosystems shape Northern Hemisphere
2871 atmospheric CO₂ seasonal amplification, *PNAS*, 117 (35), 21079-21087, doi:10.1073/pnas.1914135117,
2872 2020.
- 2873 Lintunen, A., Paljakka, T., Salmon, Y., Dewar, R., Riikonen, A, and Hölttä, T.: The influence of soil
2874 temperature and water content on belowground hydraulic conductance and leaf gas exchange in mature trees
2875 of three boreal species, *Plant, Cell and Environment*, 43, 532-547, doi: 10.1111/pce.13709, 2020.
- 2876 Liu, Y.C., Yan, C., Feng, Z., Zheng, F., Fan, X., Zhang, Y., Li, C., Zhou, Y., Lin, Z., Guo, Y., Zhang, Y.,
2877 Ma, L., Zhou, W., Liu, Z., Dada, L., Dällenbach, K., Kontkanen, J., Cai, R., Chan, T., Chu, B., Du, W., Yao,
2878 L., Wang, Y., Cai, J., Kangasluoma, J., Kokkonen, T., Kujansuu, J., Rusanen, A., Deng, C., Fu, Y., Yin, R.,
2879 Li, X., Lu, Y., Liu, Y., Lian, C., Yang, D., Wang, W., Ge, M., Wang, Y., Worsnop, D.R., Junninen, H., He,
2880 H., Kerminen, V.-M., Zheng, J., Wang, L., Jiang, J., Petäjä, T., Bianchi, F. and Kulmala, M. : Continuous
2881 and comprehensive atmospheric observation in Beijing: a station to understand the complex urban
2882 atmospheric environment, *Big Earth Data*, 4, 295-321, 2020.
- 2883 Liu, J., Wang, L., Li, M., Liao, Z., Sun, Y., Song, T., Gao, W., Wang, Y., Li, Y., Ji, D., Hu, B., Kerminen,
2884 V.-M., Wang, Y., and Kulmala, M.: Quantifying the impact of synoptic circulation patterns on ozone
2885 variability in northern China from April to October 2013–2017, *Atmos. Chem. Phys.*, 19, 14477–14492,
2886 doi:10.5194/acp-19-14477-2019, 2019 a.
- 2887 Liu, W., Atherton, J., Möttö, M., Gastellu-Etchegorry, J.P., Malenovský, Z., Raunonen, P., Åkerblom, M.,
2888 Mäkipää, R. and Porcar-Castell, A.: Simulating solar-induced chlorophyll fluorescence in a boreal forest
2889 stand reconstructed from terrestrial laser scanning measurements, *Remote Sensing of Environment*, 232,
2890 111274, 2019b.
- 2891 Liu, Y., de Leeuw, G., Kerminen, V.-M., Zhang, J., Zhou, P., Nie, W., Qi, X., Hong, J., Wang, Y., Ding, A.,
2892 Guo, H., Krüger, O., Kulmala, M., and Petäjä, T.: Analysis of aerosol effects on warm clouds over the
2893 Yangtze River Delta from multi-sensor satellite observations, *Atmos. Chem. Phys.*, 17, 5623–5641,
2894 doi:10.5194/acp-17-5623-2017, 2017.
- 2895 Liu, Y., Zhang, J., Zhou, P., Lin, T., Hong, J., Shi, L., Yao, F., Wu, J., Guo, H., and de Leeuw, G.: Satellite-
2896 based estimate of the variability of warm cloud properties associated with aerosol and meteorological
2897 conditions, *Atmos. Chem. Phys.*, 18, 18187–18202, doi:10.5194/acp-18-18187-2018, 2018.

- 2898 López-Blanco, E., Exbrayat, J.-F., Lund, M., Christensen, T. R., Tamstorf, M. P., Slevin, D., Hugelius, G.,
 2899 Bloom, A. A., and Williams, M.: Evaluation of terrestrial pan-Arctic carbon cycling using a data-
 2900 assimilation system, *Earth Syst. Dynam.*, 10, 233–255, doi:10.5194/esd-10-233-2019, 2019.
- 2901 Lu, P., Leppäranta, M., Cheng, B., and Li, Z.: Influence of melt-pond depth and ice thickness on Arctic sea-
 2902 ice albedo and light transmittance, *Cold Regions Science and Technology*, 124, 1-10,
 2903 doi:10.1016/j.coldregions.2015.12.010, 2016.
- 2904 Lu, P., Cheng, B., Leppäranta, M., and Li, Z. J.: Partitioning of solar radiation in Arctic sea ice during melt
 2905 season, *Oceanologia*, 60(4), 464-477, doi:10.1016/j.oceano.2018.03.002, 2018a.
- 2906 Lu, P., Leppäranta, M., Cheng, B., Li, Z., Istomina, L., and Heygster, G.: The color of melt ponds on Arctic
 2907 sea ice, *The Cryosphere*, 12, 1331–1345, doi:10.5194/tc-12-1331-2018, 2018b.
- 2908 Lu, Y., Yan, C., Fu, Y., Chen, Y., Liu, Y., Yang, G., Wang, Y., Bianchi, F., Chu, B., Zhou, Y., Yin, R.,
 2909 Baalbaki, R., Garmash, O., Deng, C., Wang, W., Liu, Y.C., Petäjä, T., Kerminen, V.-M., Jiang, J., Kulmala,
 2910 M. and Wang, L. : A proxy for atmospheric daytime gaseous sulfuric acid concentration in urban Beijing,
 2911 *Atmos. Chem. Phys.* 19, 1971-1983, 2019.
- 2912 Luoma, K., Virkkula, A., Aalto, P.P., Petäjä, T., and Kulmala, M.: Over a 10-year record of aerosol optical
 2913 properties at SMEAR II, *Atmos. Chem. Phys.*, 19, 11363–11382, doi:10.5194/acp-19-11363-2019, 2019.
- 2914 Lychagin, M., Chalov, S., Kasimov, N., Shinkareva, G., Jarsjo, J., and Thorslund, J.: Surface water pathways
 2915 and fluxes of metals under changing environmental conditions and human interventions in the Selenga River
 2916 system, *Environ. Earth Sci.*, 76(1), 14, doi:10.1007/s12665-016-6304-z, 2017.
- 2917 Ma, J., Yan, X., Dong, W. et al.: Gross primary production of global forest ecosystems has been
 2918 overestimated, *Sci Rep* 5, 10820, doi:10.1038/srep10820, 2015.
- 2919 Magritsky, D. V., Frolova, N. L., Evstigneev, V. M., Povalishnikova, E. S., Kireeva, M. B., and
 2920 Pakhomova, O. M.: Long-term changes of river water inflow into the seas of the Russian Arctic sector,
 2921 *Polarforschung*, 87(2), 177-194, doi: 10.2312/polarforschung.87.2.177, 2018.
- 2922 Mahura A., Baklanov A., Sørensen, J. H., Svetlov, A., and Koshkin, V.: Assessment of Long-Range
 2923 Transport and Deposition from Cu-Ni Smelters of Russian North. In "Air, Water and Soil Quality Modelling
 2924 for Risk and Impact Assessment", Security Through Science, Series C - Environmental Security. Eds. A.
 2925 Ebel, T. Davitashvili, Springer Elsevier Publishers, pp. 115-124, 2007.
- 2926 Mahura, A., Gonzalez-Aparacio, I., Nuterman, R., and Baklanov, A.: Seasonal Impact Analysis on
 2927 Population due to Continuous Sulphur Emissions from Severonikel Smelters of the Kola Peninsula.
 2928 *Geography, Environment, Sustainability*, 11(1), 130-144, doi:10.24057/2071-9388-2018-11-1-130-144,
 2929 2018.

- 2930 Malkhazova, S. M., Mironova, V. A., Orlov, D. S., and Adishcheva, O. S.: Influence of climatic factor on
 2931 naturally determined diseases in a regional context, *Geography, Environment, Sustainability*, 11(1), 157-170,
 2932 doi:10.24057/2071-9388-2018-11-1-157-170, 2018.
- 2933 Malsy, M., Flörke, M., and Borchardt, D.: What drives the water quality changes in the Selenga basin:
 2934 climate change or socio-economic development?, *Reg Environ Chang.*, 17, 1977–1989 doi:10.1007/s10113-
 2935 016-1005-4, 2017.
- 2936 Mammarella, I., Nordbo, A., Rannik, Ü., Haapanala, S., Levula, J., Laakso, H., Ojala, A., Peltola, O.,
 2937 Heiskanen, J., Pumpanen, J. and Vesala, T.: Carbon dioxide and energy fluxes over a small boreal lake in
 2938 Southern Finland, *J. Geophys. Res.: Biogeosciences*, 120(7), 1296-1314, doi:10.1002/2014jg002873, 2015.
- 2939 Manasyrov, R. M., Vorobyev, S. N., Loiko, S. V., Krivtsov, I. V., Shirokova, L. S., Shevchenko, V. P.,
 2940 Kirpotin, S. N., Kulizhsky, S. P., Kolesnichenko, L. G., Zemtsov, V. A. and Sinkinov, V. V.: Seasonal
 2941 dynamics of thermokarst lake chemical composition in discontinuous permafrost zone of Western Siberia,
 2942 *Biogeosciences*, 12, 3009-3028, 2015.
- 2943 Marelle, L., Raut, J. C., Law, K. S., and Duclaux, O.: Current and future arctic aerosols and ozone from
 2944 remote emissions and emerging local sources-modeled source contributions and radiative effects, *J.*
 2945 *Geophys. Res.: Atmos.*, 123(22), 12942-12963, doi:10.1029/2018jd028863, 2018.
- 2946 Maslov, A. V., Shevchenko, V. P., Bobrov, V. A., Belogub, E. V., Ershova, V. B., Vereshchagin, O. S., and
 2947 Khvorov, P. V.: Mineralogical-geochemical features of ice-rafted sediments in some arctic regions,
 2948 *Lithology and Mineral Resources*, 53(2), 110-129, doi:10.1134/s0024490218020037, 2018a.
- 2949 Maslov, A. V., Shevchenko, V. P., Kuznetsov, A. B., and Stein, R.: Geochemical and Sr-Nd-Pb-isotope
 2950 characteristics of ice-rafted sediments of the Arctic Ocean, *Geochem. Int.*, 56(8), 751-765,
 2951 doi:10.1134/s0016702918080050, 2018b.
- 2952 Matkala, L., Kulmala, L., Kolari, P., Aurela, M., and Bäck, J.: Resilience of carbon dioxide and water
 2953 exchange to extreme weather events in subarctic Scots pine and Norway spruce stands, *Agricultural and*
 2954 *Forest Meteorology*, 296, 108239, 2020.
- 2955 McCusker, K., Fyfe, J., and Sigmond, M.: Twenty-five winters of unexpected Eurasian cooling unlikely due
 2956 to Arctic sea-ice loss, *Nature Geoscience* 9, 838–842, doi:10.1038/ngeo2820, 2016.
- 2957 Meinander, O., Heikkinen, E., Aurela, M., and Hyvärinen, A.: Sampling, Filtering, and Analysis Protocols to
 2958 Detect Black Carbon, Organic Carbon, and Total Carbon in Seasonal Surface Snow in an Urban Background
 2959 and Arctic Finland (>60° N), *Atmosphere*, 11, 923. doi:10.3390/atmos11090923, 2020a.
- 2960 Meinander, O., Kontu, A., Kouznetsov, R., Sofiev, M.: Snow Samples Combined with Long-Range
 2961 Transport Modeling to Reveal the Origin and Temporal Variability of Black Carbon in Seasonal Snow in
 2962 Sodankylä (67° N), *Front. Earth Sci.*, 8, 13,
 2963 <https://www.frontiersin.org/articles/10.3389/feart.2020.00153/full>, 2020b.

- 2964 Merkouriadi, I., Cheng, B., Graham, R. M., Rösel, A., and Granskog, M. A.: Critical role of snow on sea ice
 2965 growth in the Atlantic sector of the Arctic Ocean. *Geophysical Research Letters*, 44.
 2966 doi:10.1002/2017GL075494, 2017
- 2967 Merkouriadi, I., Cheng, B., Graham, R. M., Rösel, A., and Granskog, M. A.: Critical role of snow on sea ice
 2968 growth in the Atlantic sector of the Arctic Ocean, *Geophys. Res. Lett.*, 44, doi: 10.1002/2017GL075494,
 2969 2018.
- 2970 Mikhailov, E. F., Mironova, S. Y., Makarova, M. V., Vlasenko, S. S., Ryshkevich, T. I., Panov, A. V., and
 2971 Andreae, M. O.: Studying seasonal variations in carbonaceous aerosol particles in the atmosphere over
 2972 central Siberia, *Izv. Atmos. Oceanic Phys.*, 51(4), 423-430, doi:10.1134/s000143381504009x, 2015a.
- 2973 Mikhailov, E. F., Mironov, G. N., Pöhlker, C., Chi, X., Krüger, M. L., Shiraiwa, M., Förster, J.-D., Pöschl,
 2974 U., Vlasenko, S. S., Ryshkevich, T. I., Weigand, M., Kilcoyne, A. L. D., and Andreae, M. O.: Chemical
 2975 composition, microstructure, and hygroscopic properties of aerosol particles at the Zotino Tall Tower
 2976 Observatory (ZOTTO), Siberia, during a summer campaign, *Atmos. Chem. Phys.*, 15, 8847–8869,
 2977 doi:10.5194/acp-15-8847-2015, 2015b.
- 2978 Mikhailov, E. F., Mironova, S., Mironov, G., Vlasenko, S., Panov, A., Chi, X., Walter, D., Carbone, S.,
 2979 Artaxo, P., Heimann, M., Lavric, J., Pöschl, U., and Andreae, M. O.: Long-term measurements (2010–2014)
 2980 of carbonaceous aerosol and carbon monoxide at the Zotino Tall Tower Observatory (ZOTTO) in central
 2981 Siberia, *Atmos. Chem. Phys.*, 17, 14365–14392, doi:10.5194/acp-17-14365-2017, 2017.
- 2982 Mikola, J., Virtanen, T., Linkosalmi, M., Vähä, E., Nyman, J., Postanogova, O., Räsänen, A., Kotze, D. J.,
 2983 Laurila, T., Juutinen, S., Kondratyev, V., and Aurela, M.: Spatial variation and linkages of soil and
 2984 vegetation in the Siberian Arctic tundra – coupling field observations with remote sensing data,
 2985 *Biogeosciences*, 15, 2781–2801, doi:10.5194/bg-15-2781-2018, 2018.
- 2986 Miles, V. V., and Esau, I.: Spatial heterogeneity of greening and browning between and within bioclimatic
 2987 zones in northern West Siberia, *Environ. Res. Lett.*, 11(11), 12, doi:10.1088/1748-9326/11/11/115002, 2016.
- 2988 Miles, V., and Esau, I.: Seasonal and Spatial Characteristics of Urban Heat Islands (UHIs) in Northern West
 2989 Siberian Cities., *Remote Sens.*, 9, 989, 2017.
- 2990 Miles, M. W., Miles, V., and Esau, I.: Varying climate response across the tundra, forest–tundra and boreal
 2991 forest biomes in northern West Siberia, *Environ. Res. Lett.*, 14, 075008, doi:10.1088/1748-9326/ab2364,
 2992 2019.
- 2993 Miles, V., and Esau, I.: Surface urban heat islands in 57 cities across different climates in northern
 2994 Fennoscandia, *Urban Climate*, 31, 10.1016/j.uclim.2019.100575, 2020.
- 2995 Miles, V.: Arctic surface Urban Heat Island (UHI), MODIS Land Surface Temperature (LST) data, 2000-
 2996 2016. Arctic Data Center. doi:10.18739/A2TB0XW4T, 2020.

- 2997 MNRE (2019): Methods for calculating emissions of pollutants into the atmosphere from stationary sources.
2998 Ministry of Natural Resources and Ecology. In Russian
2999 (www.mnr.gov.ru/docs/metodiki_rascheta_vybrosov_vrednykh_zagryaznyayushchikh_veshchestv_v_atmosf_ernyy_vozdukh_statsionarn/perechen), 2019.
3000
3001
- 3002 Mori, M., Watanabe, M., Shiogama, H., Inoue, J., and Kimoto, M.: Robust Arctic sea-ice influence on the
3003 frequent Eurasian cold winters in past decades, *Nat. Geosci.*, 7, 869–873, doi:10.1038/ngeo2277, 2014.
- 3004 Mori, M., Kosaka, Y., Watanabe, M., Nakamura, H., and Kimoto, M.: A reconciled estimate of the influence
3005 of Arctic sea-ice loss on recent Eurasian cooling, *Nat. Clim. Change*, 9, 123–129, doi: 10.1038/s41558-018-
3006 0379-3, 2019.
- 3007 Morozov, E. A., Kondrik, D. V., Chepikova, S. S., and Pozdnyakov, D. V.: Atmospheric columnar CO₂
3008 enhancement over *E. huxleyi* blooms: case studies in the North Atlantic and Arctic waters. *Transactions of*
3009 *the Karelian Research Centre of the Russian Academy of Sciences, Limnologoia i Oceanologia series*, 3, 1-6.
3010 doi:10.17076/lim989, 2019.
- 3011 Myslenkov S., Medvedeva A., Arkhipkin V., Markina M., Surkova G., Krylov A., Dobrolyubov S.,
3012 Zilitinkevich S., and Koltermann P.: Long-term statistics of storms in the Baltic, Barents and White Seas and
3013 their future climate projections. *Geography, environment, sustainability*, 11, 93-112, doi:10.24057/2071-
3014 9388-2018-11-1-93-112, 2018.
- 3015 Mäki, M., Krasnov, D., Hellén, H., Noe, S. M., and Bäck, J.: Stand type affects fluxes of volatile organic
3016 compounds from the forest floor in hemiboreal and boreal climates, *Plant Soil*, 441, 363–381,
3017 doi:10.1007/s11104-019-04129-3, 2019.
- 3018 Naakka, T., Nygård, T., Vihma, T., Graversen, R., and Sedlar, J.: Atmospheric moisture transport between
3019 mid-latitudes and the Arctic: regional, seasonal and vertical distributions, *Int. J. Climatol.*, 32, 1–18,
3020 doi:10.1002/joc.5988, 2019.
- 3021 Natali, S.M., Watts, J.D., Rogers, B.M., Potter, S., Ludwig, S. M., Selbmann, A. K., Sullivan, P.F. Abbott, B.
3022 W., Arndt, K. A., Birch, L., Björkman, M.P., Bloom, A., Celis, G., Christensen, T. R., Christiansen, C. T.,
3023 Commane, R., Cooper, E. J., Crill, P., Czimeczik, C., Davydov, S., Du, J., Egan, J.E., Elberling, B.,
3024 Euskirchen, B.S., Friborg, T., Genet, H., Göckede, M., Goodrich, J.P., Grogan, P., Helbig, M., Jafarov, E.E.,
3025 Jastrow, J. D., Kalhori, A.A.M., Kim, Y. Kimball, J. S., Kutzbach, L., Lara, M. J., Larsen, K., S., Lee, B.-Y.,
3026 Liu, Z., Lorant, M. M., Lund, M., Lupascu, M., Madani, N., Malhotra, A., Matamala, R., McFarland, J.,
3027 McGuire, A. D., Michelsen, A., Minions, C., Oechel, W., Olefeldt, D., Parmentier, F.-J., Pirk, N., Poulter,
3028 B., Quinton, W., Rezanezhad, F., Risk, D., Sachs, T., Schaefer, K., Schmidt, N. M., Schuur, E., Semenchuk,
3029 P. R., Shaver, G., Sonntag, O., Starr, G., Treat, C. C., Waldrop, M. P., Wang, Y., Welker, J., Wille, C., Xu,
3030 X., Zhang, Z., Zhuang, Q., and Zona, D.: Large loss of CO₂ in winter observed across the northern
3031 permafrost region, *Nat. Clim. Chang.*, 9, 852–857, doi:10.1038/s41558-019-0592-8, 2019.

- 3032 Nikandrova, A., Tabakova, K., Manninen, A., Väänänen, R., Petäjä, T., Kulmala, M., Kerminen, V.-M., and
3033 O'Connor, E.: Combining airborne in situ and ground-based lidar measurements for attribution of aerosol
3034 layers, *Atmos. Chem. Phys.*, 18, 10575–10591, doi:10.5194/acp-18-10575-2018, 2018.
- 3035 NILU, 2013: Sandanger, T.M., Anda, E., Berglen, T.F., Evenset, A., Christensen, G., and Heimstad, E.S.:
3036 Health and environmental impacts in the Norwegian border area related to local Russian industrial emissions.
3037 Knowledge status, 40/2013, 2013.
- 3038 Nissen, C., Munnich, M., Grube, M., and Haumann, N.: Factors controlling coccolithophore biogeography in
3039 the Southern Ocean, *Biogeosciences*, 15(22), 6997-7024, doi:10.5194/bg-15-6997-2018, 2018.
- 3040 Nitzbon, J., Langer, M., Westermann, S., Martina, L., Aas, K. S., and Boike, J.: Pathways of ice-wedge
3041 degradation in polygonal tundra under different hydrological conditions, *Cryosphere*, 13(4), 1089-1123,
3042 doi:10.5194/tc-13-1089-2019, 2019.
- 3043 Nygård, T., Graversen, R. G., Uotila, P., Naakka, T., and Vihma, T.: Strong dependence of wintertime Arctic
3044 moisture and cloud distributions on atmospheric large-scale circulation, *J. Climate*, 32, 8771-8790, doi:
3045 10.1175/JCLI-D-19-0242.1, 2019.
- 3046 Overland, J., Dunlea, E., Box, J. E., Corell, R., Forsius, M., Kattsov, V., Olsen, M. S., Pawlak, J., Reiersen,
3047 L. O., and Wang, M.: The urgency of Arctic change, *Polar Science*, 21, 6-13,
3048 doi:10.1016/j.polar.2018.11.008, 2019.
- 3049 Paasonen, P., Peltola, M., Kontkanen, J., Junninen, H., Kerminen, V.-M., and Kulmala, M.: Comprehensive
3050 analysis of particle growth rates from nucleation mode to cloud condensation nuclei in boreal forest, *Atmos.*
3051 *Chem. Phys.*, 18, 12085–12103, doi:10.5194/acp-18-12085-2018, 2018.
- 3052 Palo, T., Vihma, T., Jaagus, J., and Jakobson, E.: Observations on temperature inversion over central Arctic
3053 sea ice in summer, *Q. J. R. Meteorol. Soc.*, 143(708), 2741-2754, doi:10.1002/qj.3123, 2017.
- 3054 Panov, A. V., Prokushkin, A. S., Bryukhanov, A. V., Korets, M. A., Ponomarev, E. I., Sidenko, N. V.,
3055 Zrazhevskaya, G. K., Timokhina, A. V., and Andreae, M. O.: A complex approach for the estimation of
3056 carbonaceous emissions from wildfires in Siberia, *Russian Meteorol. Hydrol.*, 43(5), 295-301, 2018.
- 3057 Parmentier, F. W., Christensen, T. R., Rysgaard, S., Bendtsen, J., Glud, R. N., Else, B., van Huissteden, J.,
3058 Sachs, T., Vonk, J. E., and Sejr, M. K.: A synthesis of the arctic terrestrial and marine carbon cycles under
3059 pressure from a dwindling cryosphere, *Ambio*, 46, 53–69, doi:10.1007/s13280-016-0872-8, 2017.
- 3060 Parshintsev, J., Vaikkinen, A., Lipponen, K., Vrkoslav, V., Cvačka, J., et al. : Desorption atmospheric
3061 pressure photoionization high-resolution mass spectrometry: a complementary approach for the chemical
3062 analysis of atmospheric aerosols, *Rapid Commun. Mass Spectrom.*, 29, 1233–1241, 2015.
- 3063 Passananti, M., Zapadinsky, E., Zanca, T., Kangasluoma, J., Mylly, N., Rissanen, M.P., Kurtén, T., Ehn,
3064 M., Attoui, M., and Vehkamäki, H.: How well can we predict cluster fragmentation inside a mass
3065 spectrometer? *Chem. Commun.*, 55, 5946-5949, 2019.

- 3066 Payne, R. J., Creevy, A., Malysheva, E., Ratcliffe, J., Andersen, R., Tsyganov, A. N., Rowson, J., Marcisz,
3067 K., Zielinska, M., Lamentowicz, M., Lapshina, E. D., and Mazei, Y.: Tree encroachment may lead to
3068 functionally-significant changes in peatland testate amoeba communities. *Soil Biology & Biochemistry*, 98,
3069 18-21. doi:10.1016/j.soilbio.2016.04.002, 2016.
- 3070 Peltola, O., Vesala, T., Gao, Y.; Rätty, O. et al. : Monthly gridded data product of northern wetland methane
3071 emissions based on upscaling eddy covariance observations, *Earth System Science Data*, 11, 1263-1289,
3072 doi:10.5194/essd-11-1263-2019, 2019.
- 3073 Peltoniemi, J. I., Gritsevich, M., Hakala, T., Dagsson-Waldhauserová, P., Arnalds, Ó., Anttila, K., Hannula,
3074 H.-R., Kivekäs, N., Lihavainen, H., Meinander, O., Svensson, J., Virkkula, A., and de Leeuw, G.: Soot on
3075 Snow experiment: bidirectional reflectance factor measurements of contaminated snow, *The Cryosphere*, 9,
3076 2323–2337, doi:10.5194/tc-9-2323-2015, 2015.
- 3077 Peterson, B. J., Holmes, R. M., McClelland, J. W., Vörösmarty, C. J., Lammers, R. B., Shiklomanov, A. I.,
3078 Shiklomanov, I. A., and Rahmstorf, S.: Increasing river discharge to the Arctic Ocean, *Science*, 80, 298,
3079 2171–2173, doi: 10.1126/science.1077445, 2002.
- 3080 Petäjä, T., Järvi, L., Kerminen, V.-M., Ding, A. J., Sun, J. N., Nie, W., Kujansuu, J., Virkkula, A., Yang, X.-
3081 Q., Fu, C. B., Zilitinkevich, S., and Kulmala M.: Enhanced air pollution via aerosol-boundary layer feedback
3082 in China, *Scientific Reports*, 6, 18998, doi:10.1038/srep18998, 2016.
- 3083 Petäjä, T., Duplissy, E.-M., Tabakova, K., Schmale, J., Altstädter, B., Ancellet, G., Arshinov, M., Balin, Y.,
3084 Baltensperger, U., Bange, J., Beamish, A., Belan, B., Berchet, A., Bossi, R., Cairns, W. R. L., Ebinghaus, R.,
3085 El Haddad, I., Ferreira-Araujo, B., Franck, A., Huang, L., Hyvärinen, A., Humbert, A., Kalogridis, A.-C.,
3086 Konstantinov, P., Lampert, A., MacLeod, M., Magand, O., Mahura, A., Marelle, L., Masloboev, V.,
3087 Moisseev, D., Moschos, V., Neckel, N., Onishi, T., Osterwalder, S., Ovaska, A., Paasonen, P., Panchenko,
3088 M., Pankratov, F., Pernov, J. B., Platis, A., Popovicheva, O., Raut, J.-C., Riandet, A., Sachs, T., Salvatori, R.,
3089 Salzano, R., Schröder, L., Schön, M., Shevchenko, V., Skov, H., Sonke, J. E., Spolaor, A., Stathopoulos, V.,
3090 K., Strahlendorff, M., Thomas, J. L., Vitale, V., Vratolis, S., Barbante, C., Chabrillat, S., Dommergue, A.,
3091 Eleftheriadis, K., Heilimo, J., Law, K. S., Massling, A., Noe, S. M., Paris, J.-D., Prévôt, A. S. H., Riipinen,
3092 I., Wehner, B., Xie, Z., and Lappalainen, H. K.: Overview: Integrative and Comprehensive Understanding on
3093 Polar Environments (iCUPE) – concept and initial results, *Atmos. Chem. Phys.*, 20, 8551–8592,
3094 doi:10.5194/acp-20-8551-2020, 2020a.
- 3095 Petäjä, T., Ganzei, K. S., Lappalainen, H. K., Tabakova, K., Makkonen, R., Räisänen, J., Chalov, S.,
3096 Kulmala, M., Zilitinkevich, S. S., Baklanov, P., Shakirov, R. B., Mishina, N.V., Egidarev, E.G., and
3097 Kondrat'ev, I. I.: Research agenda for the Russian Far East and utilization of multi-platform comprehensive
3098 environmental observations, *J. Big Data*, 5:3, 277-305, doi:10.1080/17538947.2020.1826589 , 2020b.

- 3099 Pietron, J., Jarsjo, J., Romanchenko, A. O., and Chalov, S. R.: Model analyses of the contribution of in-
 3100 channel processes to sediment concentration hysteresis loops, *Journal of Hydrology*, 527, 576-589.
 3101 doi:10.1016/j.jhydrol.2015.05.009, 2015.
- 3102 Pietroń, J., Nittrouer, J. A., Chalov, S. R., Dong, T. Y., Kasimov, N., Shinkareva, G., and Jarsjö, J.:
 3103 Sedimentation patterns in the Selenga River delta under changing hydroclimatic conditions, *Hydrological*
 3104 *Processes*, 32(2), 278-292, doi:10.1002/hyp.11414, 2018.
- 3105 Pirazzini, R., Leppanen, L., Picard, G., Lopez-Moreno, J. I., Marty, C., Macelloni, G., Kontu, A., Von
 3106 Lerber, A., Tanis, C.M., Schneebeil, M., De Rosnay, P., Arslan, A. N.: European in-situ snow measurements:
 3107 practices and purposes, *Sensors*, 18(7), 51, doi:10.3390/s18072016, 2018.
- 3108 Pisso, I., Myhre, C. L., Platt, S. M., Eckhardt, S., Hermansen, O., Schmidbauer, N., Mienert, J.,
 3109 Vadakkepuliambatta, S., Bauguitte, S., Pitt, J., Allen, G., Bower, K. N., O'Shea, S., Gallagher, M. W.,
 3110 Percival, C. J., Pyle, J., Cain, M., and Stohl, A.: Constraints on oceanic methane emissions west of Svalbard
 3111 from atmospheric in situ measurements and Lagrangian transport modeling, *J. Geophys. Res. Atmos.*,
 3112 121(23), 14188-14200, doi:10.1002/2016jd025590, 2016.
- 3113 Platt, S. M., Eckhardt, S., Ferré, B., Fisher, R. E., Hermansen, O., Jansson, P., Lowry, D., Nisbet, E. G.,
 3114 Pisso, I., Schmidbauer, N., Silyakova, A., Stohl, A., Svendby, T. M., Vadakkepuliambatta, S., Mienert, J.,
 3115 and Lund Myhre, C.: Methane at Svalbard and over the European Arctic Ocean, *Atmos. Chem. Phys.*, 18,
 3116 17207–17224, doi:10.5194/acp-18-17207-2018, 2018.
- 3117 Ponomarev, Evgenii I., Kharuk, Viacheslav I., and Ranson, Kenneth J.: Wildfires Dynamics in Siberian Larch
 3118 Forests, *Forests*, 7(6), 125, 2016.
- 3119 Popovicheva O., Evangelidou N., Eleftheriadis K., Kalogridis A. C., Sitnikov V. N., Eckhardt S., Stohl A.:
 3120 Black carbon sources constrained by observations and modeling in the Russian high Arctic, *Environmental*
 3121 *Science Technology*, 51(7), 3871-3879, 2017.
- 3122 Popovicheva, O., Diapouli, E., Makshtas, A., Shonija, N., Manousakas, M., Saraga, D., Uttal, T., and
 3123 Eleftheriadis, K.: East Siberian Arctic background and black carbon polluted aerosols at HMO Tiksi, *Science*
 3124 *of the Total Environment*, 655, 924-938, doi:10.1016/j.scitotenv.2018.11.165, 2019a.
- 3125 Popovicheva, O. B., Engling, G., Ku, I. T., Timofeev, M. A., and Shonija, N. K.: Aerosol emissions from
 3126 long-lasting smoldering of boreal peatlands: chemical composition, markers, and microstructure, *Aerosol*
 3127 *and Air Quality Research*, 19(3), 484-503, doi:10.4209/aaqr.2018.08.0302, 2019b.
- 3128 Popovicheva, O. B., Padoan, S., Schnelle-Kreis, J., Nguyen, D. L., Adam, T.W., Kistler, M., Steinkogler, T.,
 3129 Kasper-Giebl, A., Zimmermann, R., and Chubarova, N. E.: Spring aerosol in urban atmosphere of megacity:
 3130 analytical and statistical assessment for source impacts, *Aerosol and Air Quality Research*, 20, 702–719,
 3131 2020a.

- 3132 Popovicheva O., Ivanov A., and Vojtisek M.: Functional Factors of Biomass Burning Contribution to Spring
 3133 Aerosol Composition in a Megacity: Combined FTIR-PCA Analyses, *Atmosphere*, 11, 319-339, 2019b.
- 3134 Popovicheva, O., Volpert, E., Sitnikov, N., Chichayeva, M., and Padoan, S.: Black carbon in spring aerosols
 3135 of Moscow urban background, *Geography, Environment, Sustainability*, 13, 1, 233-243, 2020c
- 3136 Pozdnyakov D. V., Pettersson L. H., and Korosov A. A.: Exploring the Marine Ecology from Space.
 3137 Springer, Switzerland, 2017.
- 3138 Pozdnyakov, D. V., Kondrik, D.V., Kazakov, E. E., and Chepikova, S.: Environmental conditions favoring
 3139 coccolithophore blooms in subarctic and arctic seas: a 20-year satellite and multi-dimensional statistical
 3140 study, *Proc. SPIE 11150, Remote Sensing of the Ocean, Sea Ice, Coastal Waters, and Large Water Regions*,
 3141 111501W, 14 October 2019, doi: 10.1117/12.2547868, 2019.
- 3142 Pozdnyakov D., Kondrik D., and Chepikova S.: Origination of *E. huxleyi* extraordinary bloom outbursts in
 3143 the Bering Sea between the late 1990s and early 2000s, and in 2018-2019: A hypothesis, *Fisheries*
 3144 *Oceanography*, submitted, 2020.
- 3145 Preis, Y. I., Simonova, G. V., Voropay, N. N., and Dyukarev, E. A.: Estimation of the influence of
 3146 hydrothermal conditions on the carbon isotope composition in *Sphagnum* mosses of bogs of Western Siberia,
 3147 *IOP Conf. Series: Earth Environ. Sci.*, 211, doi:10.1088/1755-1315/211/1/012031, 2018.
- 3148 Pugachev S. P., Pipko I. I., Shakhova, N. E., Shirshin, E. A., Perminova, I. V., Gustafsson, O., Bondur, V. G.,
 3149 Ruban, A. S., and Semiletov, I. P.: Dissolved organic matter and its optical characteristics in the Laptev and
 3150 East Siberian seas: spatial distribution and interannual variability (2003–2011), *Ocean Sci.*, 14, 87–103,
 3151 doi:10.5194/os-14-87-2018, 2018.
- 3152 Pulliainen, J., Aurela, M., Laurila, T., Aalto, T., Takala, M., Salminen, M., Kulmala, M., Barr, A., Heimann,
 3153 M., Lindroth, A., Laaksonen, A., Derksen, C., Mäkelä, A., Markkanen, T., Lemmetyinen, J., Susiluoto, J.,
 3154 Dengel, S., Mammarella, I., Tuovinen, J.-P., and Vesala, T.: Early snowmelt significantly enhances boreal
 3155 springtime carbon uptake, *PNAS*, 114(42), 11081-11086, doi:10.1073/pnas.1707889114, 2017.
- 3156 Pulliainen, J., Luojus, K., Derksen, C., Mudryk, L., Lemmetyinen, J., Salminen, M., Ikonen, J., Takala, M.,
 3157 Cohen, J., Smolander, T., and Norberg, J.: Patterns and trends of Northern Hemisphere snow mass from
 3158 1980 to 2018, *Nature* 581, 294–298, doi:10.1038/s41586-020-2258-0, 2020.
- 3159 Pärn, J., Verhoeven, J.T., Butterbach-Bahl, K., Dise, N.B., Ullah, S., Aasa, A., Egorov, S., Espenberg, M.,
 3160 Järveoja, J., Jauhainen, J. and Kasak, K.: Nitrogen-rich organic soils under warm well-drained conditions
 3161 are global nitrous oxide emission hotspots, *Nat. Commun.*, 9, 1135, doi:10.1038/s41467-018-03540-1, 2018.
- 3162 Qi, X. M., Ding, A. J., Nie, W., Petäjä, T., Kerminen, V.-M., Herrmann, E., Xie, Y. N., Zheng, L. F.,
 3163 Manninen, H., Aalto, P., Sun, J. N., Xu, Z. N., Chi, X. G., Huang, X., Boy, M., Virkkula, A., Yang, X.-Q.,
 3164 Fu, C. B., and Kulmala, M.: Aerosol size distribution and new particle formation in the western Yangtze

- 3165 River Delta of China: 2 years of measurements at the SORPES station, *Atmos. Chem. Phys.*, 15, 12445–
 3166 12464, doi:10.5194/acp-15-12445-2015, 2015.
- 3167 Rakitin, V. S., Elansky, N. F., Wang, P., Wang, G., Pankratova, N. V., Shtabkin, Y. A., Skorokhod A.I.,
 3168 Safronov A.N., Makarova M.V., and Grechko E.I.: Changes in trends of atmospheric composition over urban
 3169 and background regions of Eurasia: estimates based on spectroscopic observations, *Geography,
 3170 Environment, Sustainability*, 11(2), 84-96, doi:10.24057/2071-9388-2018-11-2-84-96, 2018.
- 3171 Rautiainen, K., Parkkinen, T., Lemmetyinen, J., Schwank, M., Wiesmann, A., Ikonen, J., Derksen, C.,
 3172 Davydov, S., Davydova, A., Boike, J., Langer, M., Druschg, M., and Pulliainen, J.: SMOS prototype
 3173 algorithm for detecting autumn soil freezing, *Remote Sensing of Environment*, 180, 346-360,
 3174 doi:10.1016/j.rse.2016.01.012, 2016.
- 3175 Rinke, A., Segger, B., Crewell, S., Maturilli, M., Naakka, T., Nygård, T., Vihma, T., Alshawaf, F., Dick, G.,
 3176 Wickert, J., and Keller, J.: Trends of vertically integrated water vapor over the Arctic during 1979-2016:
 3177 Consistent moistening all over?, *J. Climate*, 32, 6097–6116, doi:10.1175/JCLI-D-19-0092.1, 2019.
- 3178 Ripple, W. J., Wolf, C., Newsome, T. M., Galetti, M., Alamgir, M., Crist, E., Mahmoud, M. I., Laurance, W.
 3179 F., and 15,364 scientist signatories from 184 countries. World scientists' warning to humanity: A second
 3180 notice, *BioScience*, 67(12), 1026-1028, 2017.
- 3181 Rivero-Calle, S., Gnanadesikan, A., Del Castillo, C., Balch, W., and Guikema, S.: Multidecadal increase in
 3182 North Atlantic coccolithophores and the potential role of rising CO₂, *Science*, 350 (6267), 1533-1537, doi:
 3183 10.1126/science.aaa8026, 2015.
- 3184 Romanowsky, E., Handorf, D., Jaiser, R., Wohltmann, I., Dorn, W., Ukita, J., Cohen, J., Dethloff, K., and
 3185 Rex, M.: The role of stratospheric ozone for Arctic-midlatitude linkages, *Sci. Rep.* 9, 7962,
 3186 doi:10.1038/s41598-019-43823-1, 2019.
- 3187 Romanowsky, V. E., and Osterkamp, T. E.: Effects of unfrozen water on heat and mass transport processes in
 3188 the active layer and permafrost, *Permafrost Periglac. Process*, 11, 219–39, 2000.
- 3189 Roshydromet & GGO (2019): The State of Atmospheric Pollution in Cities on the Territory of Russia for
 3190 2018. Yearbook. Federal Service on Hydrometeorology and Monitoring Environment, Roshydromet & A.I.
 3191 Voeikov Main Geophysical Observatory, ISBN 978-5-9500883-8-4, St.Petersburg, 250 p., In Russian
 3192 (http://voeikovmgo.ru/images/stories/publications/2019/ejegodnik_zagr_atm_2018+.pdf)
 3193
- 3194 Rost, B., and Riebesell, U.: Coccolithophores and the biological pump: responses to environmental changes,
 3195 in: *Coccolithophores, from molecular processes to global impact*, edited by: Thierstein, H. R., Young, J. R.,
 3196 99–125, Springer, Heidelberg, Germany, 2004.
- 3197 Ryazanova, A., and Voropay, N. N.: Droughts and Excessive Moisture Events in Southern Siberia in the
 3198 Late XXth - Early XXIst Centuries, *IOP Conf. Ser.: Earth Environ. Sci.*, 96, 012015, 2017.

- 3199 Räisänen, J.: Effect of atmospheric circulation on recent temperature changes in Finland, *Clim. Dyn.*, 53,
3200 5675–5687, doi:10.1007/s00382-019-04890-2, 2019.
- 3201 Räisänen, J.: Effect of atmospheric circulation on surface air temperature trends in years 1979–2018. *Clim.*
3202 *Dyn.*, 56, 2303–2320, doi:10.1007/s00382-020-05590-y, 2021.
- 3203 Saarela, T., Rissanen, A. J., Ojala, A. et al.: CH₄ oxidation in a boreal lake during the development of
3204 hypolimnetic hypoxia, *Aquat Sci*, 82, 19, /doi.org/10.1007/s00027-019-0690-8, 2020.
- 3205 Salmon, Y., Lintunen, A., Dayet, A., Chan, T., Dewar, R., Vesala, T. and Hölttä, T.: Leaf carbon and water
3206 status control stomatal and non-stomatal limitations of photosynthesis in trees, *New Phytologist* 226, 690-
3207 703. doi: 10.1111/nph.16436, 2020.
- 3208 Santalahti, M., Sun, H., Sietiö, O.M., Köster, K., Berninger, F., Laurila, T., Pumpanen, J., and Heinonsalo,
3209 J.: Reindeer grazing alter soil fungal community structure and litter decomposition related enzyme activities
3210 in boreal coniferous forests in Finnish Lapland, *App. Soil Ecol.*, 132, 74-82,
3211 doi:10.1016/j.apsoil.2018.08.013, 2018.
- 3212 Schallhart, S., Rantala, P., Kajos, M. K., Aalto, J., Mammarella, I., Ruuskanen, T. M., and Kulmala, M.:
3213 Temporal variation of VOC fluxes measured with PTR-TOF above a boreal forest, *Atmospheric Chemistry*
3214 *and Physics*, 18(2), 815-832. doi:10.5194/acp-18-815-2018, 2018.
- 3215 Schmale, J., Arnold, S. R., Law, K. S., Thorp, T., Anenberg, S., Simpson, W. R., Mao, J. and Pratt, K. A.:
3216 Local Arctic air pollution: a neglected but serious problem, *Earths Future*, 6(10), 1385-1412,
3217 doi:10.1029/2018ef000952, 2018a.
- 3218 Schmale, J., Henning, S., Decesari, S., Henzing, B., Keskinen, H., Sellegri, K., Ovadnevaite, J., Pöhlker, M.
3219 L., Brito, J., Bougiatioti, A., Kristensson, A., Kalivitis, N., Stavroulas, I., Carbone, S., Jefferson, A., Park,
3220 M., Schlag, P., Iwamoto, Y., Aalto, P., Äijälä, M., Bukowiecki, N., Ehn, M., Frank, G., Fröhlich, R.,
3221 Frumau, A., Herrmann, E., Herrmann, H., Holzinger, R., Kos, G., Kulmala, M., Mihalopoulos, N., Nenes,
3222 A., O'Dowd, C., Petäjä, T., Picard, D., Pöhlker, C., Pöschl, U., Poulain, L., Prévôt, A. S. H., Swietlicki, E.,
3223 Andreae, M. O., Artaxo, P., Wiedensohler, A., Ogren, J., Matsuki, A., Yum, S. S., Stratmann, F.,
3224 Baltensperger, U., and Gysel, M.: Long-term cloud condensation nuclei number concentration, particle
3225 number size distribution and chemical composition measurements at regionally representative observatories,
3226 *Atmos. Chem. Phys.*, 18, 2853–2881, doi:10.5194/acp-18-2853-2018, 2018b.
- 3227 Schmeisser, L., Backman, J., Ogren, J. A., Andrews, E., Asmi, E., Starkweather, S., Uttal, T., Fiebig, M.,
3228 Sharma, S., Eleftheriadis, K., Vratolis, S., Bergin, M., Tunved, P., and Jefferson, A.: Seasonality of aerosol
3229 optical properties in the Arctic, *Atmos. Chem. Phys.*, 18, 11599–11622, doi:10.5194/acp-18-11599-2018,
3230 2018.
- 3231 Schuur, E. A. G., Bockheim, J., Canadell, J. G., Euskirchen, E., Field, C. B., Goryachkin, S. V., Hagemann,
3232 S., Kuhry, P., Lafleur, P.M., Lee, H., Mazhitova, G., Nelson, F. E., Rinke, A., Romanovsky, V. E.,

- 3233 Shiklomanov, N., Tarnocai, C., Venevsky, S., Vogel, J. G., and Zimov, S. A.: Vulnerability of permafrost
3234 carbon to climate change: implications for the global carbon cycle, *BioScience*, 58(8), 701–714,
3235 doi:10.1641/B580807, 2008.
- 3236 Schuur, E. A. G., McGuire, A. D., Romanovsky, V., Schädel, C., and Mack, M.: Chapter 11: Arctic and
3237 boreal carbon, in: *Second State of the Carbon Cycle Report (SOCCR2): A Sustained Assessment Report*,
3238 edited by: Cavallaro, N., Shrestha, G., Birdsey, R., Mayes, M. A., Najjar, R. G., Reed, S. C., Romero-
3239 Lankao, P., and Zhu, Z., U.S. Global Change Research Program, Washington, DC, USA, 428-468,
3240 doi:10.7930/SOCCR2.2018.Ch11, 2018.
- 3241 Scott, C. E., Monks, S. A., Spracklen, D. V., Arnold, S. R., Forster, P. M., Rap, A., Äijälä, M., Artaxo, P.,
3242 Carslaw, K. S., Chipperfield, M. P., Ehn, M., Gilardoni, S., Heikkinen, L., Kulmala, M., Petäjä, T.,
3243 Reddington, C. L. S., Rizzo, L. V., Swietlicki, E., Vignati, E., and Wilson, C.: Impact on short-lived climate
3244 forcers increases projected warming due to deforestation, *Nat. Commun.*, 9, 9, doi:10.1038/s41467-017-
3245 02412-4, 2018.
- 3246 Shakhova, N., Semiletov, I., and Belcheva, N.: The great Siberian rivers as a source of methane on the
3247 Russian Arctic shelf, *Dokl. Earth Sci.*, 415, 734–736, doi: 10.1134/S1028334X07050169, 2007.
- 3248 Shalina, E. V., and Sandven, S.: Snow depth on Arctic sea ice from historical in situ data, *Cryosphere*, 12(6),
3249 1867-1886, doi:10.5194/tc-12-1867-2018, 2018.
- 3250 Shen, Y., Virkkula, A., Ding, A., Wang, J., Chi, X., Nie, W., Qi, X., Huang, X., Liu, Q., Zheng, L., Xu, Z.,
3251 Petäjä, T., Aalto, P. P., Fu, C., and Kulmala, M.: Aerosol optical properties at SORPES in Nanjing, east
3252 China, *Atmos. Chem. Phys.*, 18, 5265–5292, doi: 10.5194/acp-18-5265-2018, 2018.
- 3253 Shen, Y., Virkkula, A., Ding, A., Luoma, K., Keskinen, H., Aalto, P. P., Chi, X., Qi, X., Nie, W., Huang, X.,
3254 Petäjä, T., Kulmala, M., and Kerminen, V.-M.: Estimating cloud condensation nuclei number concentrations
3255 using aerosol optical properties: role of particle number size distribution and parameterization, *Atmos.*
3256 *Chem. Phys.*, 19, 15483–15502, doi:10.5194/acp-19-15483-2019, 2019.
- 3257 Shestakova, T. A., Gutierrez, E., Valeriano, C., Lapshina, E., and Voltas, J.: Recent loss of sensitivity to
3258 summer temperature constrains tree growth synchrony among boreal Eurasian forests, *Agr. Forest Meteorol.*,
3259 268, 318-330, doi:10.1016/j.agrformet.2019.01.039, 2019.
- 3260 Shevchenko, V. P., Starodymova, D. P., Vinogradova, A. A., Lisitzin, A. P., Makarov, V. I., Popova, S. A.,
3261 Sivonen, V. V., and Sivonen, V. P.: Elemental and organic carbon in atmospheric aerosols over the
3262 northwestern coast of Kandalaksha Bay of the White Sea, *Dokl. Earth Sci.*, 461(1), 242-246,
3263 doi:10.1134/s1028334x1503006x, 2015.
- 3264 Shevchenko, V. P., Maslov, A. V., and Stein, R.: Distribution of some rare and trace elements in ice-rafted
3265 sediments in the Yermak Plateau area, the Arctic Ocean, *Oceanol.*, 57(6), 855-863,
3266 doi:10.1134/s0001437017060157, 2017a.

- 3267 Shevchenko, V. P., Pokrovsky, O. S., Vorobyev, S. N., Krickov, I. V., Manasypov, R. M., Politova, N. V.,
3268 Kopysov, S. G., Dara, O. M., Auda, Y., Shirokova, L. S., Kolesnichenko, L. G., Zemtsov, V. A., and
3269 Kirpotin, S. N.: Impact of snow deposition on major and trace element concentrations and elementary fluxes
3270 in surface waters of the Western Siberian Lowland across a 1700 km latitudinal gradient, *Hydrol. Earth Syst.*
3271 *Sci.*, 21, 5725–5746, doi:10.5194/hess-21-5725-2017, 2017b.
- 3272 Shevchenko, V. P., Kopeikin, V. M., Novigatsky, A. N., and Malafeev, G. V.: Black carbon in the
3273 atmospheric boundary layer over the North Atlantic and the Russian Arctic seas in June–September 2017,
3274 *Oceanol.*, 59(5), doi:10.1134/S0001437019050199, 692–696, 2019.
- 3275 Shevnina, E., Kourzeneva, E., Kovalenko, V., and Vihma, T.: Assessment of extreme flood events in a
3276 changing climate for a long-term planning of socio-economic infrastructure in the Russian Arctic, *Hydrol.*
3277 *Earth Syst. Sci.*, 21(5), 2559-2578, doi:10.5194/hess-21-2559-2017, 2017.
- 3278 Shevnina, E., Silaev, A., and Vihma, T.: Probabilistic projections of annual runoff and potential hydropower
3279 production in Finland, *Universal Journal of Geoscience*, 7(2), 43-55, doi:10.13189/ujg.2019.070201, 2019.
- 3280 Shiklomanov, A.I., and Lammers, R.B.: Record Russian river discharge in 2007 and the limits of analysis,
3281 *Environ. Res. Lett.*, 4, doi: 10.1088/1748-9326/4/4/045015, 2009.
- 3282 Shinkareva G. L., Lychagin M. Y., Tarasov M. K., Pietron J., Chichaeva M. A., and Chalov S. R.:
3283 Biogeochemical specialization of macrophytes and their role as a biofilter in the Selenga delta, *Geography,*
3284 *Environment, Sustainability*, 12(3), 240-263, 2019.
- 3285 Silkin, V. A., Pautova, L., Giordano, M., Chasovnikov, V., Vostokov, S., Podymov, O., Parkhomova, S., and
3286 Moskalenko, L.: Drivers of phytoplankton blooms in the northeastern Black Sea, *Mar. Pollution Bull.*, 138,
3287 274-284, doi:10.1016/j.marpolbul.2018.11.042, 2018.
- 3288 Sizov O. S., and Lobotrosova S. A.: Features of revegetation of drift sand sites in the northern taiga subzone
3289 of Western Siberia. *Earth Cryosphere*, (3), 3–13, doi:10.21782/kz1560-7496-2016-3(3-13), 2016.
- 3290 Skorokhod, A. I., Berezina, E. V., Moiseenko, K. B., Elansky, N. F., and Belikov, I. B.: Benzene and toluene
3291 in the surface air of northern Eurasia from TROICA-12 campaign along the Trans-Siberian Railway, *Atmos.*
3292 *Chem. Phys.*, 17(8), 5501-5514, doi:10.5194/acp-17-5501-2017, 2017.
- 3293 Slukovskaya, M. V., Vasenev, V. I., Ivashchenko, K. V., Morev, D. V., Drogobuzhskaya, S. V., Ivanova, L.
3294 A., and Kremenetskaya, I. P.: Technosols on mining wastes in the subarctic: Efficiency of remediation under
3295 Cu-Ni atmospheric pollution, *Int. Soil Water Conserv. Res.*, 7(3), 297-307, doi:10.1016/j.iswcr.2019.04.002,
3296 2019.
- 3297 Smith, L.: *The new north: The world in 2050*, Profile Books, London, UK, 2011.
- 3298 Song, S., Li, C., Shi, X., Zhao, S., Li, Z., Bai, Y., Cao, X., Wang, Q., Huotari, J., Tulonen, T., Uusheimo, S.,
3299 Leppäranta, M., and Arvola, L.: Under-ice metabolism in a shallow lake (Wuliangsuhai) in Inner Mongolia,
3300 in cold and arid climate zone, *Freshw. Biol.*, 1–11, 2019.

- 3301 Spengler, T., Renfrew, I. A., Terpstra, A., Tjernström, M., Screen, J., Brooks, I. M., Andrew Carleton, A.,
 3302 Chechin, D., Chen, L., Doyle, J., Esau, I., Hezel, P. J., Jung, T., Kohyama, T., Lüpkes, C., McCusker, C. E.,
 3303 Nygård, T., Sergeev, D., Shupe, M. D., Sodemann, H., and Vihma, T.: High-latitude dynamics of
 3304 atmosphere–ice–ocean interactions, *Bull. Am. Meteorol. Soc.*, 97(9), ES179–ES182, doi:10.1175/bams-d-15-
 3305 00302.1, 2016.
- 3306 Sporre, M. K., Blichner, S. M., Karsset, I. H. H., Makkonen, R., and Berntsen, T. K.: BVOC–aerosol–climate
 3307 feedbacks investigated using NorESM, *Atmos. Chem. Phys.*, 19, 4763–4782, doi:10.5194/acp-19-4763-
 3308 2019, 2019.
- 3309 Starodymova, D. P., Shevchenko, V. P., Sivonen, V. P., and Sivonen, V. V.: Material and elemental
 3310 composition of surface aerosols on the north-western coast of the Kandalaksha Bay of the White Sea, *Atmos.*
 3311 *Oceanic Opt.*, 29(6), 507–511, doi:10.1134/s1024856016060154, 2016.
- 3312 Sun, H., Santalahti, M., Pumpanen, J., Koster, K., Berninger, F., Raffaello, T., Asiegbu, F. O., and
 3313 Heinonsalo, J.: Bacterial community structure and function shift across a northern boreal forest fire
 3314 chronosequence, *Scientific Rep.*, 6, 12, doi:10.1038/srep32411, 2016.
- 3315 Sun, Y., Frankenberg C., Wood JD, Schimel DS., Jung, M., Guanter L., Drewry, DT., Verma, M., Porcar-
 3316 Castell, A., Griffis, TJ., Gu, L., Magney, S., Köhler P., Evans B., and Yuen, K.: OCO-2 advances
 3317 photosynthesis observation from space via solar-induced chlorophyll fluorescence, *Science* 358, 189,
 3318 doi:10.1126/science.aam5747, 2017.
- 3319 Suomi, I., Gryning, S-E., O'Connor E.J., and Vihma, T.: Methodology for obtaining wind gusts
 3320 using Doppler lidar, *Quarterly Journal of the Royal Meteorological Society*, 143, 2061–2072,
 3321 doi.org/10.1002/qj.3059, 2016.
- 3322 Svensson, J., Virkkula, A., Meinander, O., Kivekäs, N., Hannula, H.-R., Järvinen, O., Peltoniemi, J.I.,
 3323 Gritsevich, M., Heikkilä, A., Kontu, A., Neitola, K., Brus, D., DagssonWaldhauserova, P., Anttila, K.,
 3324 Vehkamäki, M., Hienola, A., de Leeuw, G., and Lihavainen, H.: Soot-doped natural snow and its albedo —
 3325 results from field experiments, *Boreal Environment Research*, 21, 481–503, 2016.
- 3326 Svensson, J., Ström, J., Kivekäs, N., Dkhar, N. B., Tayal, S., Sharma, V. P., Jutila, A., Backman, J.,
 3327 Virkkula, A., Ruppel, M., Hyvärinen, A., Kontu, A., Hannula, H.-R., Leppäranta, M., Hooda, R. K., Korhola,
 3328 A., Asmi, E., and Lihavainen, H.: Light absorption of dust and elemental carbon in snow in the Indian
 3329 Himalayas and the Finnish Arctic, *Atmos. Meas. Tech.*, 11, 1403–1416, doi:10.5194/amt-11-1403-2018,
 3330 2018.
- 3331 Svensson, J., Ström, J., and Virkkula, A.: Multiple-scattering correction factor of quartz filters and the effect
 3332 of filtering particles mixed in water: implications for analyses of light absorption in snow samples, *Atmos.*
 3333 *Meas. Tech.*, 12, 5913–5925, doi:10.5194/amt-12-5913-2019, 2019.

- 3334 Taylor, K. E., Stouffer, R. J., and Meehl, G. A.: An overview of CMIP5 and the experiment design, *Bull.*
 3335 *Am. Meteorol. Soc.*, 93, 485–498, doi: 10.1175/BAMS-D-11-00094.1, 2012.
- 3336 Taylor, A., Brownlee, C., and Wheeler, G.: Coccolithophore cell biology: chalking up progress, *Ann. Rev.*
 3337 *Mar. Sci.*, 9, 283–310, doi:10.1146/annurev-marine-122414-034032, 2017.
- 3338 Terentieva, I. E., Glagolev, M. V., Lapshina, E. D., Sabrekov, A. F., and Maksyutov, S.: Mapping of West
 3339 Siberian taiga wetland complexes using Landsat imagery: implications for methane emissions,
 3340 *Biogeosciences*, 13, 4615–4626, doi:10.5194/bg-13-4615-2016, 2016.
- 3341 Thompson, R. L., Sasakawa, M., Machida, T., Aalto, T., Worthy, D., Lavric, J. V., Lund Myhre, C., and
 3342 Stohl, A.: Methane fluxes in the high northern latitudes for 2005–2013 estimated using a Bayesian
 3343 atmospheric inversion, *Atmos. Chem. Phys.*, 17, 3553–3572, doi:10.5194/acp-17-3553-2017, 2017.
- 3344 Thonat, T., Saunio, M., Bousquet, P., Pison, I., Tan, Z., Zhuang, Q., Crill, P. M., Thornton, B. F., Bastviken,
 3345 D., Dlugokencky, E. J., Zimov, N., Laurila, T., Hatakka, J., Hermansen, O., and Worthy, D. E. J.:
 3346 Detectability of Arctic methane sources at six sites performing continuous atmospheric measurements,
 3347 *Atmos. Chem. Phys.*, 17, 8371–8394, doi:10.5194/acp-17-8371-2017, 2017.
- 3348 Thorslund, J., Jarsjo, J., Wallstedt, T., Morth, C. M., Lychagin, M. Y., and Chalov, S. R.: Speciation and
 3349 hydrological transport of metals in non-acidic river systems of the Lake Baikal basin: Field data and model
 3350 predictions, *Reg. Environ. Chang.*, 17(7), 2007–2021, doi:10.1007/s10113-016-0982-7, 2017.
- 3351 Tian, Z. X., Cheng, B., Zhao, J. C., Vihma, T., Zhang, W. L., Li, Z. J., and Zhang, Z. H.: Observed and
 3352 modelled snow and ice thickness in the Arctic Ocean with CHINARE buoy data, *Acta Oceanologica Sinica*,
 3353 36(8), 66–75, doi:10.1007/s13131-017-1020-4, 2017.
- 3354 Tillman, H., Yang, J. and Nielsson, E.: The Polar Silk Road: China's New Frontier of International
 3355 Cooperation, *China Quarterly of International Strategic Studies*, 4, 10.1142/S2377740018500215, 2018.
- 3356 Timokhina, A. V., Prokushkin, A. S., Onuchin, A. A., Panov, A. V., Kofman, G. B., and Heimann, M.:
 3357 Variability of ground CO₂ concentration in the middle taiga subzone of the Yenisei region of Siberia, *Russ.*
 3358 *J. Ecol.*, 46, 143–151, doi:10.1134/s1067413615020125, 2015a.
- 3359 Timokhina, A. V., Prokushkin, A. S., Onuchin, A. A., Panov, A. V., Kofman, G. B., Verkhovets, S. V., and
 3360 Heimann, M., Long-term trend in CO₂ concentration in the surface atmosphere over Central Siberia, *Russ.*
 3361 *Meteorol. Hydrol.*, 40, 186–190, 2015b.
- 3362 Tsuruta, A., Aalto, T., Backman, L., Hakkarainen, J., ... and Peters, W.: Global methane emission estimates
 3363 for 2000–2012 from CarbonTracker Europe-CH₄ v1.0. *Geosci. Model Dev.*, 10, 1261–1289, 2017.
- 3364 Tuovinen, J-P., Aurela, M., Hatakka, J., Räsänen, A., ... Laurila, T.: Interpreting eddy covariance data from
 3365 heterogeneous Siberian tundra: land-cover-specific methane fluxes and spatial representativeness,
 3366 *Biogeosciences*, 16, 255–274, 2019.

- 3367 Uotila, P., Vihma, T., and Haapala, J.: Atmospheric and oceanic conditions and the extremely low Bothnian
3368 Bay sea ice extent in 2014/2015, 42, 7740-7749, *Geophysical Research and Letters*, 2015.
- 3369 Uotila, P., Iovino, D., Vancoppenolle, M., Lensu, M., and Rousset, C., Comparing sea ice, hydrography and
3370 circulation between NEMO3.6 LIM3 and LIM2, *Geosci. Model Dev.*, 10, 1009–1031, doi:10.5194/gmd-10-
3371 1009-2017, 2017.
- 3372 Uotila, P., Goosse, H., Haines, K., Chevallier, M., Barthélemy, A., Bricaud, C., Carton, J., Fučkar, N.,
3373 Garric, G., Iovino, D., Kauker, F., Korhonen, M., Lien, V. S., Marnela, M., Massonnet, F., Mignac, D.,
3374 Peterson, K. A., Sadikni, R., Shi, L., Tietsche, S., Toyoda, T., Xie, J., and Zhang, A.: An assessment of ten
3375 ocean reanalyses in the polar regions, *Clim Dyn* 52, 1613–1650, doi:10.1007/s00382-018-4242-z, 2019.
- 3376 Uttal, T., Starkweather, S., Drummond, J. R., Vihma, T., Makshtas, A. P., Darby, L. S., Burkhart, J. F., Cox,
3377 C. J., Schmeisser, L. N., Haiden, T., Maturilli, M., Shupe, M. D., De Boer, G., Saha, A., Grachev, A. A.,
3378 Crepinsek, S. M., Bruhwiler, L., Goodison, B., McArthur, B., Walden, V. P., Dlugokencky, E. J., P. Persson,
3379 O., Lesins, G., Laurila, T., Ogren, J. A., Stone, R., Long, C. N., Sharma, S., Massling, A., Turner, D. D.,
3380 Stanitski, D. M., Asmi, E., Aurela, M., Skov, H., Eleftheriadis, K., Virkkula, A., Platt, A., Førland, E. J.,
3381 Iijima, Y., Nielsen, I. E., Bergin, M. H., Candlish, L., Zimov, N. S., Zimov, S. A., O'Neill, N. T., Fogal, P.
3382 F., Kivi, R., Konopleva-Akish, E. A., Verlinde, J., Kustov, V. Y., Vasel, B., Ivakhov, V. M., Viisanen Y.,
3383 and Intrieri, J. M.: International Arctic Systems for Observing the Atmosphere: An International Polar Year
3384 Legacy Consortium, *Bull. Amer. Meteor. Soc.*, 97, 1033–1056, doi:10.1175/BAMS-D-14-00145.1, 2016.
- 3385 Vanhatalo, A., Ghirardo, A., Juurola, E., Schnitzler, J.-P., Zimmer, I., Hellén, H., Hakola, H., and Bäck, J.:
3386 Long-term dynamics of monoterpene synthase activities, monoterpene storage pools and emissions in boreal
3387 Scots pine, *Biogeosciences*, 15, 5047–5060, doi:10.5194/bg-15-5047-2018, 2018.
- 3388 Varentsov, M., Konstantinov, P., Baklanov, A., Esau, I., Miles, V., and Davy, R.: Anthropogenic and natural
3389 drivers of a strong winter urban heat island in a typical Arctic city, *Atmos. Chem. Phys.*, 18(23), 17573-
3390 17587, doi:10.5194/acp-18-17573-2018, 2018a.
- 3391 Varentsov, M., Wouters, H., Platonov, V., and Konstantinov, P.: Megacity-induced mesoclimatic effects in
3392 the lower atmosphere: a modeling study for multiple summers over Moscow, Russia, *Atmos.*, 9(2), 24,
3393 doi:10.3390/atmos9020050, 2018b.
- 3394 Vasileva, A., Moiseenko, K., Skorokhod, A., Belikov, I., Kopeikin, V., and Lavrova, O.: Emission ratios of
3395 trace gases and particles for Siberian forest fires on the basis of mobile ground observations, *Atmos. Chem.*
3396 *Phys.*, 17(20), 12303-12325, doi:10.5194/acp-17-12303-2017, 2017.
- 3397 Vestenius, M., Hellén, H., Levula, J., Kuronen, P., Helminen, K. J., Nieminen, T., Kulmala, M., and Hakola,
3398 H.: Acidic reaction products of monoterpenes and sesquiterpenes in atmospheric fine particles in a boreal
3399 forest, *Atmos. Chem. Phys.*, 14, 7883–7893, doi:10.5194/acp-14-7883-2014, 2014.

- 3400 Vihma, T., Uotila, P., Sandven, S., Pozdnyakov, D., Makshtas, A., Pelyasov, A., Pirazzini, R., Danielsen, F.,
 3401 Chalov, S., Lappalainen, H. K., Ivanov, V., Frolov, I., Albin, A., Cheng, B., Dobrolyubov, S., Arkhipkin, V.,
 3402 Myslenkov, S., Petäjä, T., and Kulmala, M.: Towards an advanced observation system for the marine Arctic
 3403 in the framework of the Pan-Eurasian Experiment (PEEX), *Atmos. Chem. Phys.*, 19, 1941-1970,
 3404 doi:10.5194/acp-19-1941-2019, 2019.
- 3405 Vihma, T., Graverson, R., Chen, L., Dörthe H., Skific, N., Francis, J.A., Tyrrell, N., Hall, R., Hanna, E.,
 3406 Uotila, P., Dethloff, K., Karpechko, A. Y., Björnsson, H. and Overland, J. E.: Effects of the tropospheric
 3407 large-scale circulation on European winter temperatures during the period of amplified Arctic warming, *Int J*
 3408 *Climatol.*, 40, 509– 529, doi:10.1002/joc.6225, 2020
- 3409 Virkkula, A., Chi, X., Ding, A., Shen, Y., Nie, W., Qi, X., Zheng, L., Huang, X., Xie, Y., Wang, J., Petäjä,
 3410 T., and Kulmala, M.: On the interpretation of the loading correction of the aethalometer, *Atmos. Meas.*
 3411 *Tech.*, 8, 4415-4427, doi:10.5194/amt-8-4415-2015, 2015.
- 3412 Voigt, C., Marushchak, M.E., Lamprecht, R.E., et al.: Nitrous oxide emissions from thawing permafrost,
 3413 *PNAS* May 2017, 201702902; DOI: 10.1073/pnas.1702902114.
- 3414 Voigt, C., Lamprecht, R. E., Marushchak, M. E., Lind, S. E., Novakovskiy, A., Aurela, M., Martikainen, P. J.
 3415 and Biasi, C.: Warming of subarctic tundra increases emissions of all three important greenhouse gases -
 3416 carbon dioxide, methane, and nitrous oxide, *Glob. Change Biol.*, 23(8), 3121-3138, doi:10.1111/gcb.13563,
 3417 2016.
- 3418 Voropay, N. N., Kichigina, N. V.: Long-term changes in the hydroclimatic characteristics in the Baikal
 3419 region, *IOP Conf. Ser.: Earth Environ. Sci.*, 107, 012042, 2018.
- 3420 Voropay N.N., Ryazanova A.A., Dyukarev E.A. Variability of vegetation index NDVI during periods of
 3421 drought in the Tomsk Region, *IOP Conf. Series: Earth Environ. Sci.*, 381, 012096, doi:10.1088/1755-
 3422 1315/381/1/012096, 2019.
- 3423 Walker, X. J., Baltzer, J. L., Cumming, S. G., Day, N. J., Ebert, C., Goetz, S., Johnstone, J. F., Potter, S.,
 3424 Rogers, B. M., Schuur, E. A. G., Turetsky, M. R., and Mack, M. C., Increasing wildfires threaten historic
 3425 carbon sink of boreal forest soils, *Nature*, 572, 520-523, doi:10.1038/s41586-019-1474-y, 2019.
- 3426 Walsh, M. G., de Smalen, A. W., and Mor, S. M.: Climatic influence on anthrax suitability in warming
 3427 northern latitudes, *Sci Rep*, 8(1), 9269, doi:10.1038/s41598-018-27604-w, 2018.
- 3428 van Vuuren, D. P., Edmonds, J., Kainuma, M., Riahi, K., Thomson, A., Hibbard, K., Hurtt, G. C., Kram, T.,
 3429 Krey, V., Lamarque, J. F., Masui, T., Meinshausen, M., Nakicenovic, N., Smith, S. J., and Rose, S. K.: The
 3430 representative concentration pathways: an overview, *Clim. Chang.*, 109, 5-31, doi:10.1007/s10584-011-
 3431 0148-z, 2011.
- 3432 Wang, J., Ge, X., Chen, Y., Shen, Y., Zhang, Q., Sun, Y., Xu, J., Ge, S., Yu, H., and Chen, M.: Highly time-
 3433 resolved urban aerosol characteristics during springtime in Yangtze River Delta, China: insights from soot

- 3434 particle aerosol mass spectrometry, *Atmos. Chem. Phys.*, 16, 9109–9127, doi:10.5194/acp-16-9109-2016,
3435 2016.
- 3436 Wang, J., Zhao, B., Wang, S., Yang, F., Xing, J., Morawska, L., Ding, A., Kulmala, M., Kerminen, V.-M.,
3437 Kujansuu, J., Wang, Z., Ding, D., Zhang, X., Wang, H., Tian, M., Petäjä, T., Jiang, J., and Hao J.: Particulate
3438 matter pollution over China and the effects of control policies, *Sci. Total Environ.*, 584-585, 426-447, 2017a.
- 3439 Wang, Z. B., Wu, Z. J., Yue, D. L., Shang, D. J., Guo, S., Sun, J. Y., Ding, A. J., Wang, L., Jiang, J. K., Guo,
3440 H., Gao, J., Cheung, H. C., Morawska, L., Keywood, M., and Hu, M.: New particle formation in China:
3441 Current knowledge and further directions, *Sci. Total Environ.*, 577, 258–266,
3442 doi:10.1016/j.scitotenv.2016.10.177, 2017b.
- 3443 Wang, Z., Huang, X., and Ding, A.: Dome effect of black carbon and its key influencing factors, *Atmos.*
3444 *Chem. Phys.*, 18, 2821-2834, 2018b.
- 3445 Wang, P. C., Elansky, N. F., Timofeev, Y. M., Wang, G. C., Golitsyn, G. S., Makarova, M. V., Rakitin, V.
3446 S., Shtabkin, Yu., Skorokhod, A. I., Grechko, E. I., Fokeeva, E. V., Safronov, A. N., Ran, L., and Wang, T.:
3447 Long-term trends of carbon monoxide total columnar amount in urban areas and background regions:
3448 ground- and satellite-based spectroscopic measurements, *Adv. Atmos. Sci.*, 35(7), 785-795,
3449 doi:10.1007/s00376-017-6327-8, 2018a.
- 3450 Wang, Y., Wang, Y., Wang, L., Petäjä, T., Zha, Q., Gong, C., Li, S., Pan, Y., Hu, B., Xin, J., and Kulmala,
3451 M.: Increased inorganic aerosol fraction contributes to air pollution and haze in China, *Atmos. Chem. Phys.*,
3452 19, 5881–5888, doi:10.5194/acp-19-5881-2019, 2019.
- 3453 Wang, Y.H., Yu, M., Wang, Y., Tang, G., Song, T., Zhou, P., Liu, Z., Hu, B., Ji, D.S., Wang, L., Zhu, X.,
3454 Yan, C., Ehn, M., Gao, W.K., Pan, Y.P., Xin, J.Y., Sung, Y., Kerminen, V.-M., Kulmala, M. and Petäjä, T.:
3455 Rapid formation of intense haze episode via aerosol-boundary layer feedback in Beijing, *Atmos. Chem.*
3456 *Phys.*, 10, 45-53, 2020.
- 3457 Wei, L. X., Deng, X. H., Cheng, B., Vihma, T., Hannula, H. R., Qin, T., and Pulliainen, J.: The impact of
3458 meteorological conditions on snow and ice thickness in an Arctic lake, *Tellus A: Dyn. Meteorol. Oceanogr.*,
3459 68, 12, doi:10.3402/tellusa.v68.31590, 2016.
- 3460 Wickström, S., Jonassen, M., Vihma, T., and Uotila, P.: Trends in cyclones in the high latitude North
3461 Atlantic during 1979-2016, *Q. J. R. Meteorol. Soc.*, 146, 762– 779, doi:10.1002/qj.3707, 2020.
- 3462 Wiedensohler, A., Ma, N., Birmili, W., Heintzenberg, J., Ditas, F., Andreae, M. O., and Panov, A.:
3463 Infrequent new particle formation over the remote boreal forest of Siberia, *Atmos. Environ.*, 200, 167-169,
3464 doi:10.1016/j.atmosenv.2018.12.013, 2019.
- 3465 Wild, B., Andersson, A., Bröder, L., Vonk, J., Hugelius, G., McClelland, J.W., Song, W., Raymond, P.A.,
3466 and Gustafsson, Ö.: Rivers across the Siberian Arctic unearth the patterns of carbon release from thawing
3467 permafrost *Proceedings of the National Academy of Sciences*, 116 (21) 10280-10285., 2019.

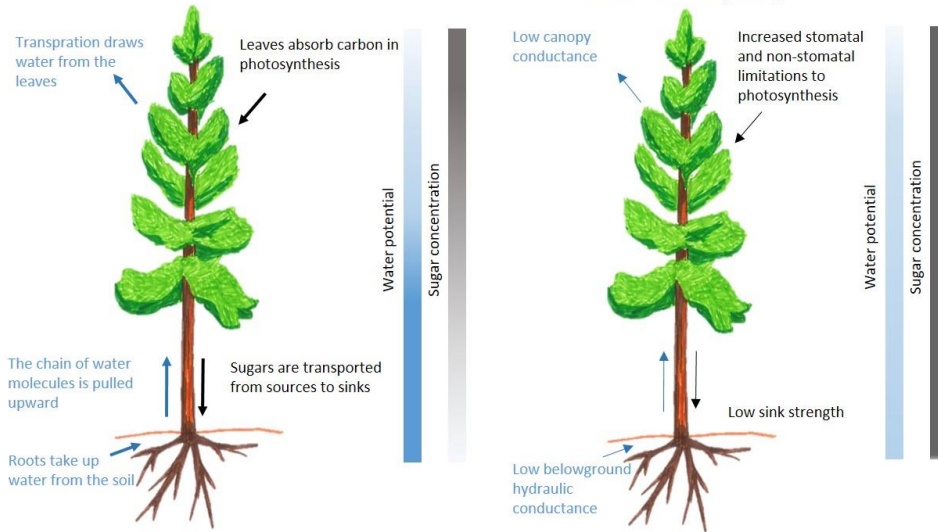
- 3468 Williams, P. J., and Smith, M. W.: The Frozen Earth: Fundamentals of Geocryology, Cambridge University
3469 Press, Cambridge, UK, 1989.
- 3470 WMO, 2019 Guidance on Integrated Urban Hydrometeorological, Climate and Environmental Services.
3471 Volume 1: Concept and Methodology, Grimmond, S., Bouchet, S., Molina, L., Baklanov, A., Joe, P. et al.,
3472 WMO-No. 1234, https://library.wmo.int/doc_num.php?explnum_id=9903, 2019.
- 3473 Wolf-Grosse, T., Esau, I., and Reuder, J.: The large-scale circulation during air quality hazards in Bergen,
3474 Norway, *Tellus A: Dyn. Meteorol. Oceanogr.*, 69, 16, doi:10.1080/16000870.2017.1406265, 2017a.
- 3475 Wolf-Grosse, T., Esau, I., and Reuder, J.: Sensitivity of local air quality to the interplay between small- and
3476 large-scale circulations: a large-eddy simulation study, *Atmos. Chem. Phys.*, 17(11), 7261-7276,
3477 doi:10.5194/acp-17-7261-2017, 2017b.
- 3478 Xausa, F., Paasonen, P., Makkonen, R., Arshinov, M., Ding, A., Denier Van Der Gon, H., Kerminen, V.-M.,
3479 and Kulmala, M.: Advancing global aerosol simulations with size-segregated anthropogenic particle number
3480 emissions, *Atmos. Chem. Phys.*, 18, 10039–10054, doi:10.5194/acp-18-10039-2018, 2018.
- 3481 Xiao, S., Wang, M. Y., Yao, L., Zhou, B., Yang, X., Chen, J. M., Wang, D. F., Fu, Q. Y., Worsnop, D. R.
3482 and Wang, L.: Strong atmospheric new particle formation in winter in urban Shanghai, China, *Atmos. Chem.*
3483 *Phys.*, 15, 1769-1781, 2015.
- 3484 Xie, Y. N., Ding, A. J., Nie, W., Mao, H. T., Qi, X. M., Huang, X., Xu, Z., Kerminen, V. K., Petäjä, T., Chi,
3485 X., Virkkula, A., Boy, M., Xue, L., Guo, J., Sun, J., Yang, X., Kulmala, M., and Fu, C. B.: Enhanced sulfate
3486 formation by nitrogen dioxide: Implications from in situ observations at the SORPES station, *J Geophys.*
3487 *Res.: Atmos.*, 120(24), 12679-12694, doi:10.1002/2015jd023607, 2015.
- 3488 Yan, C., Yin, R., Lu, Y., Dada, L., Yang, D., Fu, Y., Kontkanen, J., Deng, C., Garmash, O., Ruan, J.,
3489 Baalbaki, R., Schervish, M., Cai, R., Bloss, M., Chan, T., Chen, T., Chen, Q., Chen, X., Chen, Y., Chu, B.,
3490 Dällenbach, K., Foreback, B., He, X., Heikkinen, L., Jokinen, T., Junninen, H., Kangasluoma, J., Kokkonen,
3491 T., Kurppa, M., Lehtipalo, K., Li, H., Li, H., Li, X., Liu, Y. Ma, Q., Paasonen, P., Rantala, P., Pileci, R. E.,
3492 Rusanen, A., Sarnela, N., Simonen, P., Wang, S., Wang, W., Wang, Y. Xue, M., Yang, G., Yao, L., Zhou,
3493 Y., Kujansuu, J., Petäjä, T., Nie, W., Ma, N., Ge, M., He, H., Donahue, N. M., Worsnop, D. R., Kerminen,
3494 V.-M., Wang, L., Liu, Y., Zheng, J., Kulmala, M., Jiang, J. and Bianchi, F. (2021) The synergistic role of
3495 sulfuric acid, bases, and oxidized organics governing new-particle formation in Beijing. *Geophys. Res. Lett.*
3496 (in press).
- 3497 Yang, F., Li, C., Leppäranta, M., Shi, X., Zhao, S. and Zhang, C.: Notable increases in nutrient
3498 concentrations in a shallow lake during seasonal ice growth, *Water Sci. Technol.*, 74(12), 2773–2883, 2016.
- 3499 Yang, Y., Leppäranta, M. J., Ki, Z., Cheng, B., Zhai, M., and Demchev, D.: Model simulations of the annual
3500 cycle of the landfast ice thickness in the East Siberian Sea, *Advances in Polar Sciences*, 26(2), 168-178,
3501 doi:10.13679/j.advps.2015.2.00168, 2015.

- 3502 Yao, L., Garmash, O., Bianchi, F., Zheng, J., Yan, C., Kontkanen, J., Junninen, H., Mazon, S.B., Ehn, M.,
3503 Paasonen, P., Sipilä, M., Wang, M.Y., Wang, X.K., Xiao, S., Chen, H.F., Lu, Y.Q., Zhang, B.W., Wang,
3504 D.F., Fu, Q.Y., Geng, F.H., Li, L., Wang, H.L., Qiao, L.P., Yang, X., Chen, J.M., Kerminen, V.-M., Petäjä,
3505 T., Worsnop, D.R., Kulmala, M. and Wang, L.: Atmospheric new particle formation from sulfuric acid and
3506 amines in a Chinese megacity, *Science*, 361, 278-281, 2018.
- 3507 Yasunaka, S., Siswanto, E., Olsen, A., Hoppema, M., Watanabe, E., Fransson, A., Chierici, M., Murata, A.,
3508 Lauvset, S. K., Wanninkhof, R., Takahashi, T., Kosugi, N., Omar, A. M., van Heuven, S., and Mathis, J. T.:
3509 Arctic Ocean CO₂ uptake: an improved multiyear estimate of the air–sea CO₂ flux incorporating chlorophyll
3510 a concentrations, *Biogeosciences*, 15, 1643–1661, doi:10.5194/bg-15-1643-2018, 2018.
- 3511 Ye, Z., Liu, J., Gu, A., Feng, F., Liu, Y., Bi, C., Xu, J., Li, L., Chen, H., Chen, Y., Dai, L., Zhou, Q., and Ge,
3512 X.: Chemical characterization of fine particulate matter in Changzhou, China, and source apportionment with
3513 offline aerosol mass spectrometry, *Atmos. Chem. Phys.*, 17, 2573–2592, doi:10.5194/acp-17-2573-2017,
3514 2017.
- 3515 Ylivinkka, I., Kaupinmäki, S., Virman, M., Peltola, M., Taipale, D., Petäjä, T., Kerminen, V.-M., Kulmala,
3516 M., and Ezhova, E.: Clouds over Hyytiälä, Finland: an algorithm to classify clouds based on solar radiation
3517 and cloud base height measurements, *Atmos. Meas. Tech.*, 13, 5595–5619, 2020.
- 3518 He, Y., Chen, F., Jia, H., and Valery, G.: Bondur: Different Drought Legacies between Rain-fed and
3519 Irrigated Croplands in a Typical Russian Agricultural Region, *Remote Sens.*, 12(11), 1700,
3520 doi:10.3390/rs12111700, 2020
- 3521 Zaidan, M. A., Haapasilta, V., Relan, R., Junninen, H., Aalto, P. P., Kulmala, M., Laurson, L., and Foster, A.
3522 S.: Predicting atmospheric particle formation days by Bayesian classification of the time series features,
3523 *Tellus B: Chem. Phys. Meteorol.*, 70, 10, doi:10.1080/16000889.2018.1530031, 2018a.
- 3524 Zaidan, M. A., Haapasilta, V., Relan, R., Paasonen, P., Kerminen, V.-M., Junninen, H., Kulmala, M., and
3525 Foster, A. S.: Exploring non-linear associations between atmospheric new-particle formation and ambient
3526 variables: a mutual information approach, *Atmos. Chem. Phys.*, 18, 12699-12714, doi:10.5194/acp-18-
3527 12699-2018, 2018b.
- 3528 Zanatta, M., Laj, P., Gysel, M., Baltensperger, U., Vratolis, S., Eleftheriadis, K., Kondo, Y., Dubuisson, P.,
3529 Winiarek, V., Kazadzis, S., Tunved, P., and Jacobi, H.-W.: Effects of mixing state on optical and radiative
3530 properties of black carbon in the European Arctic, *Atmos. Chem. Phys.*, 18, 14037–14057, doi:10.5194/acp-
3531 18-14037-2018, 2018.
- 3532 Zapadinsky, E., Passananti, M., Myllys, N., Kurten, T., and Vehkamäki, H.: Modeling on Fragmentation of
3533 Clusters inside a Mass Spectrometer, *Journal of Physical Chemistry, A* 123 (2), 611-624,
3534 <https://doi.org/10.1021/acs.jpca.8b10744>, 2019.

- 3535 Zha, Q., Yan, C., Junninen, H., Riva, M., Sarnela, N., Aalto, J., Quéléver, L., Schallhart, S., Dada, L.,
3536 Heikkinen, L., Peräkylä, O., Zou, J., Rose, C., Wang, Y., Mammarella, I., Katul, G., Vesala, T., Worsnop, D.
3537 R., Kulmala, M., Petäjä, T., Bianchi, F., and Ehn, M.: Vertical characterization of highly oxygenated
3538 molecules (HOMs) below and above a boreal forest canopy, *Atmos. Chem. Phys.*, 18, 17437–17450,
3539 doi:10.5194/acp-18-17437-2018, 2018.
- 3540 Zhang, J., Liu, C., and Chen, H.: The modulation of Tibetan Plateau heating on the multi-scale northernmost
3541 margin activity of East Asia summer monsoon in northern China, *Global Planet. Change*, 161, 149–161,
3542 2018.
- 3543 Zhang, S., Zhang, J. H., Bai, Y., Koju, U. A., Igbawua, T., Chang, Q., Zhang, D., and Yao, F. M.: Evaluation
3544 and improvement of the daily boreal ecosystem productivity simulator in simulating gross primary
3545 productivity at 41 flux sites across Europe, *Ecol. Model.*, 368, 205-232,
3546 doi:10.1016/j.ecolmodel.2017.11.023, 2018.
- 3547 Zhang-Turpeinen, H., Kivimäenpää, M., Aaltonen, H., Berninger, F., Köster, E., Köster, K., Menyailo, O.,
3548 Prokushkin, A., and Pumpanen, J.: Wildfire effects on BVOC emissions from boreal forest floor on
3549 permafrost soil in Siberia, *Science of the Total Environment*, 134851, doi:10.1016/j.scitotenv.2019.134851,
3550 2020.
- 3551 Zhao, H., Li, X., Zhang, Q., Jiang, X., Lin, J., Peters, G. P., Li, M., Geng, G., Zheng, B., Huo, H., Zhang, L.,
3552 Wang, H., Davis, S. J., and He, K.: Effects of atmospheric transport and trade on air pollution mortality in
3553 China, *Atmos. Chem. Phys.*, 17, 10367–10381, doi:10.5194/acp-17-10367-2017, 2017.
- 3554 Zhdanova, E. Y., Chubarova, N. Y., and Lyapustin, A. I.: Assessment of urban aerosol pollution over the
3555 Moscow megacity by the MAIAC aerosol product, *Atmos. Meas. Tech.*, 13, 877–891, doi:10.5194/amt-13-
3556 877-2020, 2020.
- 3557 Zhou, Y., Dada, L., Liu, Y., Fu, Y., Kangasluoma, J., Chan, T., Yan, C., Chu, B., Daellenbach, K. R.,
3558 Bianchi, F., Kokkonen, T. V., Liu, Y., Kujansuu, J., Kerminen, V.-M., Petäjä, T., Wang, L., Jiang, J., and
3559 Kulmala, M.: Variation of size-segregated particle number concentrations in wintertime Beijing, *Atmos.*
3560 *Chem. Phys.*, 20, 1201–1216, doi:10.5194/acp-20-1201-2020, 2020.
- 3561 Zilitinkevich, S., Druzhinin, O., Glazunov, A., Kadantsev, E., Mortikov, E., Repina, I., and Troitskaya, Y.:
3562 Dissipation rate of turbulent kinetic energy in stably stratified sheared flows, *Atmos. Chem. Phys.*, 19, 2489–
3563 2496, doi:10.5194/acp-19-2489-2019, 2019.
- 3564 Öström, E., Putian, Z., Schurgers, G., Mishurov, M., Kivekäs, N., Lihavainen, H., Ehn, M., Rissanen, M. P.,
3565 Kurtén, T., Boy, M., Swietlicki, E., and Roldin, P.: Modeling the role of highly oxidized multifunctional
3566 organic molecules for the growth of new particles over the boreal forest region, *Atmos. Chem. Phys.*, 17,
3567 8887–8901, doi:10.5194/acp-17-8887-2017, 2017.
- 3568

Non-stressed conditions

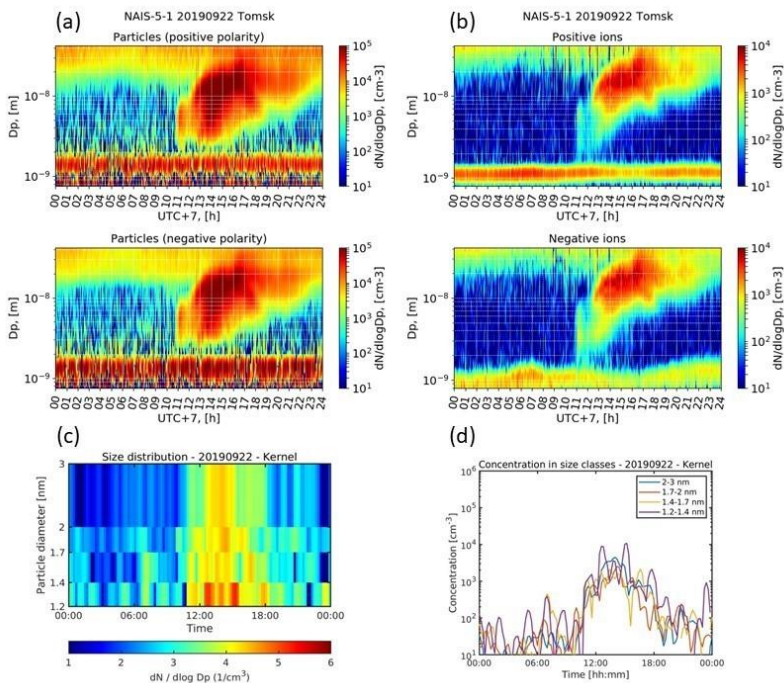
Cold soil in spring



3569

3570 Figure 1.

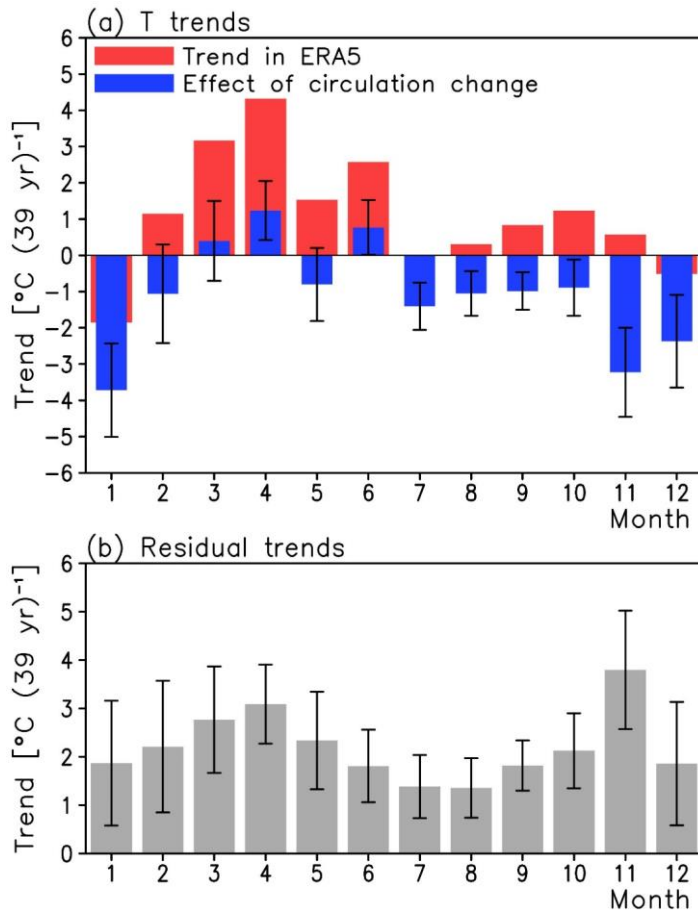
3571



3572

3573 Figure 2.

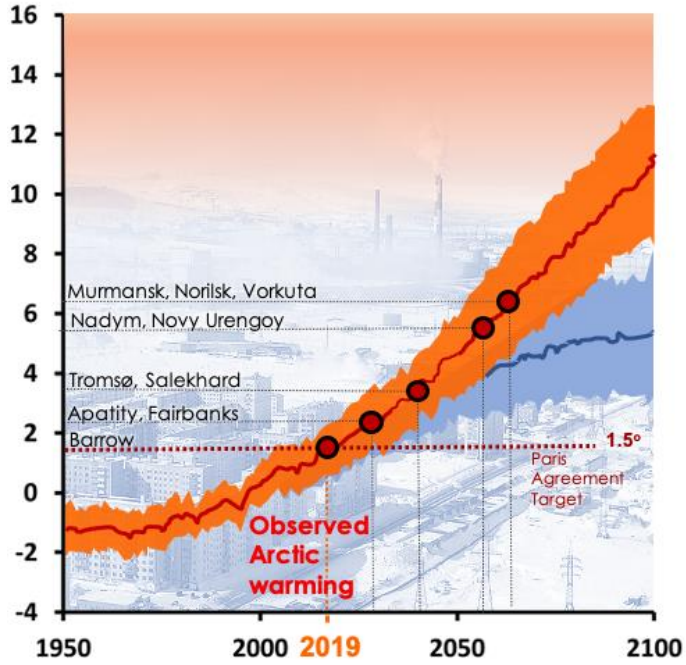
3574



3575

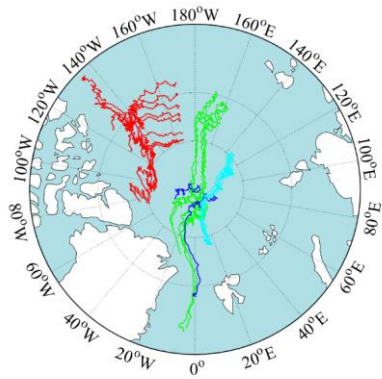
3576 Figure 3.

3577



3578

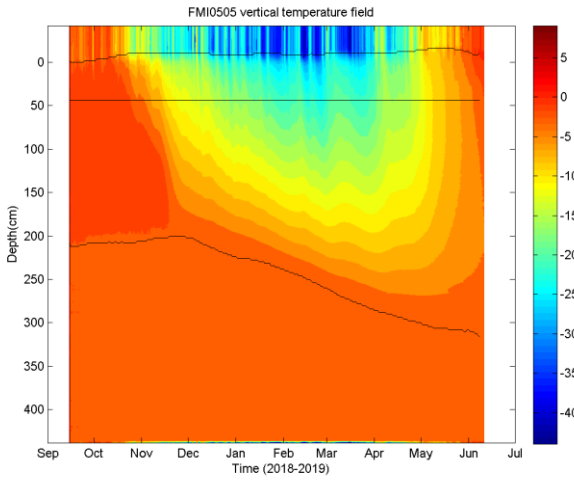
3579 Figure 4.



3580

3581 Figure 5.

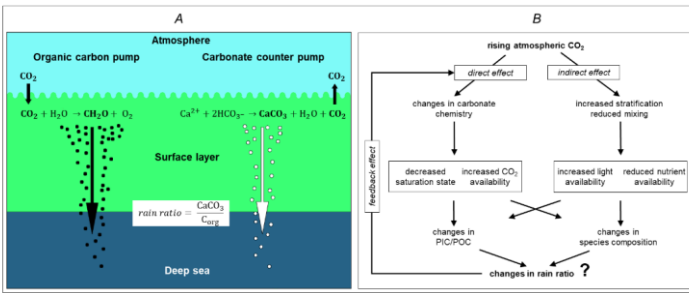
3582



3583

3584 Figure 6.

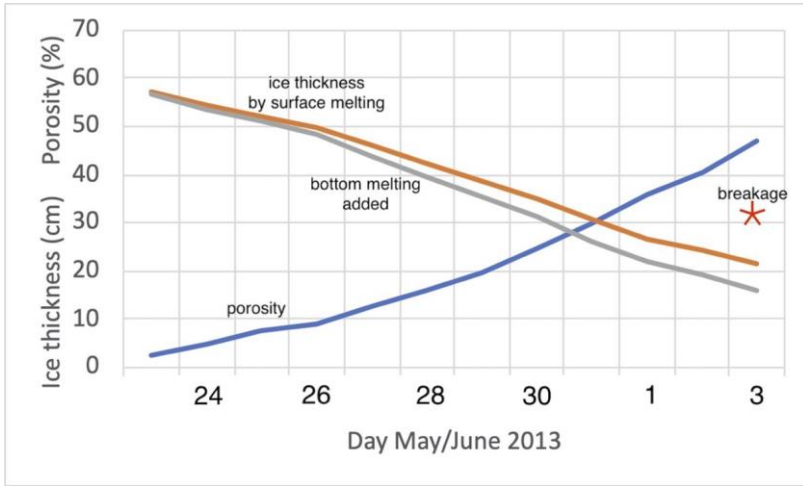
3585



3586

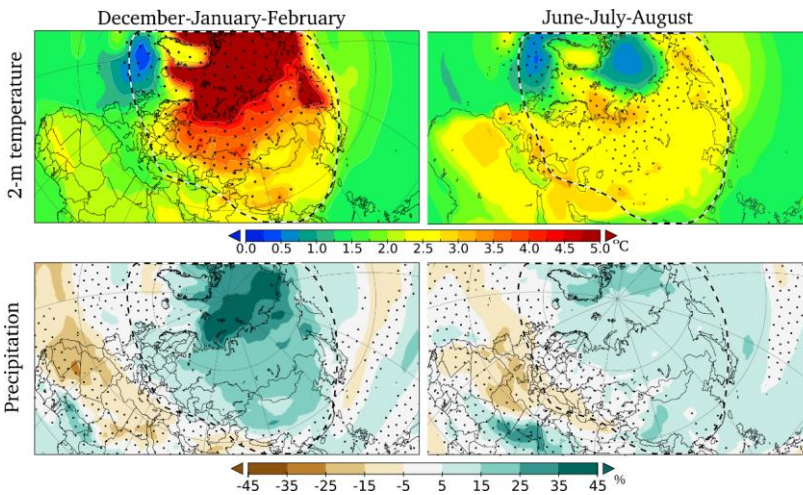
3587 Figure 7.

3588



3589

3590 Figure 8.



3591

3592 Figure 9.

3593

3594

3595

3596

3597 **Figure 1.** A recent field and modelling study shows that cold soil decreases belowground hydraulic
 3598 conductance (i.e. less root water uptake), and further canopy conductance in mature, boreal trees in spring

3599 (Lintunen et al. 2020). Cold temperature also decreases sink strength (i.e. less sugars are needed for
 3600 metabolism and growth). Low sink strength increases sugar concentration in leaves, which decreases
 3601 photosynthesis due to increased stomatal and non-stomatal limitations for photosynthesis (Hölttä et al., 2017;
 3602 Salmon et al., 2020).

3603 **Figure 2.** Example of results from the state-of-the-art aerosol instruments NAIS and PSM displaying NPF
 3604 event at Fonovaya station, Siberia, on 22.09.2019. Particles of different polarity, NAIS (a), ions of different
 3605 polarity, NAIS (b), particle number distribution at the smallest sizes, PSM (c), number concentration of the
 3606 smallest particles in different size bins, PSM (d).

3607
 3608 **Figure 3.** Linear trends of monthly mean temperature in Western Siberia (55°-65°N, 65°-90°E) in years
 3609 1979-2018. In (a), the red bars show the trend in the ERA5 reanalysis and the blue bars the circulation-
 3610 related trend. In (b), the residual trends are shown. The error bars indicate the 5-95% uncertainty range in the
 3611 circulation-related trend and the residual trend based on interannual variability. Redrawn from Räisänen
 3612 (2021).

3613

3614 **Figure 4.** The northern urban heat islands are forerunners of the global warming. Winter season future
 3615 temperatures for the Arctic (60–90°N) averaged over 36 CMIP5 global climate models and expressed as
 3616 departures from the means for the 1981–2005 period. The red line is the ensemble mean for RCP8.5, the blue
 3617 line is for RCP4.5. Shaded areas denote \pm one standard deviation from the ensemble mean (Overland et al.,
 3618 2014; and Fig. 2.15 of AMAP, 2017). The observed surface UHIs are shown as red dots collocated with the
 3619 expected future Arctic temperature anomalies, e.g., the observed wintertime urban temperature anomaly in
 3620 Nadym corresponds to the regional warming as expected to be reached by 2060. Observe that the present
 3621 Arctic climate is already 1.5°C warmer than the historical normals 1960-1990.

3622

3623 **Figure 5.** Trajectories of SIMBA buoys deployed in the Arctic in the period 2018-2019. Red: CHINARE (10
 3624 buoys), green: NABOS (5 buoys), dark blue: CAATEX (2 buoys), and light blue: MOSAiC (15 buoys).
 3625 SIMBA is a thermistor string-based ice mass balance (IMB) buoy. It measures high-resolution (2 cm)
 3626 vertical environment temperature (ET) profiles (4 times a day) through the air-snow-sea ice-ocean column.
 3627 The heating temperature (HT) measured by the thermistor string once per day is based on the use of a small
 3628 identical heater on each sensor. The ET and HT data are used to derive snow depth and ice thickness.
 3629 SIMBA uses GPS module to track the buoy location. The Iridium satellite is used for data transmission. A
 3630 total 15 SIMBA buoys have been deployed in the Arctic Ocean during the Chinese National Arctic Research
 3631 Expedition (CHINARE) 2018 and the Nansen and Amundsen Basins Observational System (NABOS) 2018
 3632 field expeditions in late autumn. In 2019 17 SIMBA buoys were deployed during the CAATEX (2) and
 3633 MOSAIC expeditions (15, leg 1).

3634

3635 **Figure 6.** SIMBA observations on the temporal evolution of the snow depth, ice thickness, and the
 3636 temperature profile from the ocean through snow and sea ice to air. The results were obtained applying the
 3637 algorithm by Liao et al. (2018). The black lines are snow surface (top), Initial freeboard (middle) and ice
 3638 base (bottom). 0 level refers to snow/ice interface. The colors indicate the temperature in °C.

3639 **Figure 7. A:** Biological pumps resulting in (i) atmospheric CO₂ sink and(ii) calcium carbonate transport
 3640 from surface to deep ocean; **B:** anticipated forward and feedback alterations in ocean ecology driven by
 3641 atmospheric CO₂ increase. PIC=particulate inorganic carbon; POC=particulate organic carbon (modified
 3642 after Rost & Riebesell, 2004).

3643 **Figure 8.** Field data for ice decay in Lake Kilpisjärvi in 2013 showing decrease of ice thickness by surface
 3644 melting and bottom melting and increase of porosity until breakage of ice cover.

3645
 3646 **Figure 9.** Changes in 2-meter temperature (°C, upper panels) and precipitation (% , lower panels) during the
 3647 21st century. Present-day climatology is averaged over years 1981-2010 and end-of-century climatology
 3648 over 2070-2099. Winter (left) and summer (right) are shown separately. Dotted areas indicate high
 3649 variability in model ensemble (for temperature: standard deviation of 21st century change exceeds 1°C; for
 3650 precipitation: standard deviation of 21st century change exceeds 100% or present-day precipitation). The
 3651 model results are from IPCC AR5, based on 42 individual models in CMIP5 experiments under the RCP4.5
 3652 scenario.

3653
 3654 **Table 1.** Systems, key topical areas, research question introduced in the PEEEX Science Plan (SP) (Kulmala
 3655 et al. 2015; 2016a, Lappalainen et al. 2018) connected to the addressed research themes over last 5 years by
 3656 the PEEEX questionnaire (APPENDIX 1). The addressed research themes and the results are overviewed in
 3657 section 3.

3658

3659

PEEX – SP System	PEEX - SP key topical area	PEEX - SP research question (Q-No)	Addressed research themes during the last 5 years
Land	Changing land ecosystem processes	How could the land regions and processes that are especially sensitive to climate change be identified, and what are the best methods to analyze their responses? (Q-1)	<ul style="list-style-type: none"> • high-latitude photosynthetic productivity and vegetation changes (greening, browning) • new methodologies determining Earth surface characteristics
Land	Risk areas of permafrost thawing	How fast will permafrost thaw proceed, and how will it affect ecosystem processes and ecosystem-atmosphere feedbacks, including hydrology and greenhouse gas fluxes ? (Q-2)	<ul style="list-style-type: none"> • soil temperature evolution • changing GHG fluxes, carbon sink-source dynamics due to permafrost thawing

Land	Ecosystem structural changes	What are the structural ecosystem changes and tipping points in the future evolution of the Pan-Eurasian ecosystem? (Q-3)	<ul style="list-style-type: none"> • changes in soil microbial activity e.g. effect of forest fires • changes of the Northern soils and functioning of the Arctic tundra in global carbon cycling context
Atmosphere	Atmospheric composition and chemistry	What are the critical atmospheric physical and chemical processes with large-scale climate implications in a northern context? (Q4)	<ul style="list-style-type: none"> • carbon (C) balance in the boreal forests; methane (CH₄) balance at the Arctic; carbon monoxide (CO), ozone (O₃) at the Northern Eurasian region • Sources and properties of atmospheric aerosols in boreal and Arctic environments • black carbon and dust in the atmosphere and on snow at the Northern high latitudes • methodological and model developments related to atmospheric chemistry and physics
Atmosphere	Urban air quality and megacities, ABL	What are the key feedbacks between air quality and climate at northern high latitudes and in China? (Q5)	<ul style="list-style-type: none"> • recent observations on air quality in China • Anthropogenic emissions and environmental pollution in Russia
Atmosphere	Weather and atmospheric circulation	How will atmospheric dynamics (synoptic scale weather, boundary layer) change in the Arctic-boreal regions? (Q6)	<ul style="list-style-type: none"> • cold & warm episodes • cyclone density dynamics • circulation effect on temperature and moisture • cloudiness in Arctic • atmospheric boundary layer (ABL) dynamics
Water	The Arctic Ocean in the climate system	How will the extent and thickness of the Arctic sea ice and terrestrial snow cover change? (Q-7)	<ul style="list-style-type: none"> • Sea ice dynamics and thermodynamics with atmospheric and ocean dynamics • Snow depth/mass and sea ice thickness • Sea ice research supporting navigation • Ocean floor, sediments: composition and fluxes • River runoff effecting the hydrological processes at coastal marine environments in Russia
Water	Arctic marine ecosystem	What is the joint effect of Arctic warming, ocean freshening, pollution load and acidification on the Arctic marine ecosystem, primary production and carbon cycle? (Q-8)	<ul style="list-style-type: none"> • Living marine organisms weaken or even subdue CO₂ accumulation

Water	Lakes and large-scale river systems	What is the future role of Arctic-boreal lakes, wetlands and large river systems, including thermokarst lakes and running waters of all size, in biogeochemical cycles, and how will these changes affect societies) ? (Q-9)	<ul style="list-style-type: none"> organic carbon, carbon balance, ice cover at lakes in the Northern high latitudes specific characteristics of the Lake Baikal and Selenga River delta in Russia specific characteristics of Asian water lakes
Society	Anthropogenic impact	How will human actions such as land-use changes, energy production, the use of natural resources, changes in energy efficiency and the use of renewable energy sources influence further environmental changes in the region? (Q-10)	<ul style="list-style-type: none"> Mitigation e.g method for the natural risk assessment in Russia and new clean energy technologies
Society	Environmental impact	How do the changes in the physical, chemical and biological state of the different ecosystems, and the inland, water and coastal areas affect the economies and societies in the region, and vice versa? (Q-11)	<ul style="list-style-type: none"> Reindeer grazing effects on the ground vegetation structure and biomass
Society	Natural hazards	In which ways are populated areas vulnerable to climate change? How can their vulnerability be reduced and their adaptive capacities improved? What responses can be identified to mitigate and adapt to climate change? (Q-12)	<ul style="list-style-type: none"> Emerging zoonotic diseases UV variation effects on health Air pollution in different scales and environments (street-level urban air pollution, transported air pollution in urban environments, air pollution at the Arctic) and related health effects;
Feedbacks	Key topics: Atmospheric composition, biogeochemical cycles: water, C, N, P, S	How will the changing cryospheric conditions and the consequent changes in ecosystems feed back to the Arctic climate system and weather, including the risk of natural hazards? (Q-13)	<ul style="list-style-type: none"> <i>Research needs:</i> quantification of the COntinental Biosphere-Aerosol-Cloud-Climate (COBACC) feedback loop at different Northern boreal environments Gold & high region quantification of BVOC – aerosols feedback loop at the Tibetan /Himalayan Plateau:..
Feedbacks	Key topics: Atmospheric composition, biogeochemical cycles: water, C, N, P, S	What are the net effects of various feedback mechanisms on (i) land cover changes, (ii) photosynthetic activity, (iii) GHG exchange and BVOC emissions (iv) aerosol and cloud formation and radiative forcing ? How do these vary with climate change on regional and global scales? (Q-14)	<ul style="list-style-type: none"> <i>Research needs:</i> The Arctic greening and browning calls for a multi-disciplinary scientific approach together, improved modelling tools and new data in order to solve scientific questions related to the net effects of various feedback mechanisms connecting the biosphere-atmosphere - human activities

<p>Feedbacks</p>	<p>Key topics: Atmospheric composition, biogeochemical cycles: water, C, N, P, S</p>	<p>How are intensive urbanization processes changing the local and regional climate and environment? (Q-15)</p>	<ul style="list-style-type: none"> <i>Research needs:</i> accelerating urbanization calls for studies on the effects of on air pollution, local climate and the effects these changes have on global climate. Integrated studies should lead to services for society, cities helping to mitigate hazards storms, flooding, heat waves, and air pollution episodes (see also 3.2.1)
------------------	--	--	---

3660

3661 **Table 2.** Hydrogeochemical signature of large river system –Selenga River case study. The figure represent
 3662 metal(loid)s partitioning (Median values) in the Selenga river basin in the upper (Mongolian) and
 3663 downstream (Russian) part between 20 July -10 August 2011 under dominant high water (A) and 07 June -10
 3664 July 2012 under dominant low water conditions. Dark orange fill corresponds to the share of suspended
 3665 forms of elements > 75% (green) , light orange – 75-50% , light blue – 50-25%, dark blue – < 25%. The
 3666 figure indicate that in the large river system some metals are mostly found in the dissolved form (84–96% of
 3667 Mo, U, B, and Sb on an average), whereas many others predominantly existed in suspension (66–87% of Al,
 3668 Fe, Mn, Pb, Co, and Bi). A consistently increasing share of metals in suspended particulate modes (about 2–
 3669 6 times) is observed under high discharge conditions For details and other hydrological seasons refer to
 3670 (Kasimov et al., 2020b).

Commented [LHK1]: Fig 9 in the pervious version is now Table 2

A

	Fe	Al	Mn	Pb	Bi	Co	Be	V	Ni	Cr	Cd	Cu	Zn	As	B	U	Mo	Sb	Ca	Sr	Sn
Russian part of the catchment	65	69	56	46	77	59	71	65	48	29	49	41	25	22	11	5	2	1	2	3	34
Mongolian part of the catchment	98	96	100	95	87	89	71	57	56	55	71	70	86	10	19	4	2	0	11	9	58

B

	Fe	Al	Mn	Pb	Bi	Co	Be	V	Ni	Cr	Cd	Cu	Zn	As	B	U	Mo	Sb	Ca	Sr	Sn
Russian part of the catchment	60	70	52	45	75	57	41	56	40	47	19	42	26	39	18	6	4	41	2	3	15
Mongolian part of the catchment	78	83	59	72	76	59	49	43	35	49	13	62	23	12	10	1	1	42	2	2	11

3671

3672

3673

3674 **Code/Data availability:** This is an review paper and the data availability is introduced in the original articles.

3675 **Author contribution:** Co-authors have provided text and/or relevant references. Some of them have been
 3676 editors of the specific chapters of the manuscript.

3677 **Competing interests:** no specific competing interests